NUREG/IA-0480

International Agreement Report

TRACE Assessment for Effect of Spacer Grid in RBHT Reflood Heat Transfer Experiments

Prepared by:
Byung-Gil HUH, Ae-Ju CHEONG, Kyung Won LEE

Korea Institute of Nuclear Safety
Daejeon, Korea

K. Tien, NRC Project Manager

Division of Systems Analysis
Office of Nuclear Regulatory Research
U.S. Nuclear Regulatory Commission
Washington, DC20555-0001

Manuscript Completed: February 2018
Date Published: February 2018

Prepared as part of
The Agreement on Research Participation and Technical Exchange
Under the Thermal-Hydraulic Code Applications and Maintenance Program (CAMP)

Published by
U.S. Nuclear Regulatory Commission

AVAILABILITY OF REFERENCE MATERIALS IN NRC PUBLICATIONS

NRC Reference Material

As of November 1999, you may electronically access NUREG-series publications and other NRC records at the NRC's Public Electronic Reading Room at http://www.nrc.gov/reading-rm.html. Publicly released records include, to name a few, NUREG-series publications; *Federal Register* notices; applicant, licensee, and vendor documents and correspondence; NRC correspondence and internal memoranda; bulletins and information notices; inspection and investigative reports; licensee event reports; and Commission papers and their attachments.

NRC publications in the NUREG series, NRC regulations, and Title 10, "Energy," in the *Code of Federal Regulations* may also be purchased from one of these two sources.

1. **The Superintendent of Documents**
   U.S. Government Publishing Office
   Washington, DC 20402-0001
   Internet: http://bookstore.gpo.gov
   Telephone: 1-866-512-1800
   Fax: (202) 512-2104

2. **The National Technical Information Service**
   5301 Shawnee Road
   Alexandria, VA 22161-0002
   http://www.ntis.gov
   1-800-553-6847 or, locally, (703) 605-6000

A single copy of each NRC draft report for comment is available free, to the extent of supply, upon written request as follows:

U.S. Nuclear Regulatory Commission
Office of Administration
Multimedia, Graphics and Storage & Distribution Branch
Washington, DC 20555-0001
E-mail: distribution.resource@nrc.gov
Facsimile: (301) 415-2289

Some publications in the NUREG series that are posted at the NRC's Web site address http://www.nrc.gov/reading-rm/doc-collections/nuregs are updated periodically and may differ from the last printed version. Although references to material found on a Web site bear the date the material was accessed, the material available on the date cited may subsequently be removed from the site.

Non-NRC Reference Material

Documents available from public and special technical libraries include all open literature items, such as books, journal articles, transactions, *Federal Register* notices, Federal and State legislation, and congressional reports. Such documents as theses, dissertations, foreign reports and translations, and non-NRC conference proceedings may be purchased from their sponsoring organization.

Copies of industry codes and standards used in a substantive manner in the NRC regulatory process are maintained at—

The NRC Technical Library
Two White Flint North
11545 Rockville Pike
Rockville, MD 20852-2738

These standards are available in the library for reference use by the public. Codes and standards are usually copyrighted and may be purchased from the originating organization or, if they are American National Standards, from—

American National Standards Institute
11 West 42nd Street
New York, NY 10036-8002
http://www.ansi.org
(212) 642-4900

Legally binding regulatory requirements are stated only in laws; NRC regulations; licenses, including technical specifications; or orders, not in NUREG-series publications. The views expressed in contractor-prepared publications in this series are not necessarily those of the NRC.

The NUREG series comprises (1) technical and administrative reports and books prepared by the staff (NUREG-XXXX) or agency contractors (NUREG/CR-XXXX), (2) proceedings of conferences (NUREG/CP-XXXX), (3) reports resulting from international agreements (NUREG/IA-XXXX), (4) brochures (NUREG/BR-XXXX), and (5) compilations of legal decisions and orders of the Commission and Atomic and Safety Licensing Boards and of Directors' decisions under Section 2.206 of NRC's regulations (NUREG-0750).

NUREG/IA-0480

International Agreement Report

TRACE Assessment for Effect of Spacer Grid in RBHT Reflood Heat Transfer Experiments

Prepared by:
Byung-Gil HUH, Ae-Ju CHEONG, Kyung Won LEE

Korea Institute of Nuclear Safety
Daejeon, Korea

K. Tien, NRC Project Manager

Division of Systems Analysis
Office of Nuclear Regulatory Research
U.S. Nuclear Regulatory Commission
Washington, DC 20555-0001

Manuscript Completed: February 2018
Date Published: February 2018

Prepared as part of
The Agreement on Research Participation and Technical Exchange
Under the Thermal-Hydraulic Code Applications and Maintenance Program (CAMP)

Published by
U.S. Nuclear Regulatory Commission

ABSTRACT

The effects of the spacer grid model in the TRACE V5.0 patch4 were evaluated for Rod Bundle Heat Transfer (RBHT) reflood heat transfer experiments. The RBHT test section was modeled in the VESSEL and HTSTR components of TRACE. Two PIPE components were modeled as the lower plenum and upper plenum and the injected flow was provided by the FILL component that was connected to the bottom of the lower plenum. The BREAK component was used to set the pressure boundary at the top of the test section. The main parameters of the spacer grid were defined by the experimental data and seven mixing vane grids were modeled in the test section of TRACE. The calculations for six tests of RBHT confirmed that when the spacer grid model was used, the rod temperatures decreased and the rods were quenched at an earlier time. This was because the spacer grid enhanced the convective heat transfer due to the flow acceleration and turbulence increase. In Test 1096 at a low power, a low reflood rate, a low pressure and a low subcooling degree, the peak rod temperature and the quenching time were most significantly affected by the spacer grid. Sensitivity studies were also performed to identify 1) the effect of the number of nodes, 2) the effect of the spacer grid parameters and 3) the effect of the mixing vane. The effect of the spacer grid model in TRACE is largely shown to simulate the RBHT reflood heat transfer experiments. However, since the droplet breakup and the grid rewetting models were not yet fully implemented, there are some limitations to quantitatively predicting their effects and the TRACE code needs to be improved for these models in the future.

CONTENTS

LIST OF FIGURES

LIST OF TABLES

EXECUTIVE SUMMARY

TRACE implemented models in 2010 that enhanced the heat transfer in the region downstream of spacer grids, but a systematic assessment of those models has not yet been performed with various post-CHF heat transfer tests such as FLECHT-SEASET, RBHT, THTF, etc. The Rod Bundle Heat Transfer (RBHT) facility conducted rod bundle heat transfer tests to support to develop reflood heat transfer models of the USNRC's thermal-hydraulic codes. In this study, calculations using TRACE V5.0 patch4 code were conducted for RBHT reflood heat transfer experiments to assess the effect of the spacer grid models of TRACE code.

For the modeling of the RBHT facility, the test section was modeled in the VESSEL component and a 7x7 heater rod bundle in the test section was modeled in HTSTR components of TRACE, which was based on a previous study. The lower plenum and upper plenum were modeled by the PIPE component. The injected flow was provided by the FILL component that connected to the bottom of the lower plenum. The BREAK component was used to set the pressure boundary at the top of the test section. The times for the injected flow and power were modified to exactly consider the experimental data. The main parameters of the spacer grid were defined by the experimental data, and seven mixing vane grids were modeled in the test section of TRACE.

The evaluations for the six tests of RBHT were performed by TRACE, and the tests covered a range of the power from 0.88 kW/m to 1.53 kW/m, the subcooling from 16 K to 86 K, the liquid injection flow rate from 0.12 kg/sec to 0.75 kg/sec and the pressure from 0.13 MPa to 0.28 MPa. When the spacer grid model was used, the rod temperatures usually decreased and the rods were quenched at an earlier time in most of the tests because the spacer grid enhanced the convective heat transfer due to the flow acceleration and the turbulence increase. In tests with high power and a high reflood rate, the effect of the spacer grid for the peak rod temperature was not big, which was due to the short heat up period and the faster rise of the liquid level. When the subcooling degree was higher, the reduced degree of quenching time due to the spacer grid was also further decreased. In Test 1096 at a low power, a low reflood rate, a low pressure and a low subcooling degree, the peak rod temperature and the quenching time were influenced most significantly by the spacer grid.

Sensitivity studies were performed to identify the effect of the number of nodes, the effect of spacer grid parameters and the effect of the mixing vane. In modeling the number of nodes of the test section as 8, 15 and 30, the coarse node case (8 nodes) had a lower peak temperature at elevation z ~ 2.77 m with the peak power. The peak rod temperature for 30 nodes was predicted to be slightly higher than that for 15 nodes, but their difference was not significant. For sensitivity calculations for 7 grid parameters, such as the spacer grid flow blockage area ratio, the mixing vane flow blockage ratio, the mixing vane angle, etc., the effect of the spacer grid flow blockage area was dominant, but the effect of other parameters was not significant for the enhancement of heat transfer due to the spacer grid. This could be because there was no full implementation of the droplet breakup model and the grid re-wetting model in TRACE. Without the mixing vane, the rod temperatures were slightly increased and the rod quenches were delayed due to the reduction of the heat transfer enhancement due to the mixing vane.

In conclusion, the effect of the spacer grid model in TRACE was shown largely to simulate the RBHT reflood heat transfer experiments. However, there are still some limitations to quantitatively predicting the effect of the droplet breakup and the grid rewetting models.

Therefore, comparative studies with other codes with a spacer grid model should be performed, and the TRACE code needs to be improved to implement the droplet breakup and the grid rewetting models in future studies

1 INTRODUCTION

A large break Loss of Coolant Accident (LOCA) is the most severe accident in the analyses of a pressurized light water reactor (PWR). In particular, the thermal-hydraulic phenomena in the core during the reflood phase needs to be accurately predicted. The reflooding typically starts by increasing the subcooled water from the bottom of core. Large amounts of steam are generated by interacting between the subcooled water and hot fuels. This steam increases the core pressure and then hinders the reflooding of water. Various heat transfer regimes such as single-phase vapor convection, nucleate boiling, transition boiling, and film boiling also occur during this phase [1]. Therefore, a heat transfer package has been developed to accurately predict complicated thermal-hydraulic phenomena during the reflooding.

Currently, spacer grids have been installed in most commercial fuel bundles, and the spacer grids may influence the thermal-hydraulic phenomena in the reflood phase of LOCA. However, the effect of the spacer grid has not been evaluated properly in various analyses and it is just considered by adding the loss coefficient at an elevation of spacer grid.

The spacer grid was originally designed to maintain a geometrical configuration of the fuel bundles, but spacer grids affect the fluid dynamics and the heat transfer in the core. The spacer grids obstacle the fluid flow in the bundles and then increase the overall pressure losses. The spacer grids also decrease the flow area by contracting and accelerating the flow, and the mixing vanes typically generate a strong swirling flow in the core, which increases the local heat transfer downstream of the spacer grid. In addition, if the spacer grids are quenched, their surfaces are covered with liquid film and provide an additional interface area between liquid and vapor. Finally, the spacer grids also break up the entrained droplets into smaller droplets and therefore the downstream vapor temperature is reduced due to the higher heat transfer of the smaller droplets and the vapor velocity increases due to the easier evaporation of the smaller droplets.

The TRACE code is the thermal-hydraulic system code and was developed by USNRC for a realistic analysis of thermal-hydraulics transients in pressurized water reactors [2]. TRACE implemented the spacer grid model in December 2010 [3]. The spacer grid models in TRACE consist of the single-phase convective enhancement model, the pressure loss model, the droplet breakup model, and the spacer grid rewet model, but the droplet breakup model and the grid re-wetting model are not fully implemented in the current TRACE. A systematic assessment of those models has not yet been performed with various post-CHF heat transfer tests such as FLECHT-SEASET, RBHT, THTF, etc. In particular, the Rod Bundle Heat Transfer (RBHT) facility have conducted rod bundle heat transfer experiments to support to develop reflood heat transfer models of the USNRC's thermal-hydraulic codes [4].

This study performed calculations using TRACE V5.0 patch4 code, which was released in April 2014, and the comparison with experimental data were made for RBHT reflood heat transfer experiments to assess the effect of the spacer grid model of the TRACE code. A brief description for RBHT facility and the spacer grid models of TRACE is made in Chapter 2. A comparative assessment of the TRACE spacer grid model against six RBHT tests is described in Chapter 3. Chapter 4 describes the results for the sensitivity analysis, such as the effect of the number of nodes, the effect of the spacer grid parameters and the effect of the mixing vane. Finally, the conclusions of this study are given in Chapter 5.

2 TEST FACILITY AND MODEL DESCRIPTION

2.1 Description for RBHT Experiment

The Rod Bundle Heat Transfer (RBHT) which was initiated at the Pennsylvania State University (PSU) in 1997 has conducted rod bundle heat transfer experiments to develop reflood heat transfer models of the USNRC's thermal-hydraulic codes [4]. This facility was designed to perform separate effects tests such as two phase level swell tests, steam flow tests with and without droplet injection, inverted annular film boiling reflood tests, and dispersed flow film boiling reflood heat transfer tests.

A schematic of the RBHT test facility is shown in Figure 2.1. The test section was comprised of a lower plenum, a low-mass housing with a heater rod bundle, and an upper plenum. This is a once-though flow facility where either water or steam can enter the lower plenum through the coolant and steam injection systems and flow upward through the rod bundle. The upper plenum serves as the first stage for phase separation and liquid collection of the two phase flow exiting the rod bundle. There are a large and a small liquid carryover tank to measure the amount of entrained liquid by steam flow. The phase separator is located downstream of the upper plenum to separate out the remaining liquid flow from the vapor. Additionally, the pressure fluctuation damping tank and steam exhaust piping are installed to damp out any pressure oscillations in the facility.

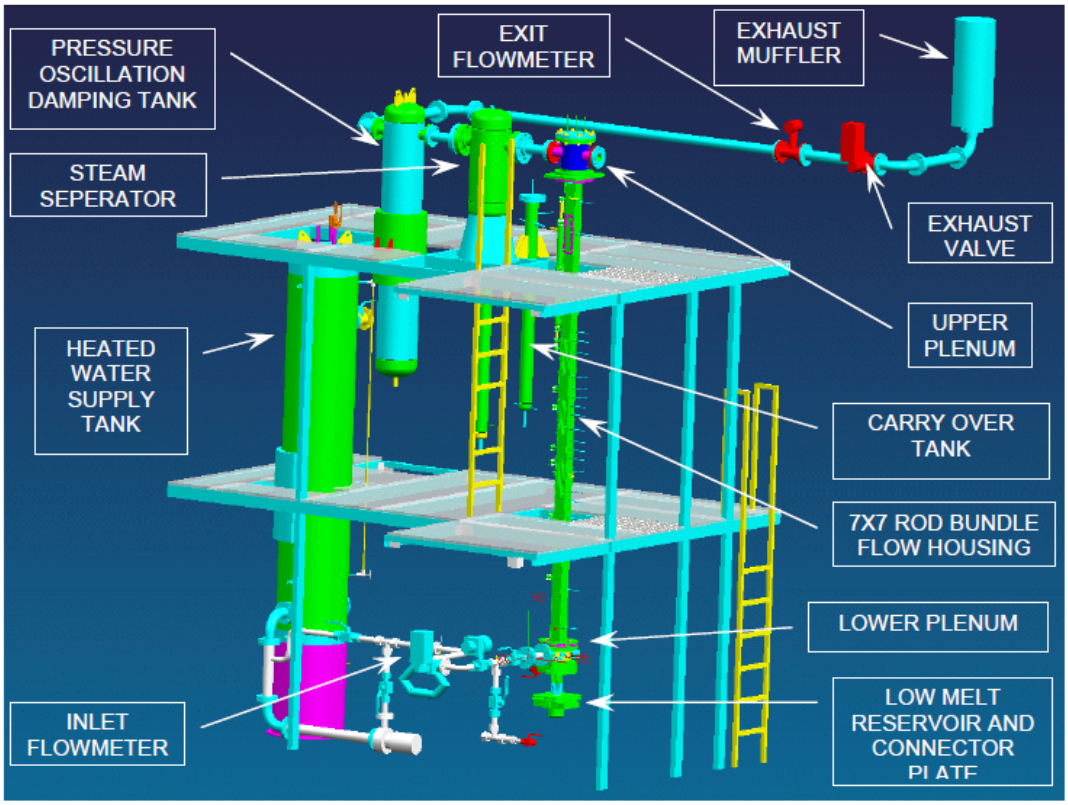

Figure 2-1 RBHT Test Facility

The test section is presented in Figure 2.2. The heater rod bundle is considered a small portion of a 17x17 PWR reactor fuel assembly. The electrical heater rods were arranged in a 7x7 array with a 9.5 mm rod diameter and a 12.6 mm pitch. The rod bundle has 45 heater rods and 4 unheated corner rods. The heater rods have a 3.66 m (12 ft.) heated length with a skewed axial power profile with the peak power located at elevation z = 2.74 m (9 ft.). The maximum-to-average power ratio (P_{max}/P_{avg}) is 1.5 at the peak power location and the bundle has a uniform radial power distribution [5].

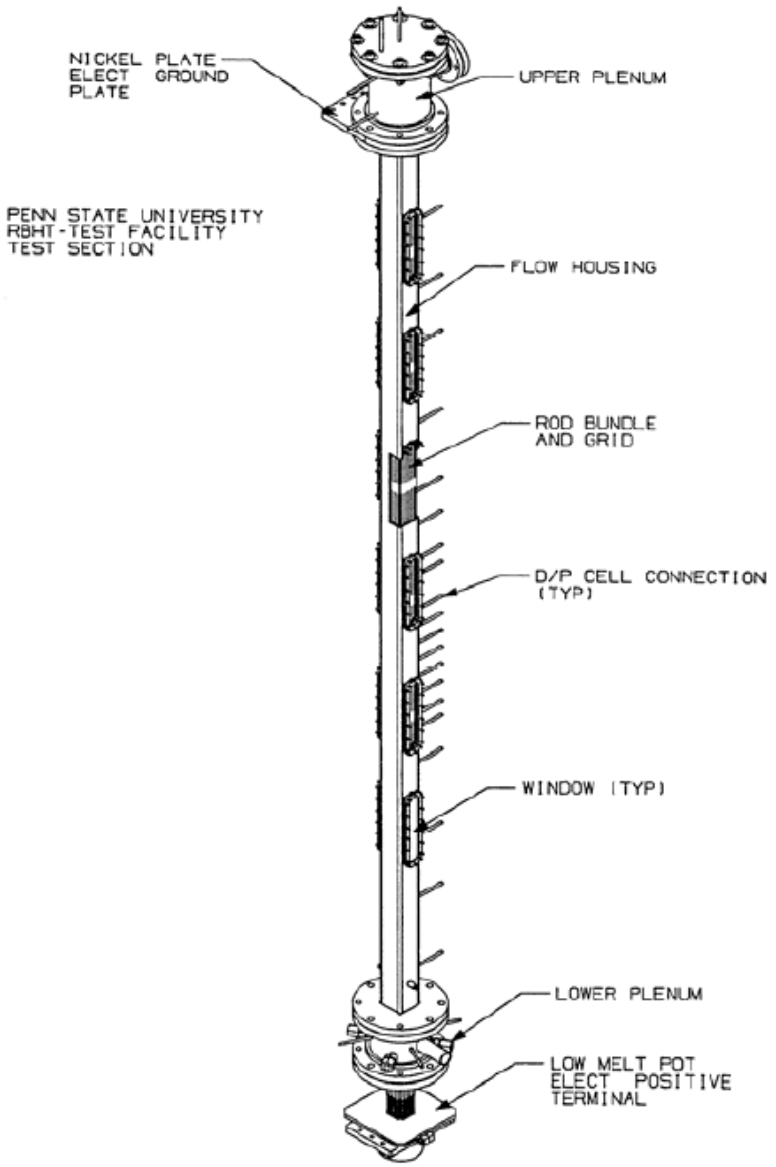

Figure 2-2 Test Section Schematic

The rod bundle has seven mixing vane grids, which is similar to a typical 17x17 PWR fuel assembly. The grid straps are made of Inconel 600 alloy sheets that are 0.51 mm thick and are 44.5 mm in height, including the mixing vane. The grids are located 522 mm apart except for the spacing between the first and second grid, which is 588 mm apart. The first grid is located

102 mm above the bottom of the heater. The blockage ratio of the spacer grids was reported to be 0.362 [6]. The flow housing has a square geometry with 90.2 x 90.2 mm inside dimensions and a 6.4 mm wall thickness. The flow housing also has six pairs of windows.

Most of the experiments used a peak cladding temperature of 1033 to 1144 K and the reflooding rates varied from 0.0254 to 0.1524 m/s. The most significant problem during the reflood tests was reported for pressure oscillations that occurred due to the control logic for the exhaust control valve [4]. Pressure variations in the test section were usually small, but there were several experiments in which pressure oscillations could not be damped.

2.2 Spacer Grid Model in TRACE

There are spacer grids in most fuel assemblies. The functions of the spacer grid are to support fuel rods vertically and laterally, to maintain the space between rods and to enhance the flow mixing. In the thermal-hydraulic aspect, the spacer grid provides flow obstacles in a core channel and then influences the heat transfer mechanism in the core. First, the spacer grid reduces the flow area and then flow acceleration occurs at the location of a spacer grid. This promotes the local convective heat transfer. Second, the spacer grids can be quenched before the fuel rod during a reflood and increase the interfacial area between liquid and vapor. Third, the spacer grids break the entrained droplets into smaller ones and this increases the interfacial heat transfer to the vapor phase.

Currently, there are four sub-models in TRACE, which are for the convective heat transfer enhancement, the pressure drop, the droplet breakup and the grid re-wetting, respectively. In this chapter, four sub-models are briefly described by referring to the TRACE theory manual [3].

1) Convective heat transfer enhancement

The Yao, Hochreiter and Leech model [7] was applied in TRACE and it can be used in both egg-crate grids and mixing vane grids. This model consists of two parts; 1) the heat transfer enhancement due to the acceleration of the flow and the increased turbulence due to the spacer grid, and 2) the effects of mixing vanes:

$$\frac{Nu}{Nu_o} = \underbrace{\left[1 + 5.55\beta^2 e^{-0.13\frac{x}{D_H}}\right]}_{Part\ 1} \underbrace{\left[1 + a^2(tan\emptyset)^2 e^{-0.034\frac{x}{D_H}}\right]^{0.4}}_{Part\ 2} \quad (1)$$

where Nu is the local Nusselt number at the wall with the grid spacer, Nu_o is the local Nusselt number at the wall without the spacer grid, β represents the spacer grid flow blockage area ratio as viewed from upstream, x is the axial distance from the downstream edge of the spacer, D_H is the hydraulic diameter of the flow channel, a is the mixing vane flow blockage area ratio when viewed from upstream, and $\emptyset$ is the angle of the vane with respect to the axial direction.

As shown in Eq. (1), this model depends on the spacer grid blockage ratio, the mixing vane blockage ratio, and the mixing vane angle. Additionally, in order to consider the increased enhancement effects for high void fraction, laminar flows, a laminar enhancement factor, F was introduced into this model as shown in TRACE theory manual [3].

2) Pressure losses

In order to consider the pressure drop due to the spacer grids, TRACE adopted the Yao, Loftus and Hochreiter [8] model. The loss coefficient for this model was improved by Rehme [9] and a 40% increase of the loss factor was also applied to account for the sharp leading edge.

$$\Delta p_{grid} = K_{grid}\frac{\rho}{2}V^2, \quad K_{grid} = 1.4\,C_V(\beta + a)^2 \tag{2}$$

where, $C_V = \begin{cases} 196Re_m^{-0.33}, & 10^3 < Re < 10^4 \\ 41Re_m^{-0.16}, & 10^4 < Re < 10^5 \\ 6.5, & 10^5 < Re \end{cases}$.

3) Droplet breakup

In the dispersed droplet flow, the droplet is split apart by the spacer gird strap. The droplet breakup model in TRACE is based on a study that was conducted by Yao, Hochreiter and Cai [10]. The shattered small droplet ratio is represented as a function of the droplet Weber number and the ratio of the Sauter mean diameter to the initial diameter. If the Weber number is greater than 250, the droplets do not have sufficient surface tension force to overcome the impact with the spacer grid straps and the droplet breakup is possible [3]. The droplet mass flow rate in the downstream cell is as follows:

$$\dot{m}_{small} = 0.6(\beta + a)\dot{m}_o, \quad \dot{m}_{large} = \dot{m}_o - \dot{m}_{small} \tag{3}$$

The diameters of the shattered droplets and the remaining large droplets are given as

$$D_{small} = 6.16We_d^{-0.53}D_o, \quad D_{large} = D_o \tag{4}$$

where $We_d = \frac{\rho_l D_d V_d^2}{\sigma_d}$ is the droplet Weber number.
This model is subject to the completion of the droplet field equation because droplets shattered from a large group are taken as the source and sink terms in the downstream axial cell. However, the droplet breakup model is not currently activated in TRACE and it has been waiting for full implementation of the droplet field.

4) Grid re-wetting

During reflood conditions, the spacer grid with no internal heat generation falls below the minimum film boiling temperature before the fuel rods. Therefore, the liquid film formed on a spacer grid increases the local interfacial area for heat transfer and then it results in significant de-superheating of the vapor. In TRACE, the modified radiation model of Paik, Hochreiter, Kelly, and Kohrt [11] was used after several simplifications. This model is about the heat transfer between fuel rods, a spacer grid, and the continuous vapor phase. The heat balance equation for the spacer grid is given as

$$\rho_{sp}C_p\frac{\partial T_{sp}}{\partial t} = \frac{WP_{grid}}{A_{grid}}\left(q''_{rad} - q''_{conv}\right) \tag{5}$$

For a detailed description of this model refer to the TRACE manual [3]. According to this model, the spacer grid temperature was calculated by the spacer grid surface area is obtained as the spacer grid height times the grid wetted perimeter multiplied by two to account for both sides of the spacer grid straps.

However, in the current TRACE, the spacer grid re-wetting model is only implemented to calculate the transient spacer grid temperatures and add the spacer grid surface area to the wallFilmArea variable if the spacer grid is quenched. Further work for a critical film thickness will be required for determining the film Nusselt number from which the film interfacial heat transfer coefficient is calculated.

3 EVALUATION FOR THE SPACER GRID MODEL ON RBHT REFLOOD TESTS

Usually, the spacer grid decreases the flow area and then enhances the convective heat transfer due to the flow acceleration and the turbulence increases. Their phenomena is shown in both egg-crate style spacer grids and mixing vane grids. The mixing vane enhances the convective heat transfer additionally in the case of mixing vane grids. In this section, the effect of the spacer grid model of TRACE was evaluated on Rod Bundle Heat Transfer (RBHT) reflood tests [4, 5]. The RBHT facility was installed to simulate the reflood thermal-hydraulic phenomena which is very important during a hypothetical large break loss of coolant accident (LOCA). The RBHT facility was designed to conduct several separate-effects tests such as single phase steam cooling, low flow boiling and dispersed flow film boiling heat transfer. The test facility consists of a test section with a lower plenum, heater rods and an upper plenum, water injection and steam injection systems, a phase separation and liquid collection systems and a pressure fluctuation damping tank as shown in Figure 3.1. This facility has the heated length of 3.66 m (12.0 ft.) of the typical pressurized water reactor (PWR) fuel assembly. The test section consists of a 7x7 rod bundle with 45 heated electrical rods and seven mixing vane grids. The electrical rods have a diameter of 9.5 mm and are arranged in a 7x7 array with a 12.6 mm pitch with 45 heater rods and four unheated rods. Tests 1096, 1108, 1170, 1196, 1285 and 1383 which were in the TRACE assessment manual [12] were selected to evaluate the effect of the spacer grid model of TRACE.

3.1 TRACE Modeling

The RBHT test section was modeled by the VESSEL and HTSTR components of TRACE as shown in Figure 3.2. The TRACE modeling was almost the same as that of the previous study [12] except for some corrections. The Vessel was divided into 17 axial levels and there were two cells between each gird. The bottom of the spacer grid was located in the bottom of the corresponding cell. Forty-five heated rods were modeled in a 7x7 array with 4 unheated rods in the corners. The heated length of the heater rod was 3.66 m with a skewed axial power profile as shown in Figure 3.2 in which the peak power was located at ~ 2.74 m (9 ft.) elevation. The power peaking (P_{max}/P_{avg}) was 1.5. Eight groups of heater rods have thermocouples at different elevations to cover the entire heated rod length. The radial location of each group is shown in Figure 3.3. The thermocouples of the heater rods are also shown in Table 3.1. The heater rod was modeled with 8 radial cells and the material properties of the previous study [12] were also used in this calculation.

Two PIPE components were modeled as the lower plenum and the upper plenum respectively. The injected flow was provided by the FILL component that was connected to the bottom of the lower plenum. The BREAK component was used to set the pressure boundary at the top of the test section. The heat loss for radiation was not considered since the heat loss for a typical reflood test was just a small fraction (~2%) of the total power (~114 kW).

As in the previous study [12], the initial temperatures of the rods were defined as the detailed temperatures which were translated from the fourth-order polynomial to the TRACE node by simple linear interpolation. The list of injected flow rates and the power for each test is shown in Table 3.2. The times for the injected flow and power were corrected to consider the experimental data exactly, especially for tests 1108, 1170 and 1196. The transient calculation was started at the time of reflood initiation.

For the spacer grid, the grid straps were made by Inconel 600 alloy sheets which were 0.51 mm (0.02 in) thick and 44.5 mm (1.75 in) high, including the mixing vanes. The grids were located 522 mm (20.55 in) apart except for the spacing between the first and second grid, which was 588 mm (23.26 in) apart [4]. The first grid was located 102 mm (4.01 in) above the bottom of the heater length. The grid locations were similar to a 17x17 PWR fuel assembly. In order to model the spacer grid, the experimental design data and the general fuel data were considered to determine some parameters. The spacer grid for TRACE was modeled as follows:

```
*n: Grid-MixingVane
*
*       gridid
        101
*       spbloc          vnbloc          phi             wetperm
        0.362           0.188           30.0            1.912
*       height          strthick        spmatid
        0.045           1.0E-3          12
```

Meaning of the grid parameters

- gridid : Grid number ID
- spbloc : Spacer grid flow blockage area ratio
- vnbloc : Mixing vane flow blockage area ratio
- phi : Mixing vane angle measured from parallel with the top of the spacer grid to the mixing vane
- wetperim : Spacer grid wetted perimeter
- height : Spacer grid axial height
- strthick : Grid strap thickness of modeled spacer grid
- spmatid : Grid material ID

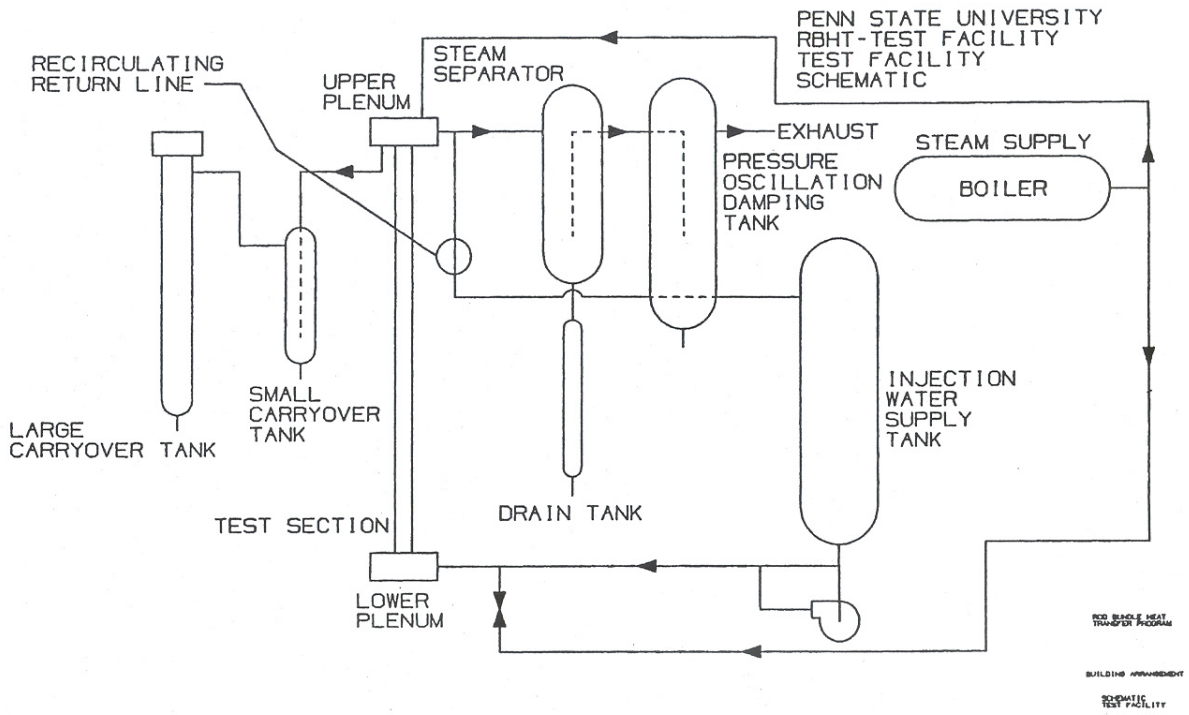

Figure 3-1 Schematics of the RBHT Test

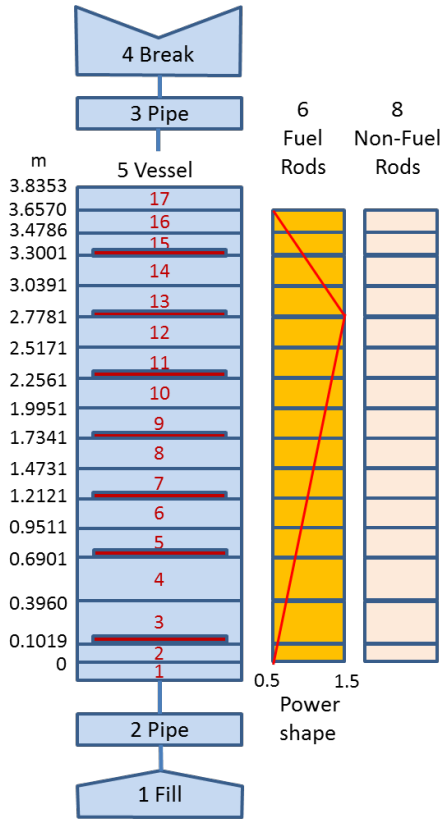

Figure 3-2 TRACE Nodalization for RBHT

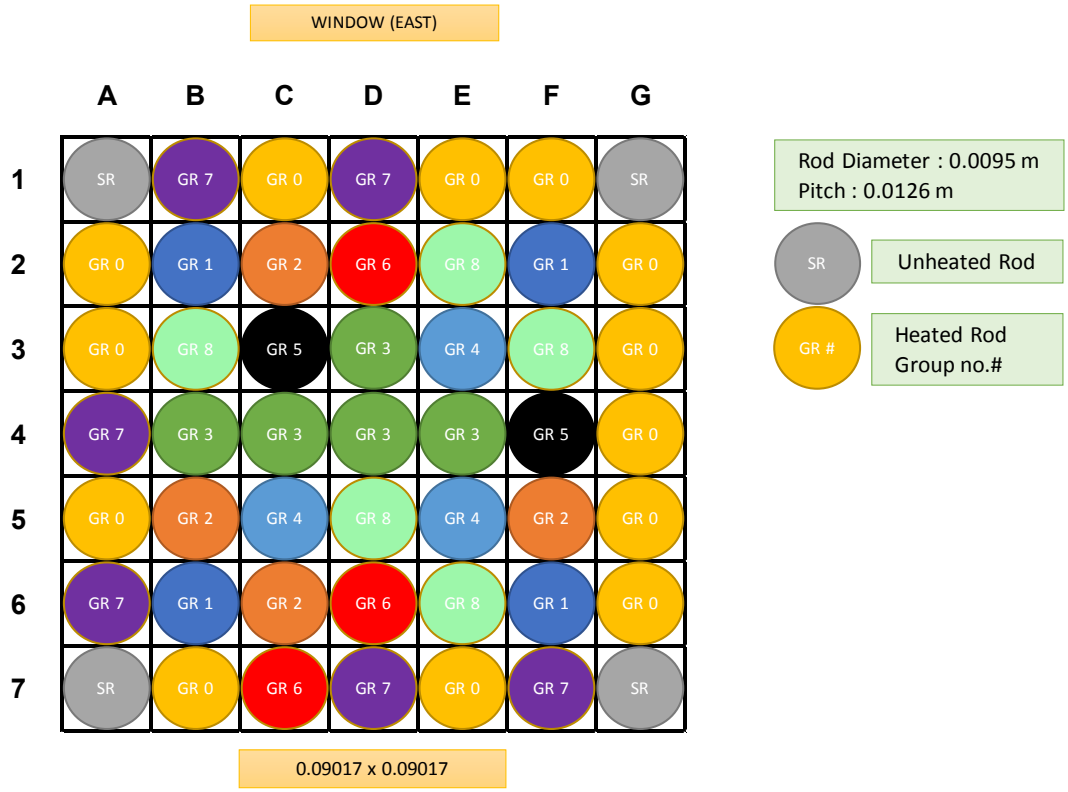

Figure 3-3 Heater Rod Location

Table 3-1 Locations of Thermocouples of Heater Rods

Spacer Grid Location from bottom		Channel Location		channel ID	Channel Location		channel ID
in	m	in	m		in	m	
		142.2	3.6119	168,192,208,224,240			
		139.3	3.5382	8,16,24,32,40,48			
		135.4	3.4392	200,216,232			
		131.5	3.3401	199,215,231			
129.92	3.3000						
					128.5	3.2639	72,136
		126.6	3.2156	198,214,230	126.6	3.2156	7,15,23,31,39,47
					124.6	3.1648	71,135
		122.7	3.1166	197,213,229			
					120.7	3.0658	70,134
		118.8	3.0175	196,212,228			
					116.8	2.9667	69,133
		115.8	2.9413	195,211,227			
		114.9	2.9185	6,14,22,30,38,46	114.9	2.9185	68,132
		113.9	2.8931	194,210,226			
					112.9	2.8677	67,131
		111	2.8194	167,191,207,223,239	111.4	2.8296	104,184
109.37	2.7780						
					109	2.7686	103,183
		106.1	2.6949	166,190,206,222,238	106.1	2.6949	66,130
					103.2	2.6213	65,129
		100.2	2.5451	165,189,205,221,237			
		97.3	2.4714	5,13,21,29,37,45	97.3	2.4714	102,182
		95.3	2.4206	164,188,204,220,236			
					94.4	2.3978	101,181
		93.4	2.3724	163,187,203,219,235			
					92.4	2.3470	100,180
		91.4	2.3216	162,186,202,218,234			
88.82	2.2560						
		88.5	2.2479	161,185,201,217,233	88.5	2.2479	99,179
					85.5	2.1717	98,178
		79.7	2.0244	4,12,20,28,36,44	79.7	2.0244	97,177
		76.7	1.9482	64,112,160,144			
		75.7	1.9228	63,111,159,143			
					74.8	1.8999	80,96,128,176,248
		73.8	1.8745	62,110,158,142			
					72.8	1.8491	79,95,127,175,247
					69.8	1.7729	78,94,126,174,246
68.27	1.7341	68.9	1.7501	3,11,19,27,35,43			
					65.9	1.6739	77,93,125,173,245
					63.9	1.6231	2,10,18,26,34,42
		63.9	1.6231	61,109,157,141	63.9	1.6231	193,209,225
					60	1.5240	76,92,124,172,244
		58	1.4732	60,108,156,140	57	1.4478	75,91,123,171,243
		55.1	1.3995	59,107,155,139			
					54.1	1.3741	74,90,122,170,242
		53.1	1.3487	58,106,154,138			
					50.1	1.2725	73,89,121,169,241
		48.1	1.2217	1,9,17,25,33,41			
47.72	1.2121						
		41.2	1.0465	57,105,153,137			
		38.2	0.9703	56,88,120,152			
		35.2	0.8941	55,87,119,151		Group Color	
		33.2	0.8433	54,86,118.150			Group 0
		29.2	0.7417	53,85,117,149			Group 1
27.17	0.6901						Group 2
		23.2	0.5893	52,84,116,148			Group 3
		16.2	0.4115	51,83,115,147			Group 4
		11.2	0.2845	50,82,114,146			Group 5
		4.2	0.1067	49,81,113,145			Group 6
4.01	0.1019						Group 7

Table 3-2 Reflood Test Injection Flow Rates and Power

Test 1096 (P=0.14 MPa)				Test 1108 (0.14 MPa)			
Time (s)	Inj. Flow (kg/s)	Time (s)	Power (W)	Time (s)	Inj. Flow (kg/s)	Time (s)	Power (W)
0.00	0.00	0.00	0.00	0.00	0.0000	0.00	0.00
0.50	0.04	0.50	72021.00	0.50	0.0626	0.50	71764.00
1.00	0.1232	1.00	143603.00	1.00	0.1251	1.00	143528.00
2.00	0.1245	1684.00	143603.00	2.00	0.1251	1381.00	143528.00
73.00	0.1245	1685.00	72021.00	1381.00	0.1251	1382.00	71764.00
197.00	0.1241	1686.00	0.00	1382.00	0.0626	1383.00	0.00
1702.00	0.1241			1383.00	0.0000		
1703.00	0.0618						
1704.00	0.0000						
Test 1170 (P=0.28 MPa)				Test 1196 (0.28 MPa)			
Time (s)	Inj. Flow (kg/s)	Time (s)	Power (W)	Time (s)	Inj. Flow (kg/s)	Time (s)	Power (W)
0.00	0.0000	0.00	0.00	0.00	0.0000	0.00	0.00
15.00	0.3768	0.50	125645.00	15.00	0.3700	0.50	125595.00
30.00	0.7536	1.00	251289.00	30.00	0.7400	1.00	251190.00
100.00	0.7536	474.00	251289.00	100.00	0.7400	496.00	251190.00
474.00	0.7536	475.00	125645.00	496.00	0.7400	497.00	125595.00
475.00	0.3768	476.00	0.00	497.00	0.3700	498.00	0.00
476.00	0.0000			498.00	0.0000		
Test 1285 (P=0.28 MPa)				Test 1383 (0.28 MPa)			
Time (s)	Inj. Flow (kg/s)	Time (s)	Power (W)	Time (s)	Inj. Flow (kg/s)	Time (s)	Power (W)
0.00	0.0000	0.50	0.00	0.00	0.00	0.50	0.00
15.00	0.4136	1.00	125944.00	0.50	0.05	1.00	71801.00
22.00	0.7334	308.00	251887.00	1.00	0.1000	891.00	143603.00
308.00	0.7415	309.00	251887.00	2.00	0.1300	892.00	143603.00
309.00	0.0000	310.00	125944.00	33.00	0.1220	893.00	71807.00
		311.00	0.00	43.00	0.1290	894.00	0.00
				70.00	0.1290		
				108.00	0.1380		
				893.00	0.1340		
				894.00	0.1340		
				895.00	0.00		

3.2 Evaluation for the Spacer Grid Model

As mentioned before, six tests were chosen for this calculation as shown in Table 3.3. The tests covered a range of power from 0.88 kW/m to 1.53 kW/m, subcooling from 16 K to 86 K, liquid injection flow rate from 0.12 kg/sec to 0.75 kg/sec and pressure from 0.13 MPa to 0.28 MPa. TRACE simulations in the assessment manual [12] showed the results for peak cladding temperature (PCT), heat transfer coefficients, quench times, liquid carry-over, steam temperature, and two-phase level swell at low pressure during a reflood test. In this study, the results for the effect of the spacer grid were shown for tests as follows:

Table 3-3 Test Matrix for TRACE Evaluation

Test ID	Reflood rate (kg/s)	Pressure (MPa)	Linear power /Rod (kW/m)	Subcooling (K)	Reflood Time (s)
1383	0.13	0.28	0.88	17	310
1096	0.12	0.14		16	225
1108	0.13	0.14		82	110
1170	0.75	0.28	1.53	16	300
1196	0.74	0.28		59	227
1285	0.74	0.28		86	115

1) Test 1383

Test 1383 was a reflood test with 0.13 kg/s (~1 in/s) at 0.28 MPa, 17 K subcooling and 0.88 kW/m linear power. Generally, the test bundle was preheated by the steam produced from the boiler and the power was turned on. When the heater rods reached a predetermined temperature, the reflood started as the liquid was injected. The pressure kept stable during the test. The collapsed liquid level in the test section increased gradually with the injected water. TRACE slightly over-predicted the liquid level. When the spacer grid model was applied, the collapsed liquid level increased slightly faster than that without the spacer grid model as shown in Figure 3.4.

The rod temperatures at various elevations are shown in Figures 3.5 through 3.9. These figures clearly showed that the rod was heated up by the initiation of the reflood, turning to reduce during the reflood, and eventually quenching. The predicted peak temperatures agreed reasonably well with the RBHT data at low elevations ($z < 1.27$ m), but showed over-estimated results at higher elevations. TRACE under-predicted the quenching time. As described in Chapter 2, the spacer grid models in TRACE were divided into four sub models: convective enhancement model, pressure loss model, droplet breakup model and spacer grid rewet model. However, the convective enhancement and pressure loss models of TRACE currently influence the rod temperatures. In order to consider the flow acceleration and the turbulence increase due to the spacer grid, the convective Nusselt number was enhanced to the nominal Nusselt number. In addition, for RBHT with the mixing vane grid, the effect of the mixing vane added to the convective enhancement. For the pressure loss, the loss coefficient for the spacer grid was calculated and added to the existing loss coefficients for the grid locations. The large loss coefficient increased the local velocity and the overall pressure drop of the test section. As would be expected, the lower rod temperatures and earlier rod quenches were predicted in the case with a spacer grid model. The effect for the rod temperature and quenching was larger with a higher elevation. At elevation z~2.77 m with the peak power, the decreasing peak rod temperature was ~ 21.7 K and the reduction of the quenching time was ~ 53 sec due to the spacer grid model.

The heat transfer coefficients (HTCs) at several elevations are given in Figures 3.10 through 3.12. Usually, when the heater rod was quenched, the heat transfer coefficient significantly increased. As shown in the figures, the HTC decreased during the rod heat up and the mixed convective heat transfer became dominant during the reflood. The heater rod during the reflood phase cooled by the steam cooling and water droplets and the HTC increased gradually. Finally, the HTC increased very rapidly at the time of rod quenching. However, TRACE did not predict the HTC decrease during the rod heat up. At the reflood initiating time, the increase in the HTC was reasonably predicted and the average HTC during the reflood roughly predicted the data,

but the trend did not agree with the RBHT data. TRACE predicted a sharp increase in the HTC much earlier than that of RBHT data since the rod quenching occurred too early. When the spacer grid model was applied, a steep increase in the HTC was expedited since the earlier rod quench occurred due to the enhancement of the convective heat transfer.

The steam temperatures at the middle elevation are shown in Figures 3.13 and 3.14. The steam temperature was over-estimated at the initial heat up after the reflood and the cooling in bundles was not enough to quench the rod. This may have resulted in a significant increase in rod temperature in the heat up region. The under-estimation of the quenching time may have come from the increase of evaporation and cooling due to the over-estimated liquid carry-over into the exit. The calculation with the spacer grid model showed a slightly higher steam temperature because of the enhancement of heat transfer.

The quenching front location and the mass flowrate at ~ 2.7 m elevation where the peak power was located are plotted in Figures 3.15 and 3.16. When the spacer grid model was applied, the quenching front arrived at ~ 2.7 m earlier around ~ 50 sec as compared to that without the spacer grid model. As shown in Figure 3.16, the local mass flowrate increased strongly at the spacer grid location and this reduced the rod temperature.

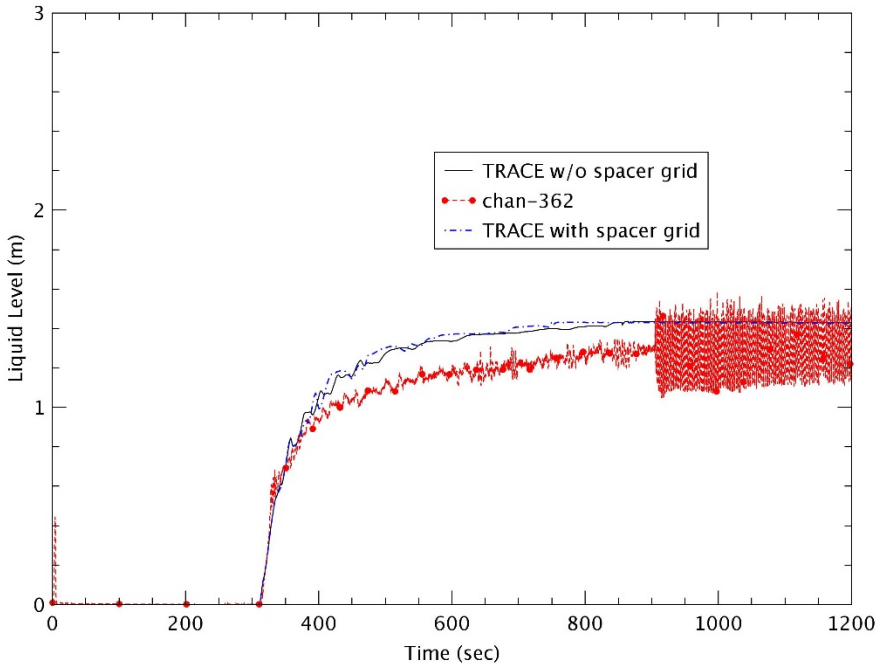

Figure 3-4 Collapsed Liquid Level – Test 1383

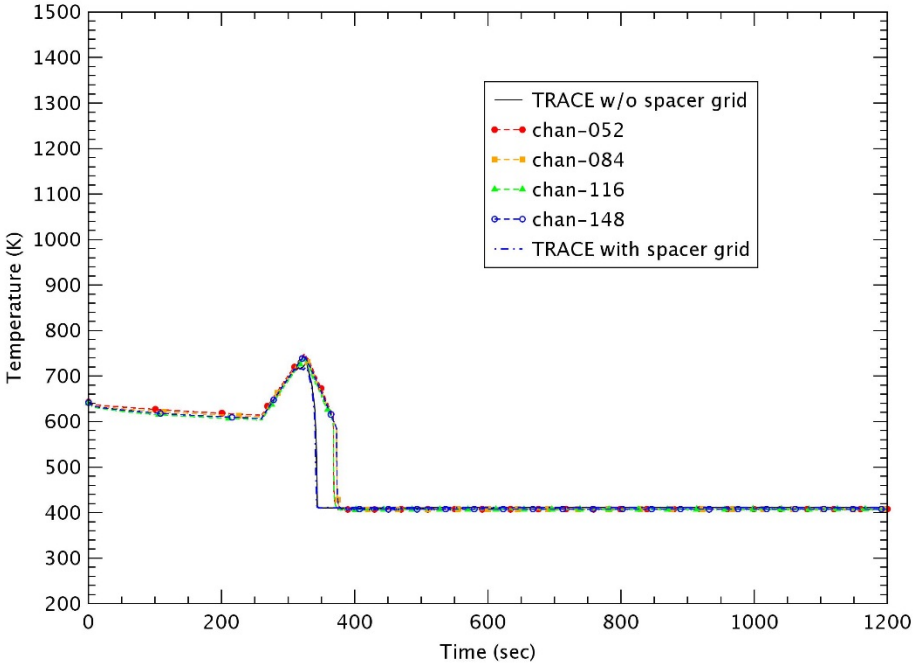

Figure 3-5 Heater Rod Temperature at 0.59 m – Test 1383

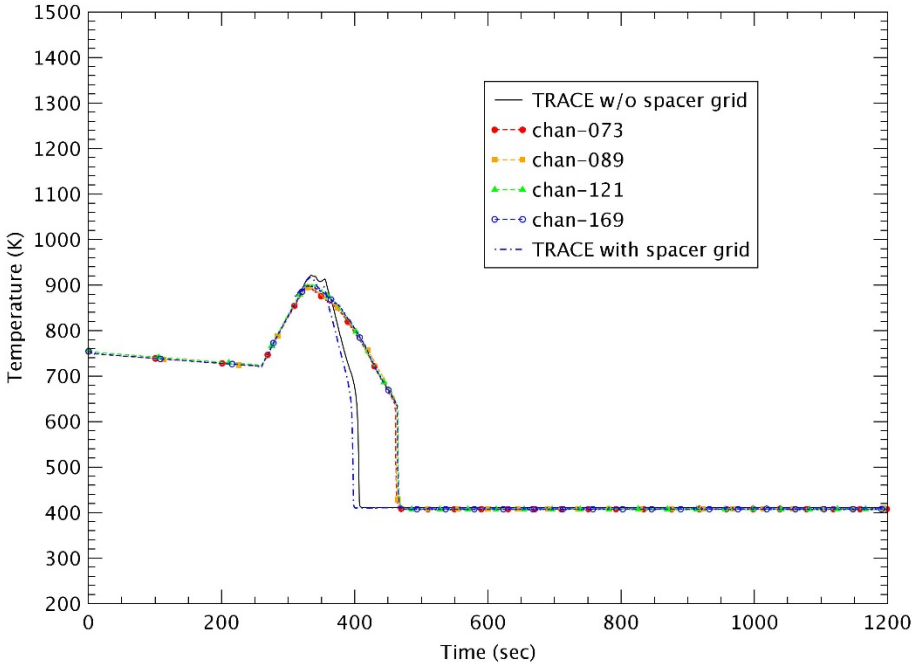

Figure 3-6 Heater Rod Temperature at 1.27 m Test 1383

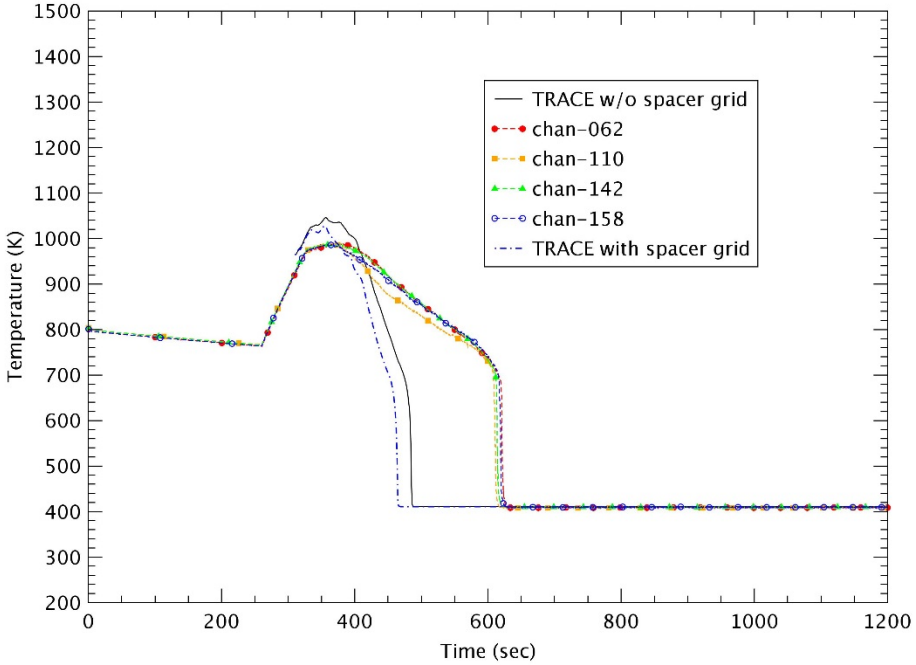

Figure 3-7 Heater Rod Temperature at 1.87 m – Test 1383

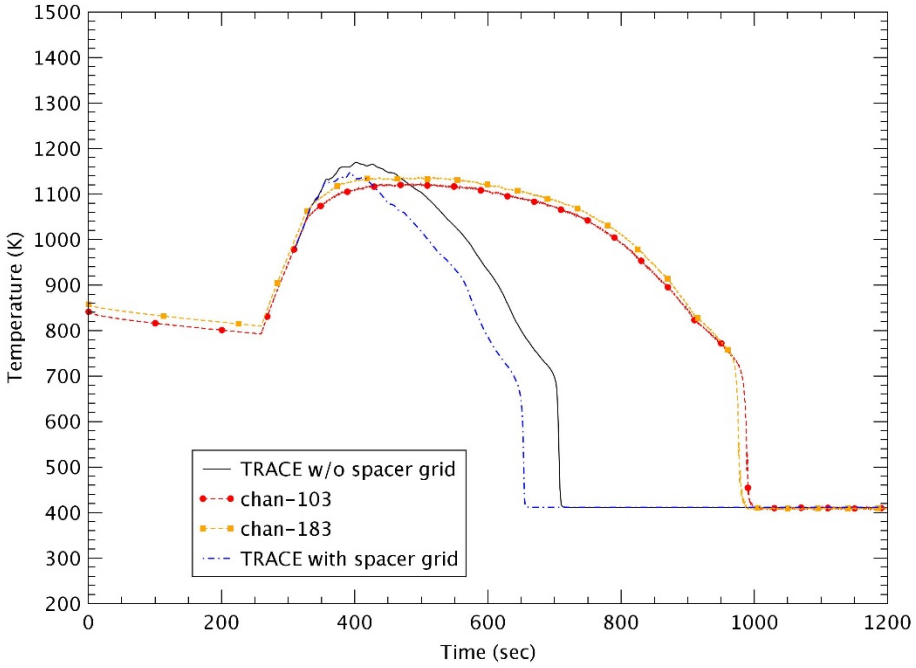

Figure 3-8 Heater Rod Temperature at 2.77 m – Test 1383

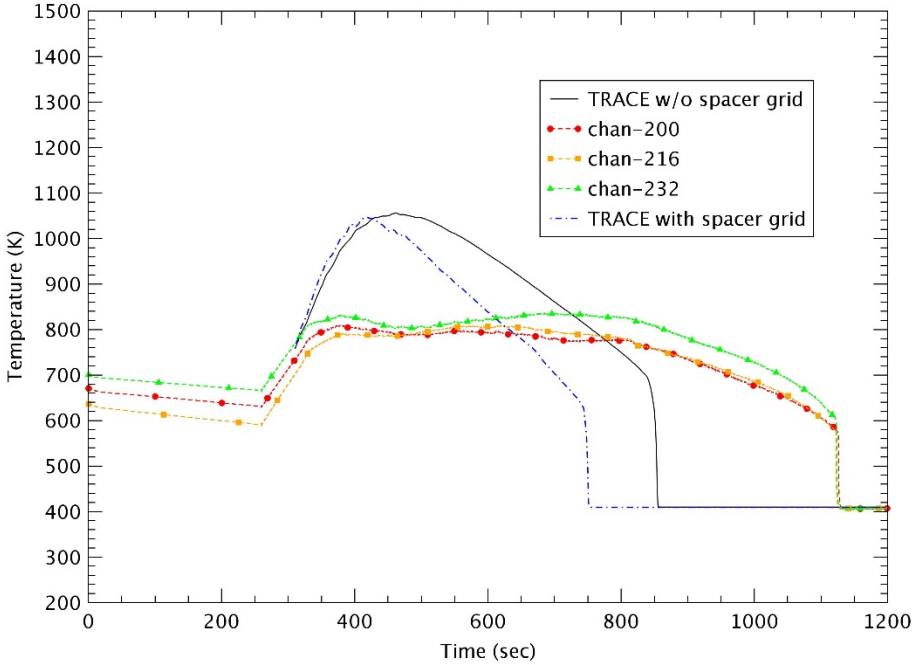

Figure 3-9 Heater Rod Temperature at 3.43 m – Test 1383

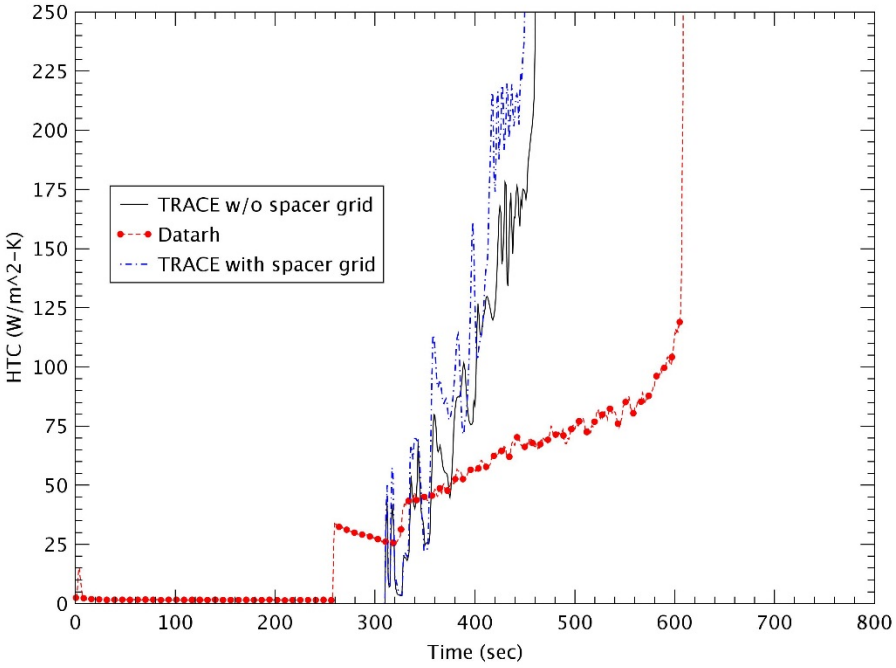

Figure 3-10 Heat Transfer Coefficient at 1.88 m – Test 1383

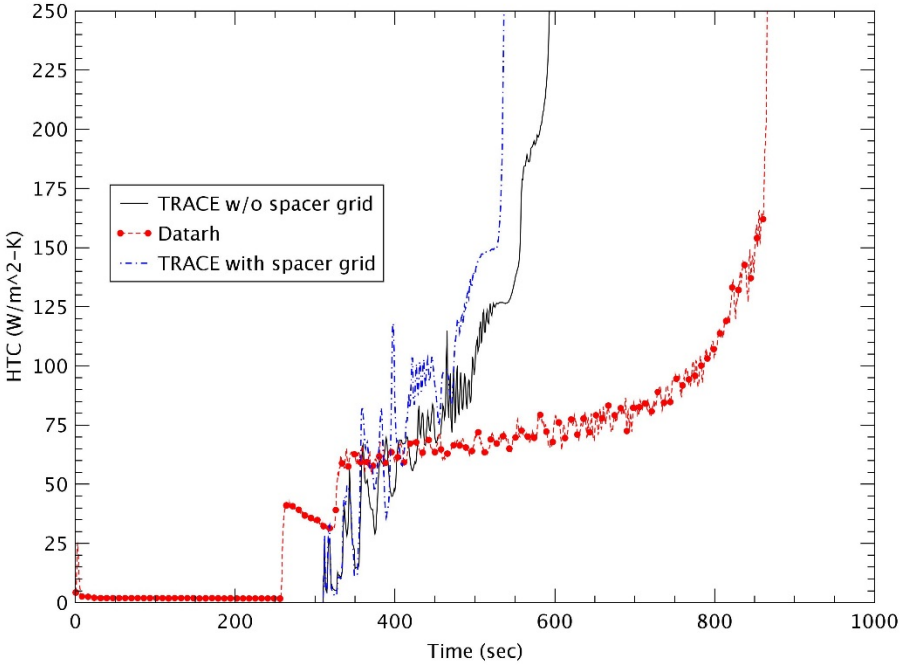

Figure 3-11 Heat Transfer Coefficient at 2.54 m – Test 1383

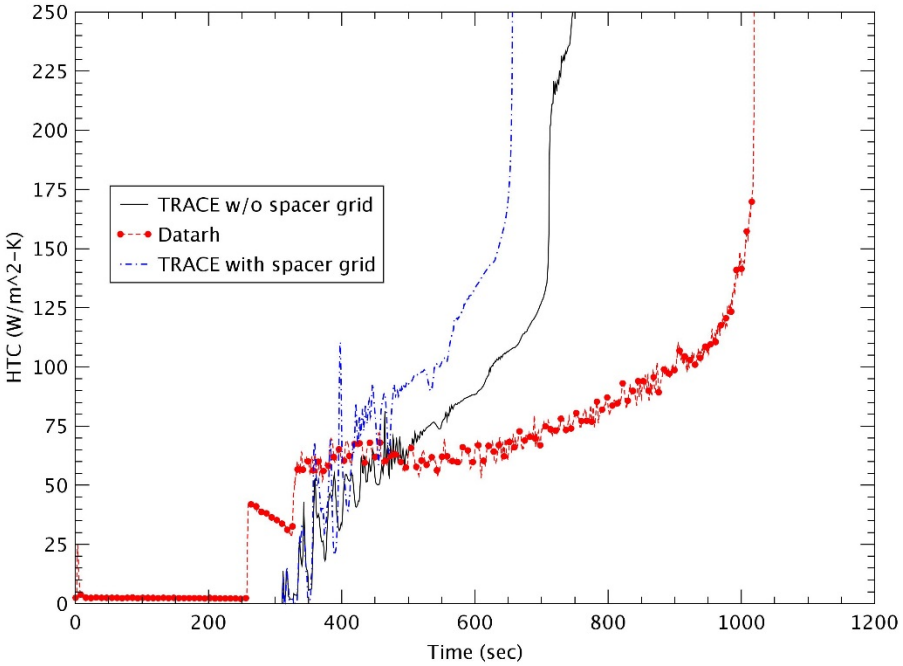

Figure 3-12 Heat Transfer Coefficient at 2.93 m – Test 1383

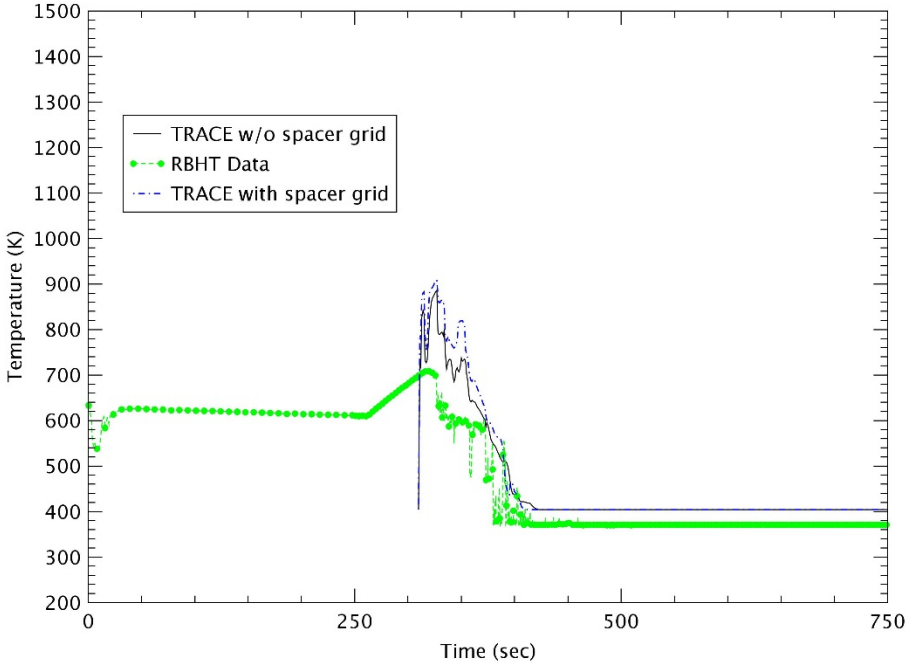

Figure 3-13 Steam Temperature at 1.40 m – Test 1383

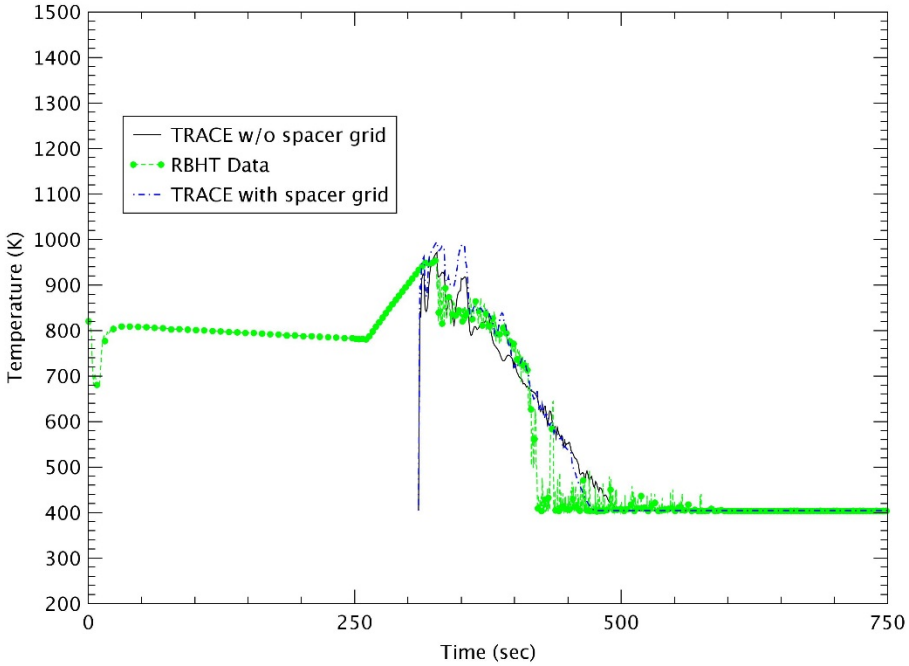

Figure 3-14 Steam Temperature at 1.88 – Test 1383

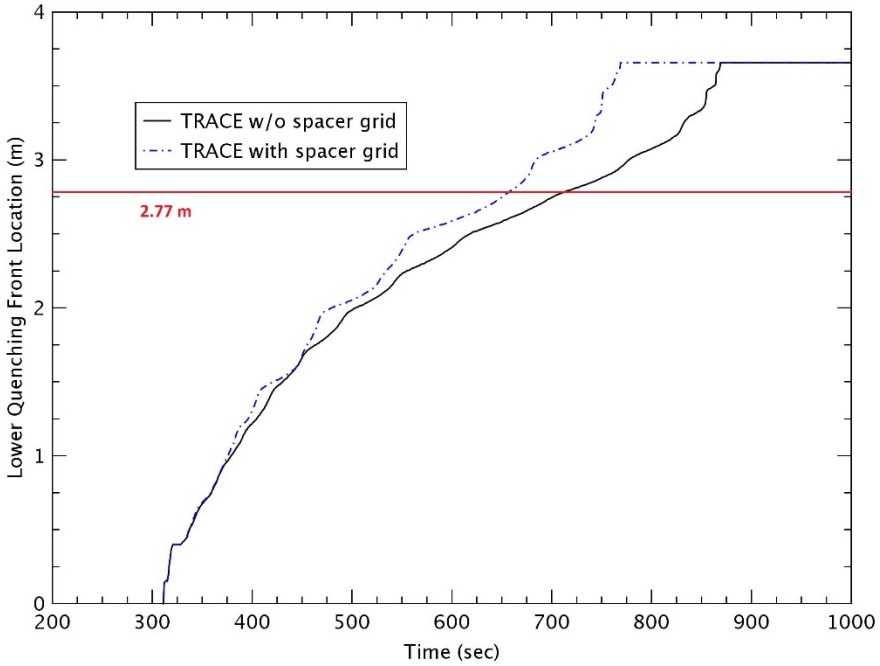

Figure 3-15 Quenching Front Location – Test 1383

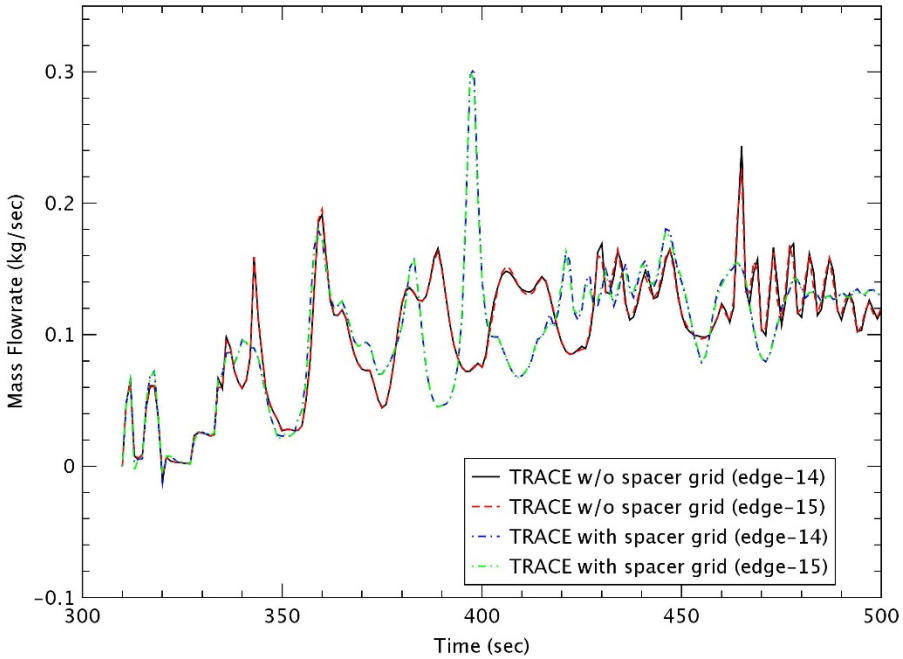

Figure 3-16 Mass flowrate around 2.77 m – Test 1383

2) Test 1096

Test 1096 was a reflood test with 0.12 kg/s (~ 1 in/s) at 0.14 MPa, 16 K subcooling and 0.88 kW/m linear power. This was the same as Test 1383, except for a decrease in pressure. Test bundles were preheated by the steam produced from the boiler and the power was turned on. When the heater rods reached a predetermined temperature, the reflood started as the liquid was injected. The collapsed liquid level is shown in Figure 3.17. The steep increase of the initial liquid level data (chan-362) at ~ 250 sec which did not show in TRACE resulted from the vaporization of the first liquid slug that was injected into the test section [12]. TRACE accurately predicted the collapsed liquid level that increased with the injected water. The collapsed liquid level with the space grid model rose faster than that without the spacer grid model.

Figures 3.18 through 3.22 represent the rod temperature at various elevations. The predictions of TRACE agreed reasonably with the RBHT data at low elevations, but consistently over-estimated the peak temperature and expedited the quenching time at higher elevations. This characteristic is also explained in Figures 3.23 through 3.25 about the HTC at various elevations. As the elevation increased, the HTCs were more under predicted at the initiating of the reflood and were more over predicted as the rod cooled. Therefore, the rod at higher elevations showed a significantly over-estimated temperature and under-estimated quenching time. When the spacer grid model was applied, the rod temperature and the HTCs show a trend similar to Test 1383. The peak rod temperature decreased significantly due to the heat transfer enhancement and then the earlier rod quenching occurred as the elevation increased. The earlier sharp growth of HTC was predicted due to the faster rod quenching in the calculation with the spacer grid model. At elevation z~2.77 with the peak power, the reduction of peak rod temperature was ~ 87.2 K and the quenching time was ~ 243 seconds earlier than that without the spacer grid model. These were the largest values in various tests. Test 1096 was a case in which all the parameters such as the reflood rate, the linear power, the subcooling degree and the system pressure had a low value. The effect of the spacer grid model was most dominant in the test matrix.

The steam temperature was predicted very well at z=1.40 m of Figure 3.26, but seems to have a faster cooling at z=1.88 m of Figure 3.27 than the RBHT data. The calculation with the spacer grid model had a slightly higher steam temperature during the reflood, which was similar to Test 1383.

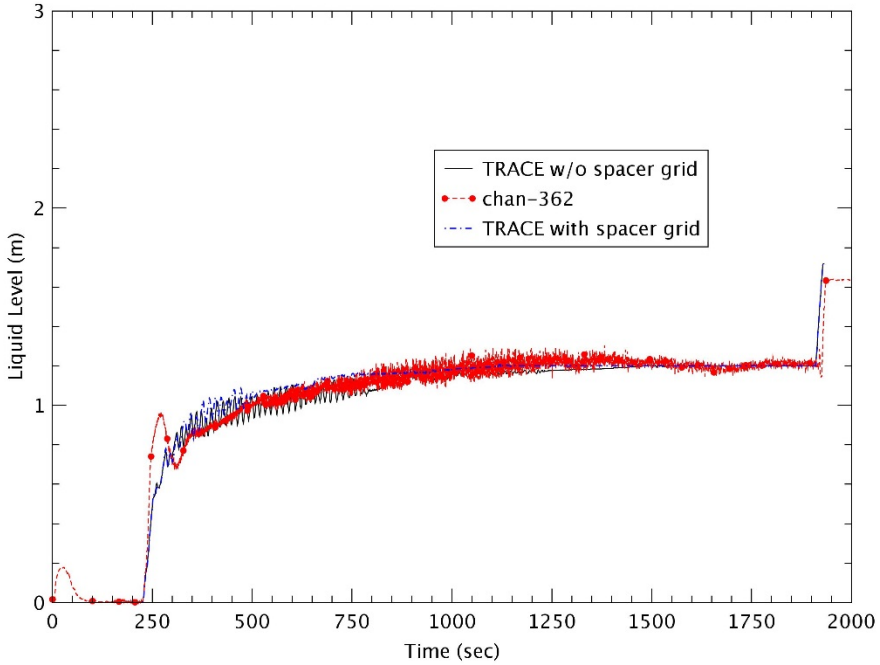

Figure 3-17 Collapsed Liquid Level – Test 1383

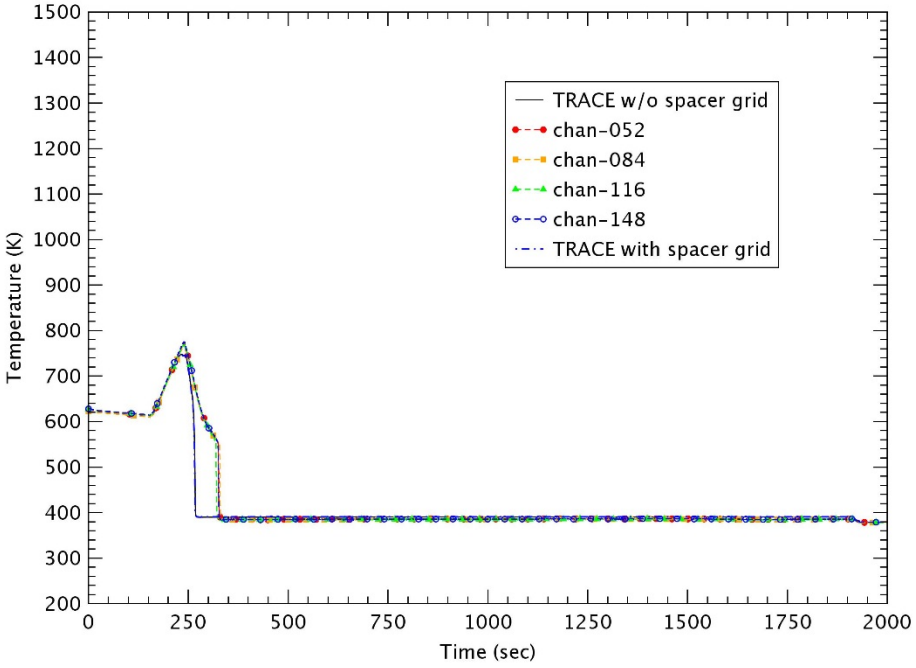

Figure 3-18 Heater Rod Temperature at 0.59 m – Test 1096

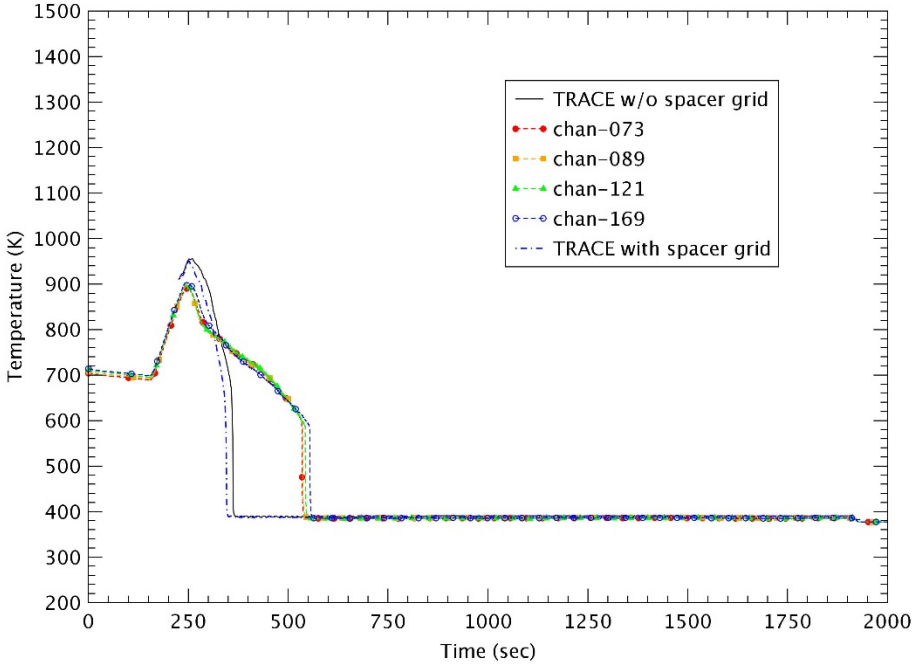

Figure 3-19 Heater Rod Temperature at 1.27 - Test 1096

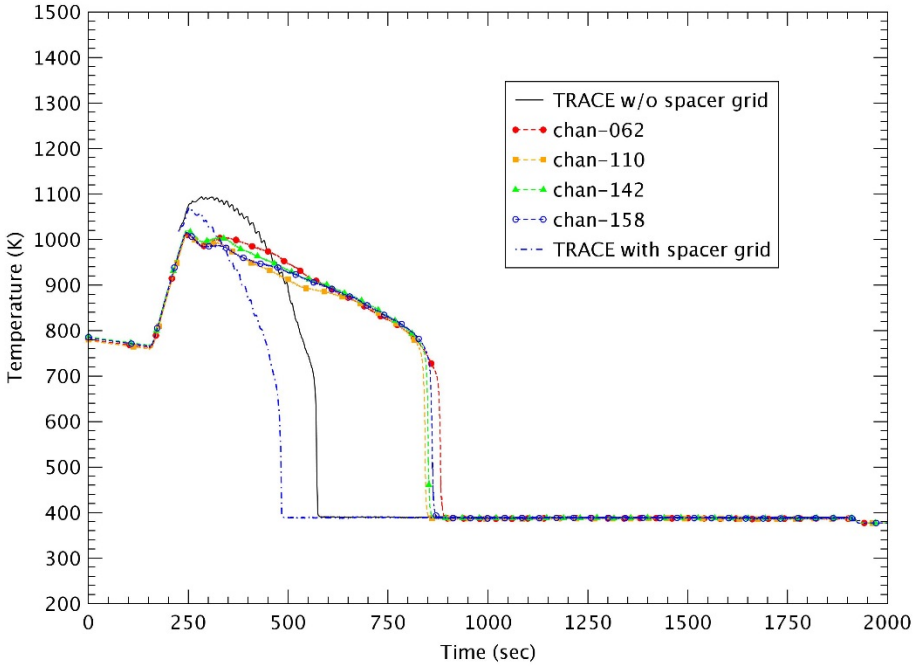

Figure 3-20 Heater Rod Temperature at 1.87 - Test 1096

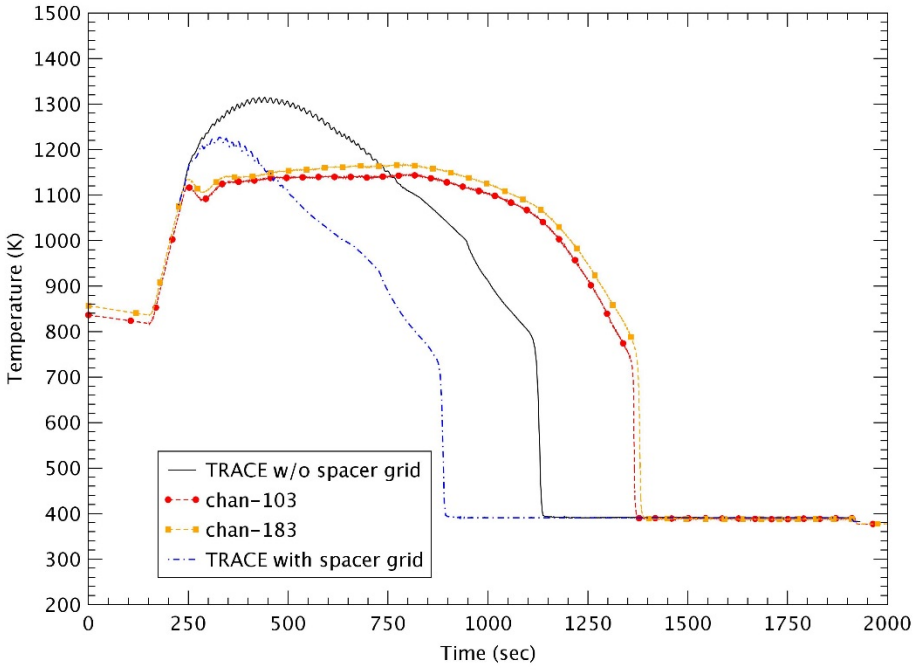

Figure 3-21 Heater Rod Temperature at 2.77 m – Test 1096

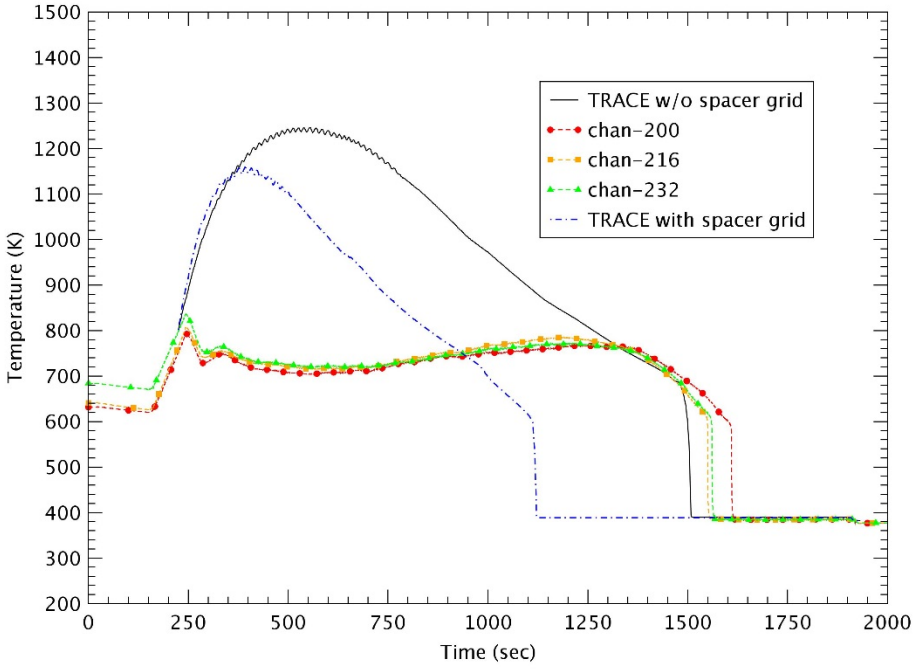

Figure 3-22 Heater Rod Temperature at 3.43 m – Test 1096

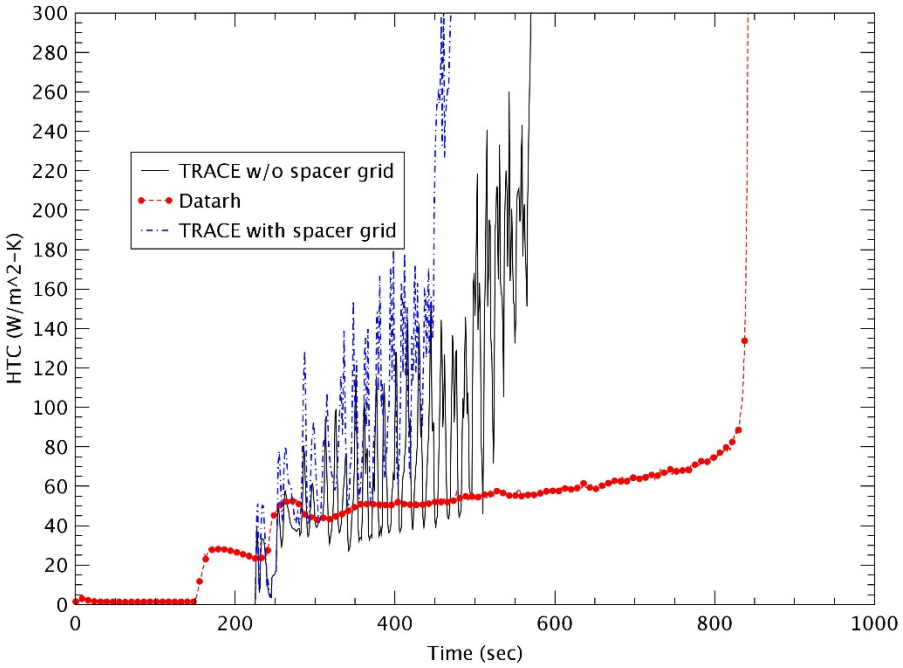

Figure 3-23 Heat Transfer Coefficient at 1.88 m – Test 1096

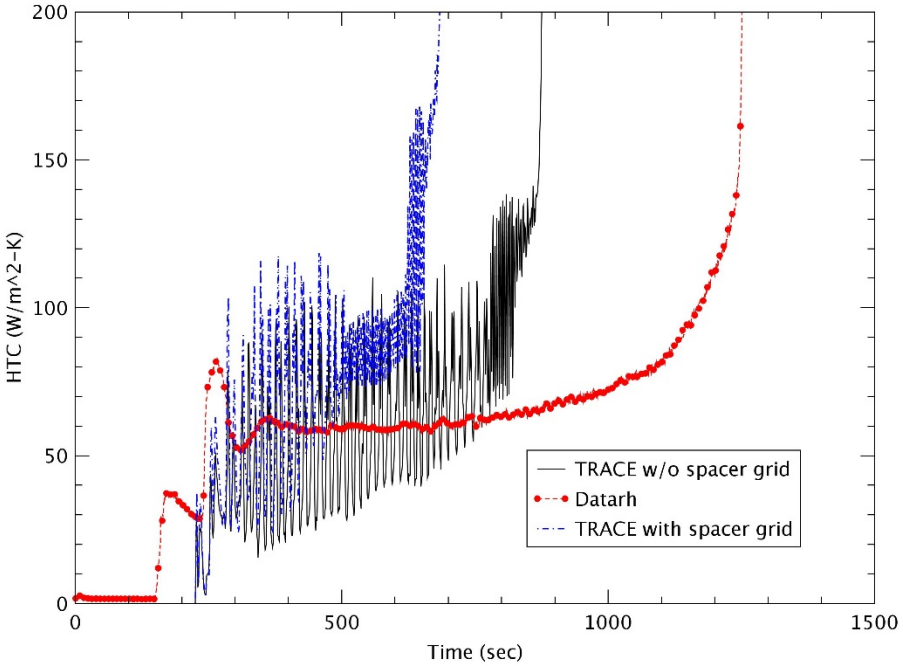

Figure 3-24 Heat Transfer Coefficient at 2.54 m – Test 1096

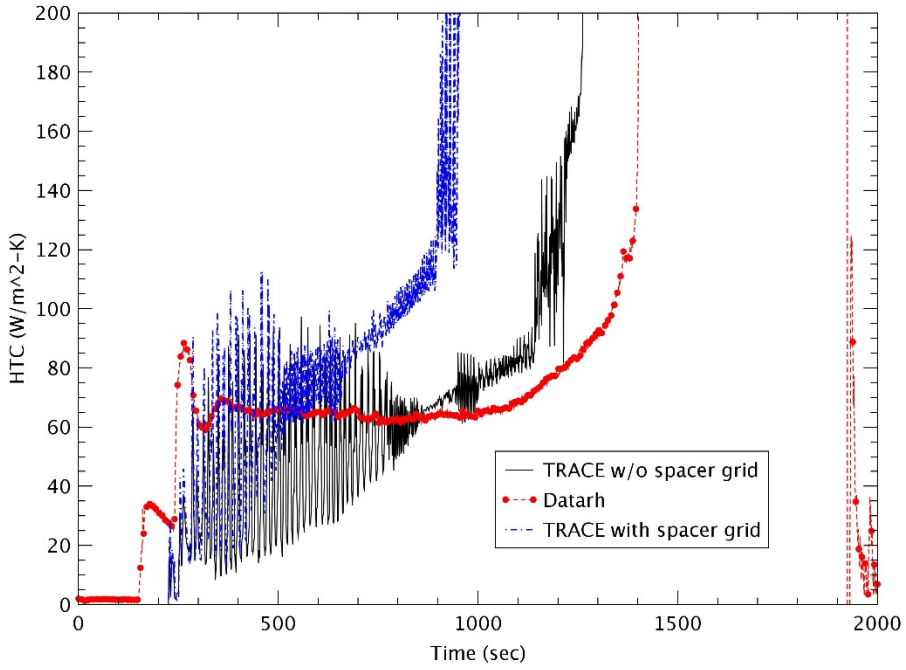

Figure 3-25 Heat Transfer Coefficient at 2.93 m – Test 1096

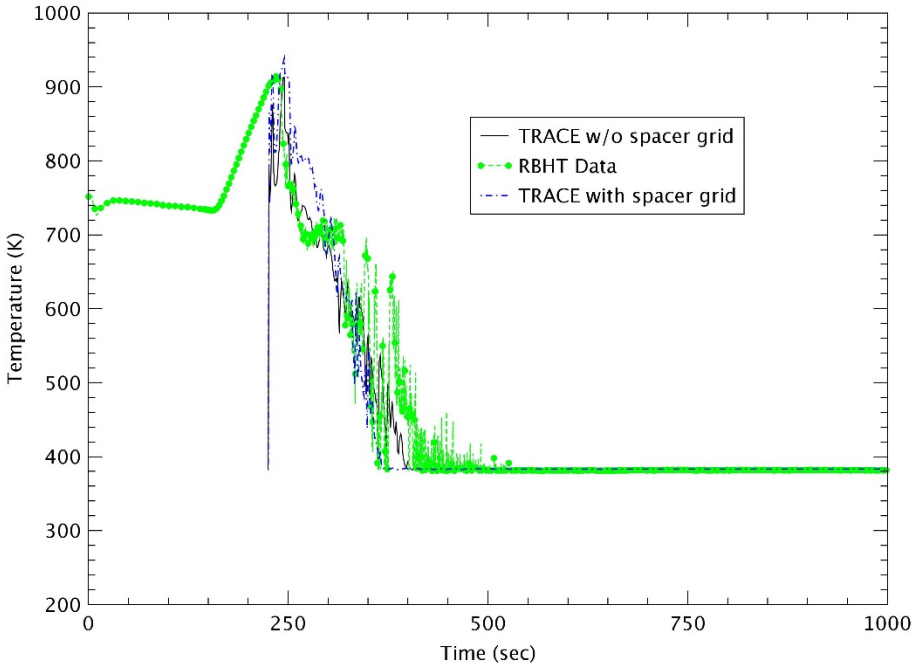

Figure 3-26 Steam Temperature at 1.40 m – Test 1096

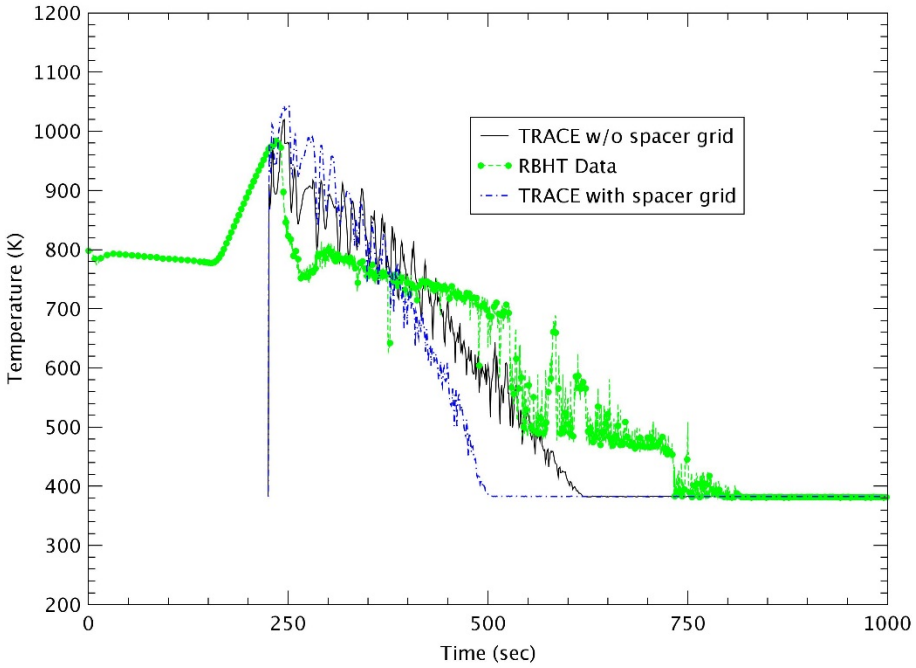

Figure 3-27 Steam Temperature at 1.88 m – Test 1096

3) Test 1108

Test 1108 was a reflood test with 0.13 kg/s (~ 1 in/s) at 0.14 MPa, 82 K subcooling and 0.88 kW/m linear power. This was the same as Test 1096 except for the subcooling degree. The test began by preheating the bundle with steam from the steam boiler. The power turned on and then when the bundle reached a predetermined temperature, the reflood water was injected into the test section. The collapsed liquid level increased steadily as the reflood proceeded and TRACE accurately predicted the experimental data as shown in Figure 3.28.

The rod temperatures at various elevations are plotted in Figures3.29 through 3.33. As only the subcooling degree increased compared to Test 1096, the lower peak rod temperature and the earlier quenching are shown in comparison with Test 1096, as expected. As in Tests 1383 and 1096, the prediction of TRACE consistently showed a higher peak rod temperature and earlier quenching times at higher elevations for the RBHT data. However, compared to Test 1096, TRACE showed a little better prediction for the peak rod temperature at elevation z~2.77 of the peak power. The HTCs of TRACE had results consistent with previous Tests as shown in Figures 3.34 through 3.36. As the spacer grid model was used, the peak rod temperature decreased and the rod was quenched earlier. The steep increase in HTC appeared earlier than the case without the spacer grid model. At elevation z~2.77 with the peak power, the decreasing amount of peak rod temperature was ~ 56.0 K and the reduction of quenching time was ~ 76 sec due to the spacer grid model. For Test 1108, the single-phase convection heat transfer was larger than that for Test 1096 due to the increase in subcooling and then the rod without the spacer grid model had a lower temperature than Test 1096. Therefore, the differences for the peak temperature and the quenching time decreased as compared to Test 1096.

The steam temperature at two elevations are shown in Figures 3.37 and 3.38. The predictions of TRACE agreed well with the RBHT data at two elevations. When the spacer grid model was used, the steam temperature had slightly higher values during the reflood.

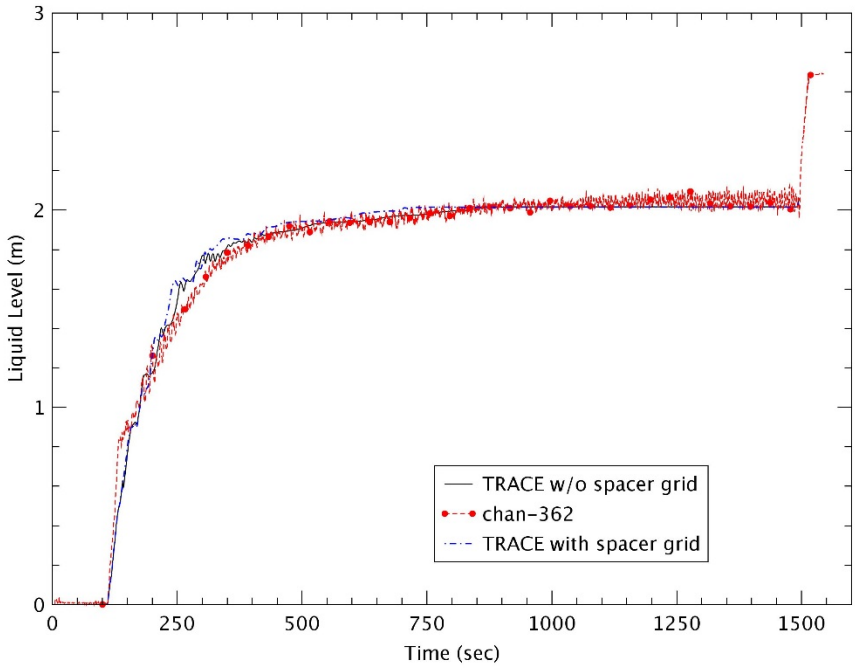

Figure 3-28 Collapsed Liquid Level – Test 1108

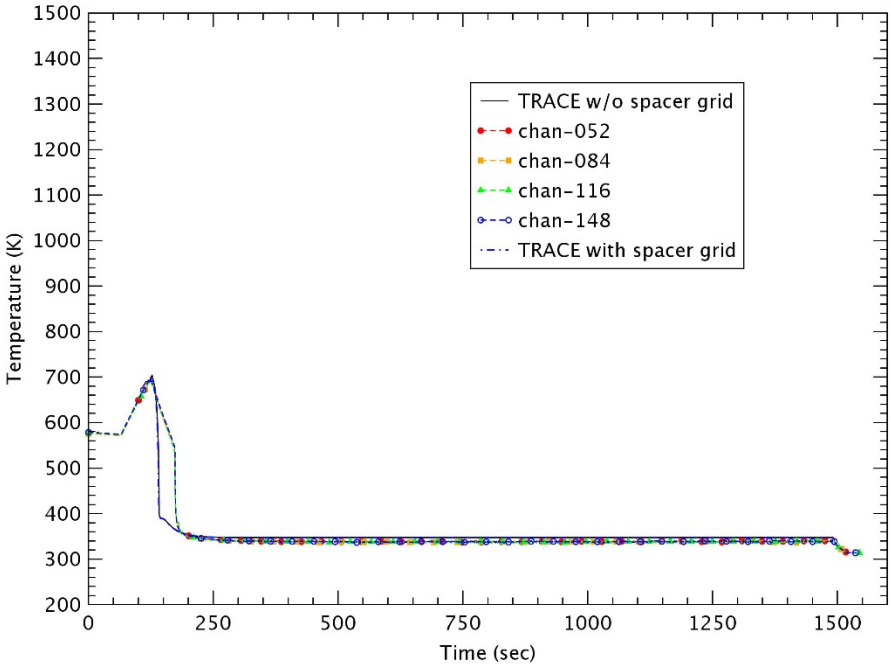

Figure 3-29 Heater Rod Temperature at 0.59 m – Test 1108

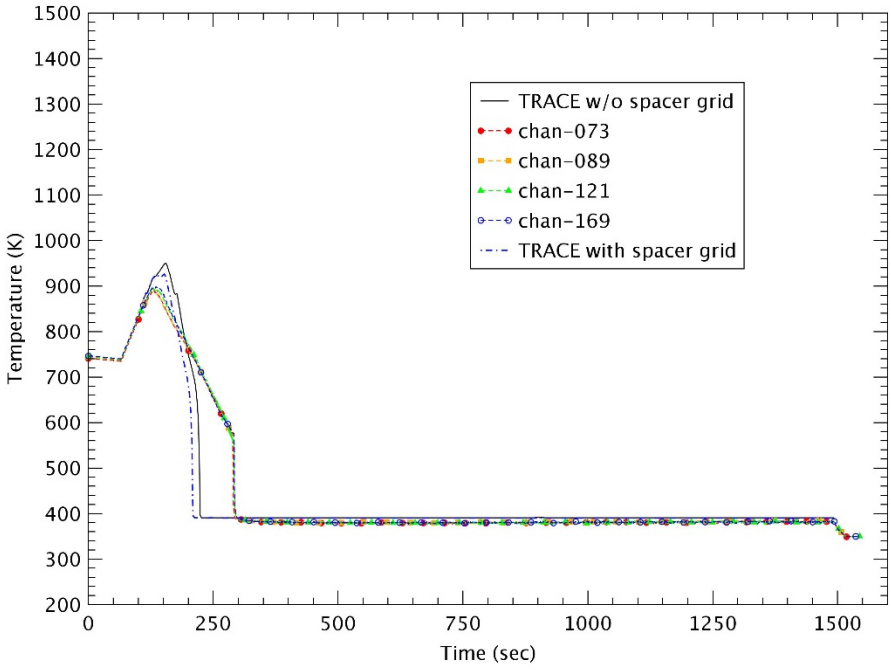

Figure 3-30 Heater Rod Temperature at 1.27 m – Test 1108

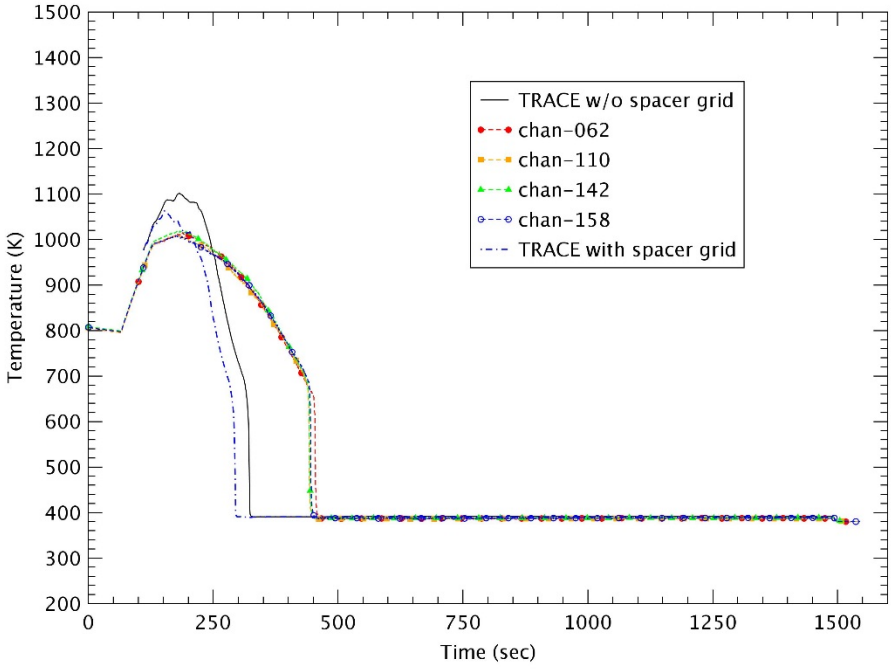

Figure 3-31 Heater Rod Temperature at 1.87 m – Test 1108

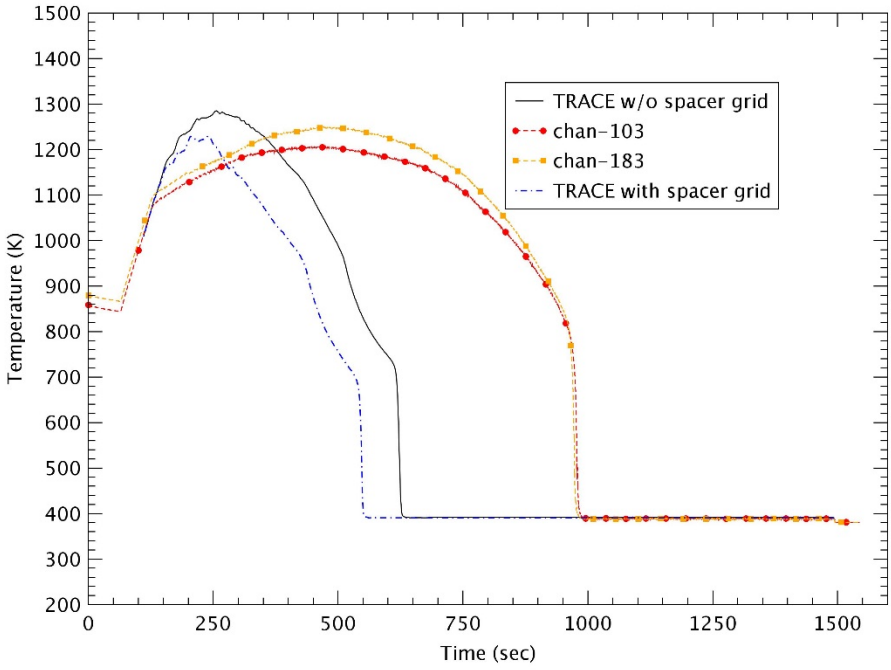

Figure 3-32 Heater Rod Temperature at 2.77 m – Test 1108

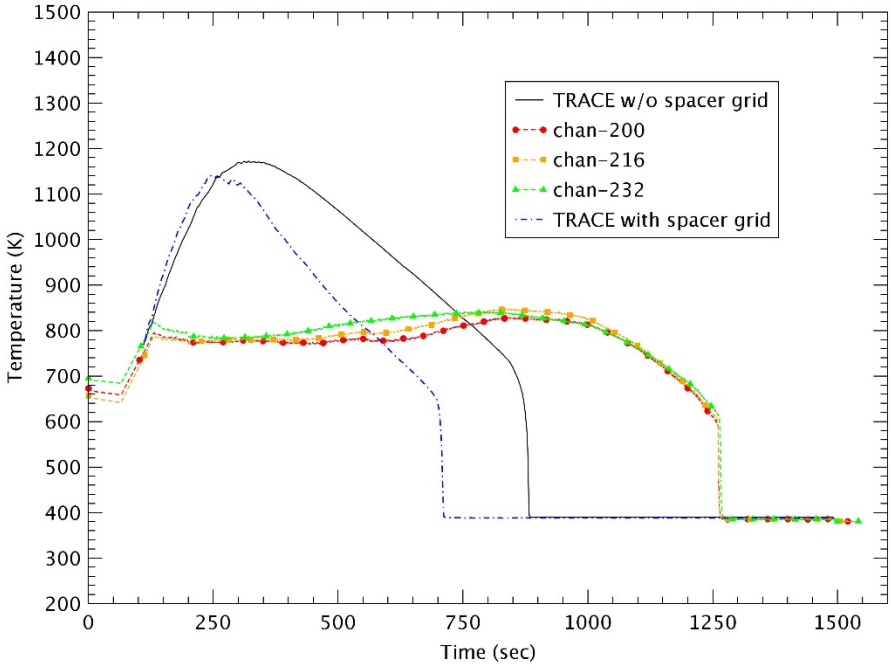

Figure 3-33 Heater Rod Temperature at 3.43 m – Test 1108

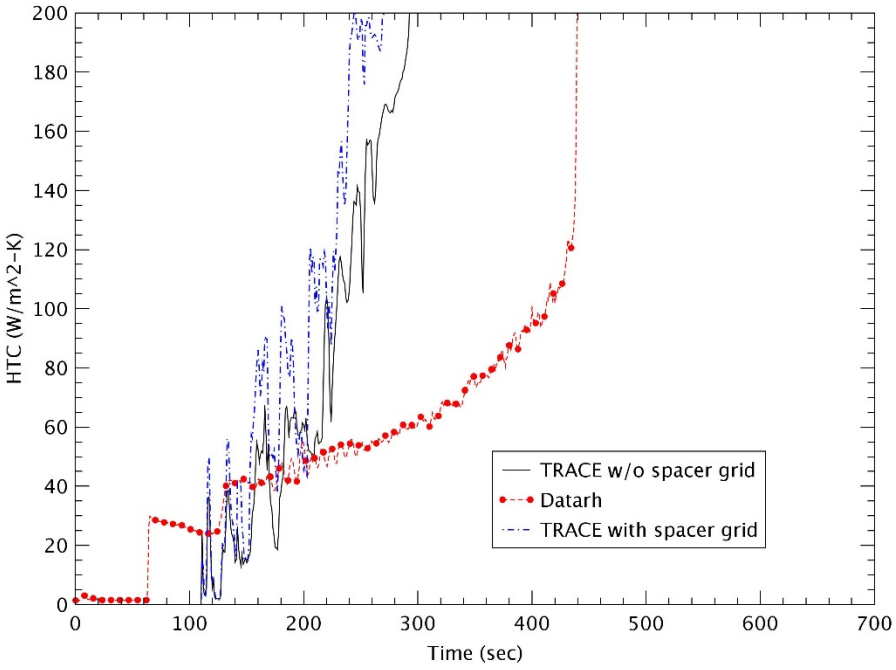

Figure 3-34 Heat Transfer Coefficient at 1.88 m – Test 1108

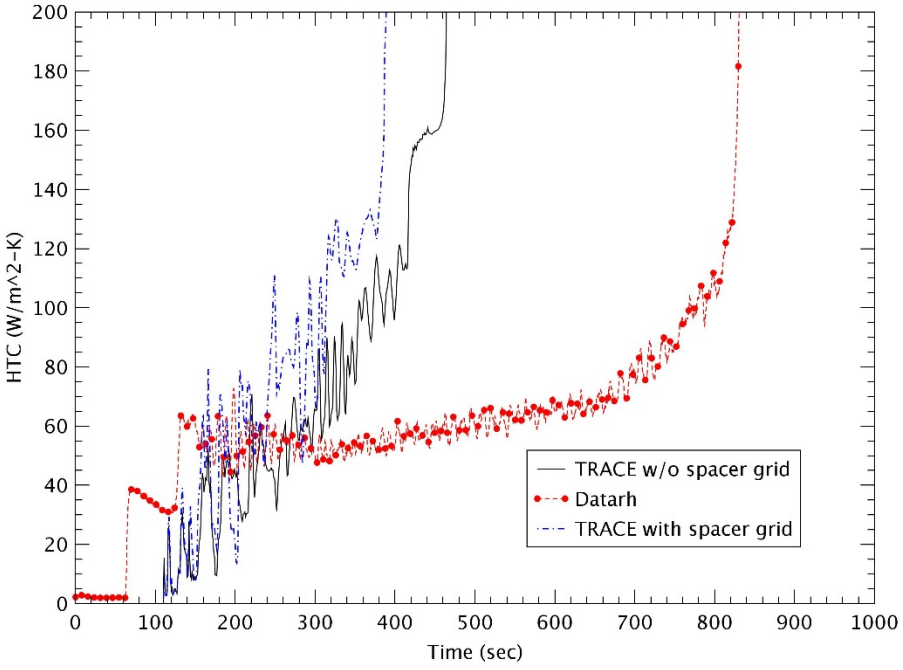

Figure 3-35 Heat Transfer Coefficient at 2.54 m – Test 1108

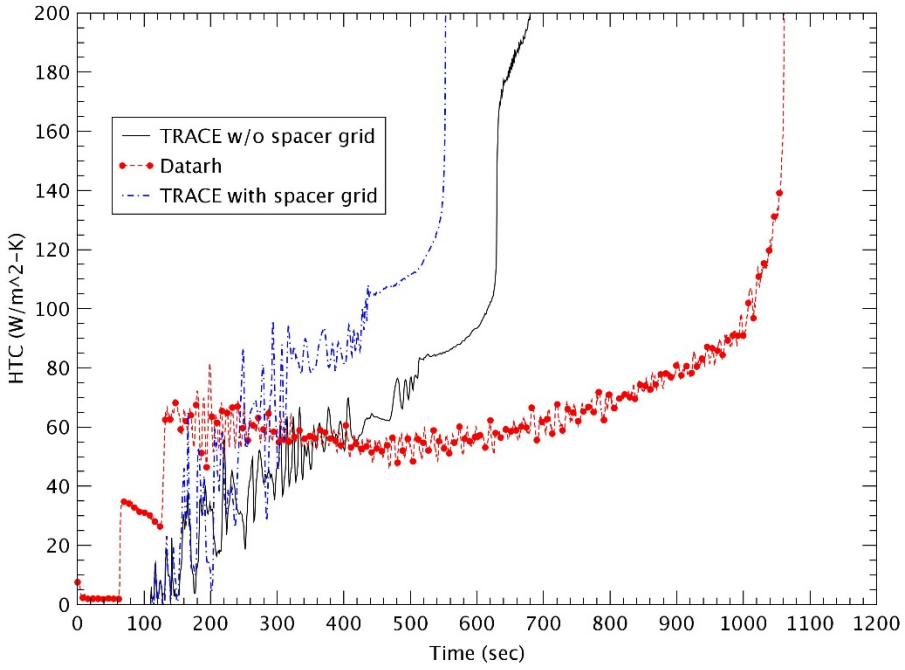

Figure 3-36 Heat Transfer Coefficient at 2.93 m – Test 1108

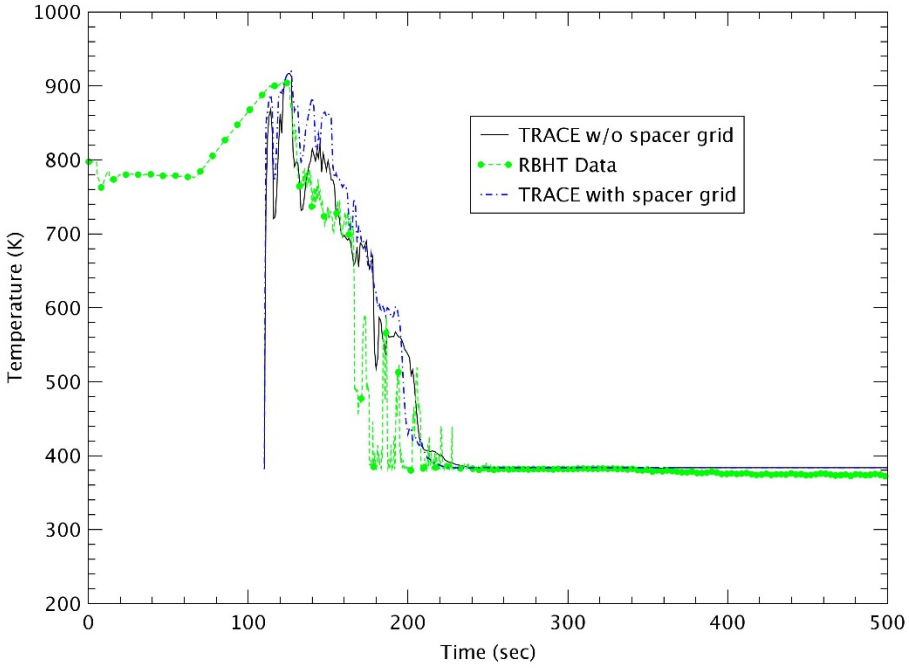

Figure 3-37 Steam Temperature at 1.40 m – Test 1108

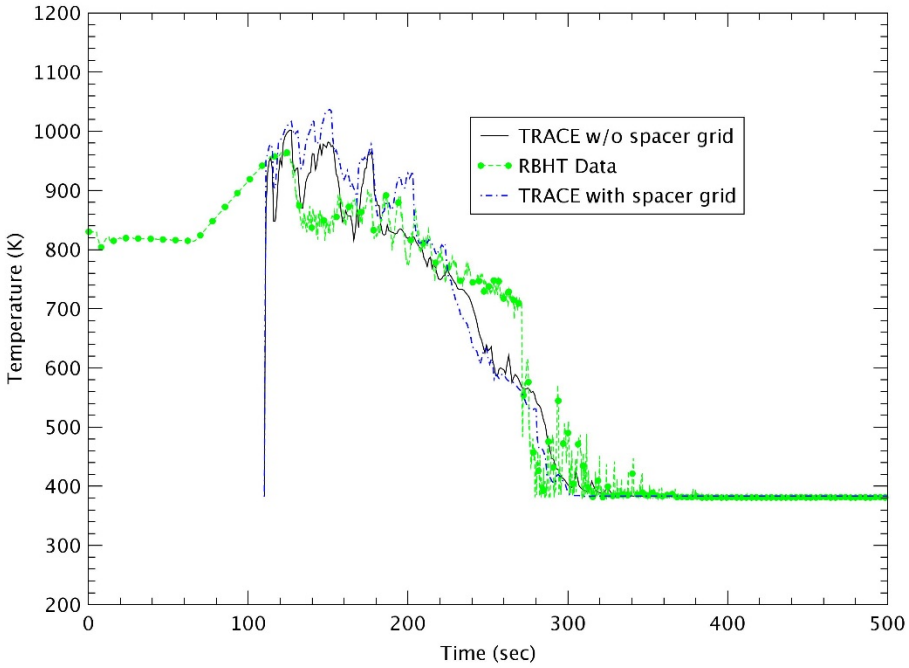

Figure 3-38 Steam Temperature at 1.88 m – Test 1108

4) Test 1170

Test 1170 was the first of three high power and high reflood rate cases in the test matrix of Table 3.3. Test 1170 was a reflood test with 0.75 kg/s (~ 6 in/s) at 0.28 MPa, which was a relatively high pressure and high reflooding rate, 16 K subcooling and 1.53 kW/m linear power.

This was the same as Test 1383 except for the reflood rate and the linear power. As in other tests, the test began by preheating the bundle with steam from the steam boiler. The power turned on and then when the bundle reached a predetermined temperature, the reflood water was injected into the test section.

Figure 3.39 gives the collapsed liquid level and shows that TRACE significantly under-predicted the liquid level. At the initiating time of reflood, the sharp increase in the liquid level could have been due to the strong rod quenching in the lower bundle due to sudden large water injection as shown in Figure 3.40. This would cause the large steam flow and the sudden increase of pressure in Figure 3.41. After that, the liquid level was fairly stable despite the large fluctuation of pressure, except for the initial increment. This phenomena was more common in the high power and the high reflood rate tests. The high liquid level for all times of the test was the unique characteristic of Test 1170, which resulted in the rod temperature and the HTCs. In the case with the spacer grid model, the earlier increase in the collapsed liquid level is shown in Figure 3.39.

Although TRACE under-estimated the collapsed liquid level, the rod temperatures were predicted reasonably well up to z=1.85 m as shown in Figures 3.42 through 3.46. The rod peak temperature had good prediction at all elevations. However, unusually, the rod quenching time was significantly over predicted at higher elevations (z >2.77 m), which was different from the results of the other tests. The delay prediction for the quenching time resulted from the high collapsed liquid level of the experiment. When the spacer grid model was used, the peak rod

temperature did not decrease much and the rod was quenched earlier. The small change in the peak temperature might have been induced from the short heat up period and the fast growth of the liquid level due to the high reflood rate, which was the characteristic in the high reflood tests. At elevation z~2.77 with the peak power, the peak rod temperature increased to ~ 1.2 K and the reduction of quenching time was ~ 114 sec due to the spacer grid model.

The HTCs at various elevations are plotted in Figures3.47 through 3.49. For Test 1170 with high power and high reflood rate, the HTCs of TRACE had better prediction results during the reflood period. The increase in HTCs at some elevations agreed well with the RBHT data at the beginning of the reflood. However, the steep growth of HTCs for the quenching was predicted at a later time due to the delay prediction of quenching. When the spacer grid model was applied, a steep increase in HTC was expedited since the earlier rod quenching occurred due to the enhancement of convective heat transfer.

The steam temperature at two elevations are shown in Figures 3.50 and 3.51. TRACE over-estimated the steam temperature for all times of the test, which is consistent with the trends of the rod temperature and HTCs. In Test 1170, the steam in the test was quenched earlier due to the high liquid level and then the rapid drop of rod temperature occurred after arriving at the peak rod temperature.

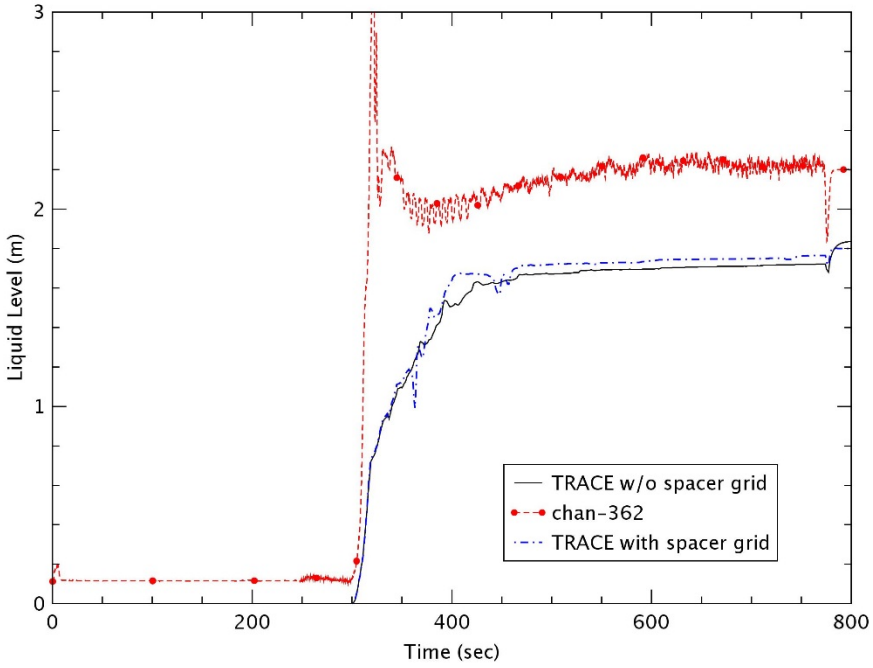

Figure 3-39 Collapsed Liquid Level – Test 1170

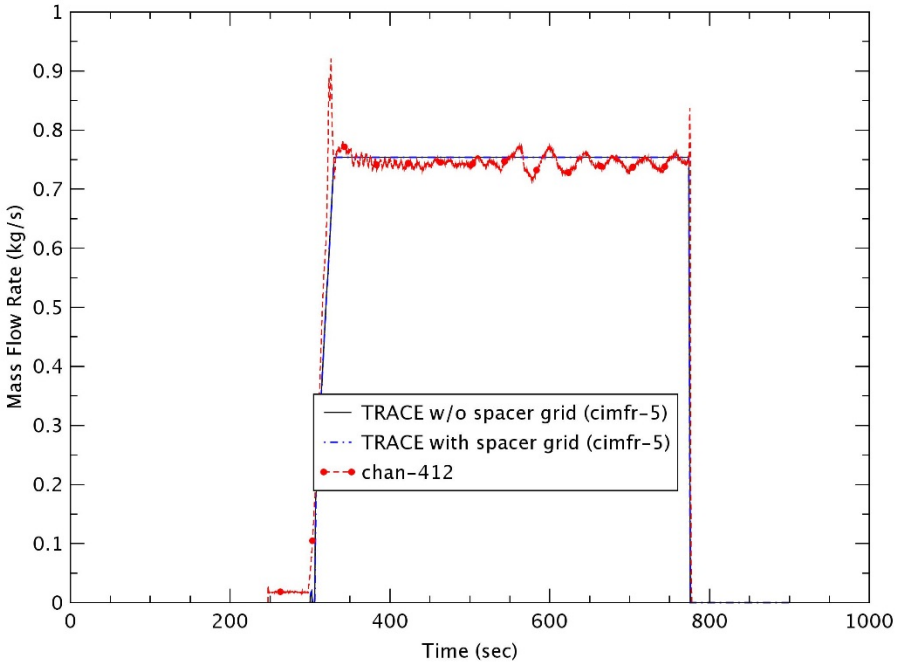

Figure 3-40 Liquid Injection Flowrate – Test 1170

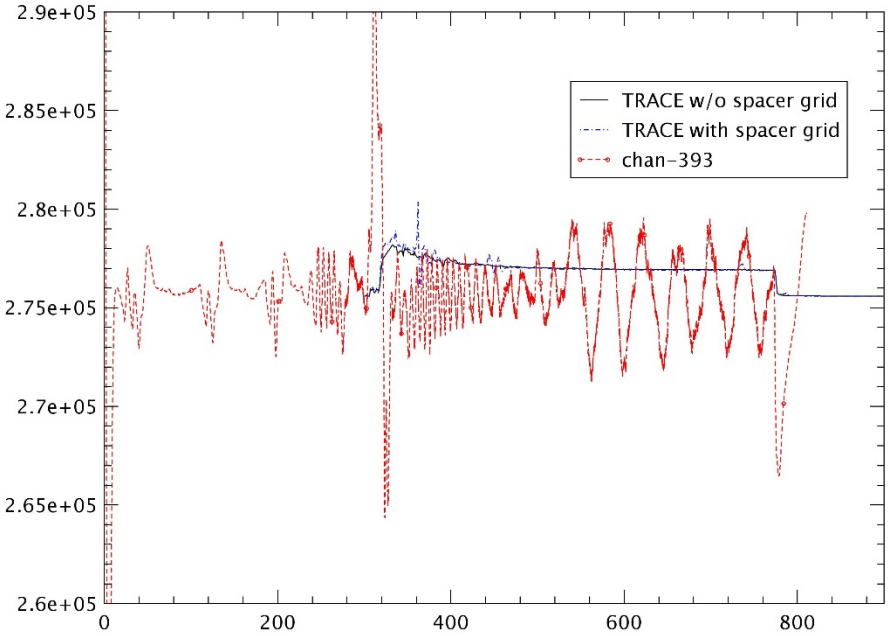

Figure 3-41 Upper Plenum Pressure – Test 1170

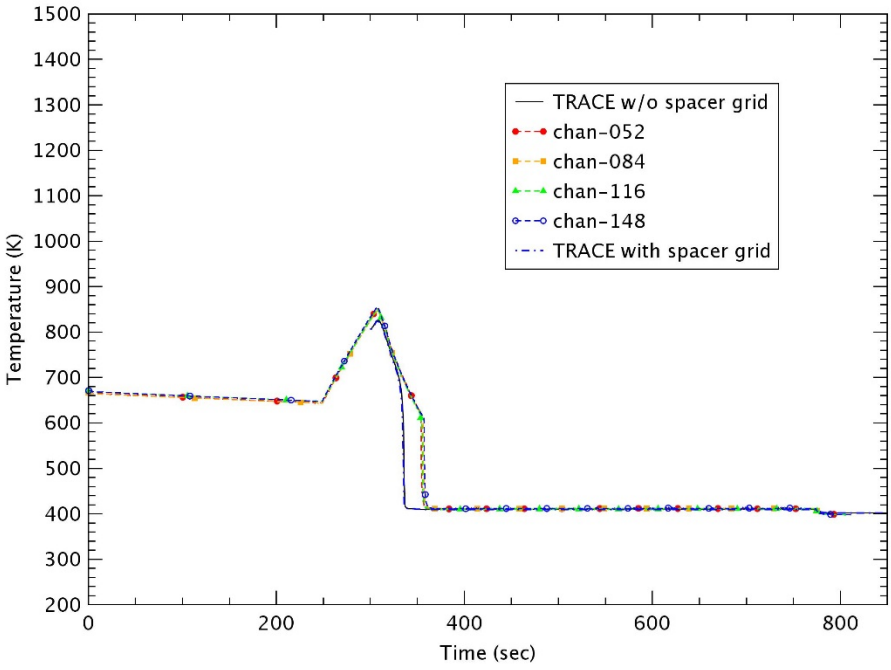

Figure 3-42 Heater Rod Temperature at 0.59 m – Test 1170

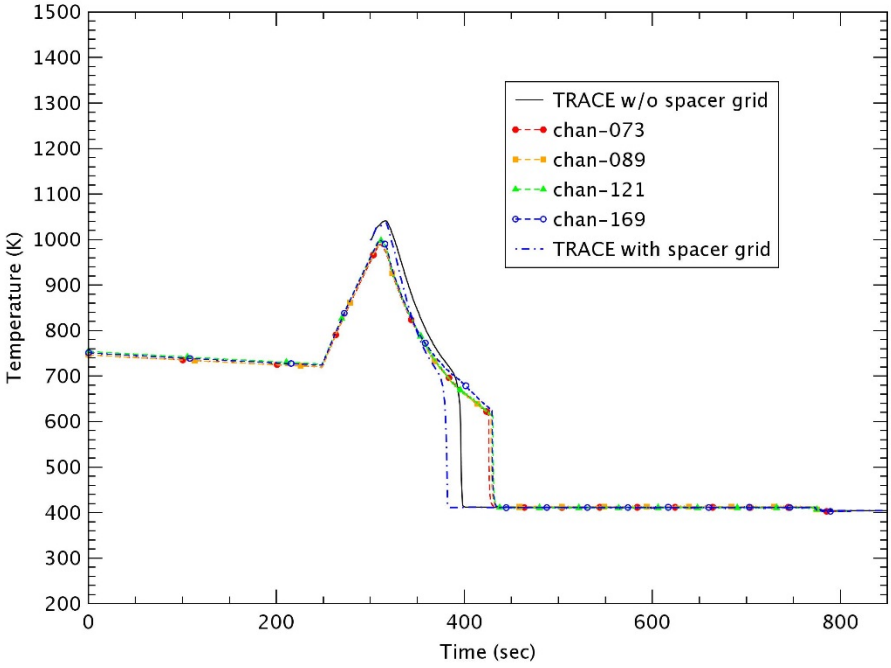

Figure 3-43 Heater Rod Temperature at 1.27 m – Test 1170

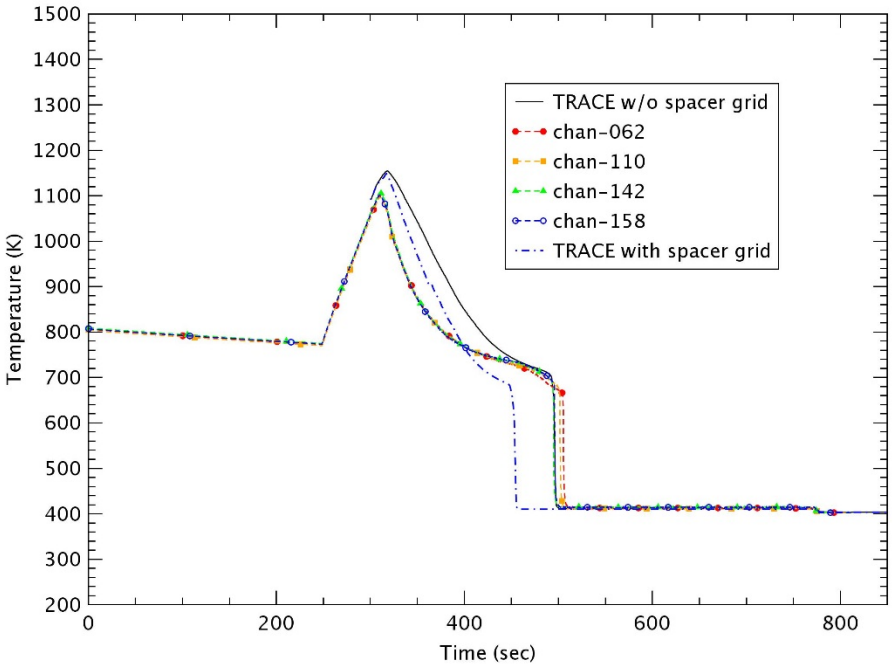

Figure 3-44 Heater Rod Temperature at 1.87 m – Test 1170

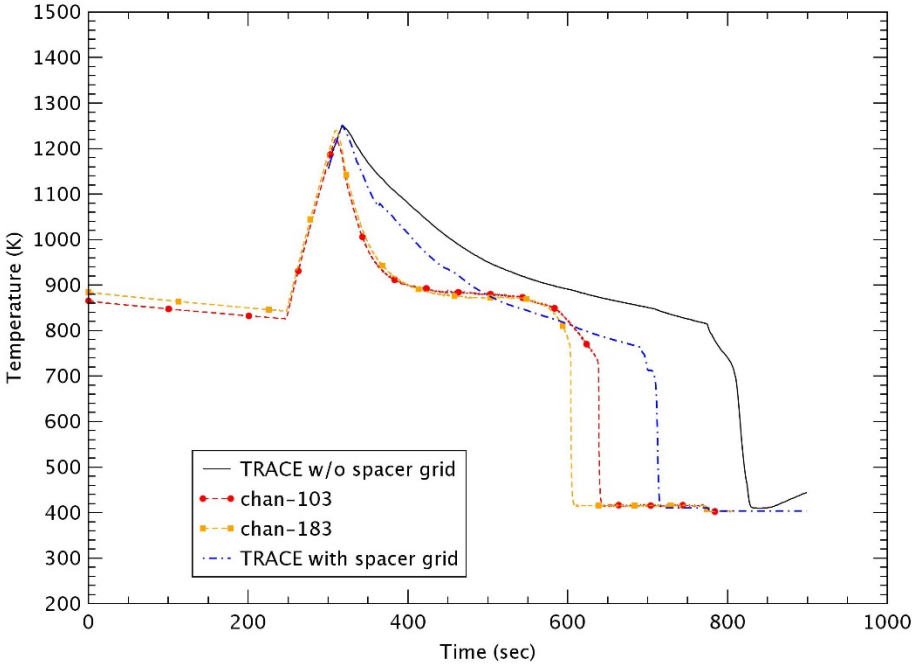

Figure 3-45 Heater Rod Temperature at 2.77 m – Test 1170

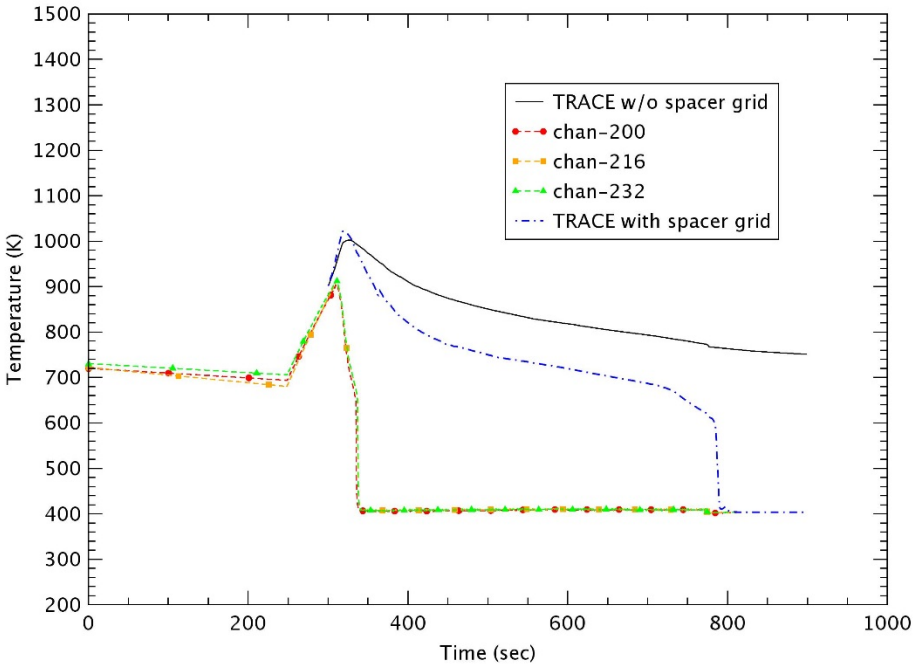

Figure 3-46 Heater Rod Temperature at 3.43 m – Test 1170

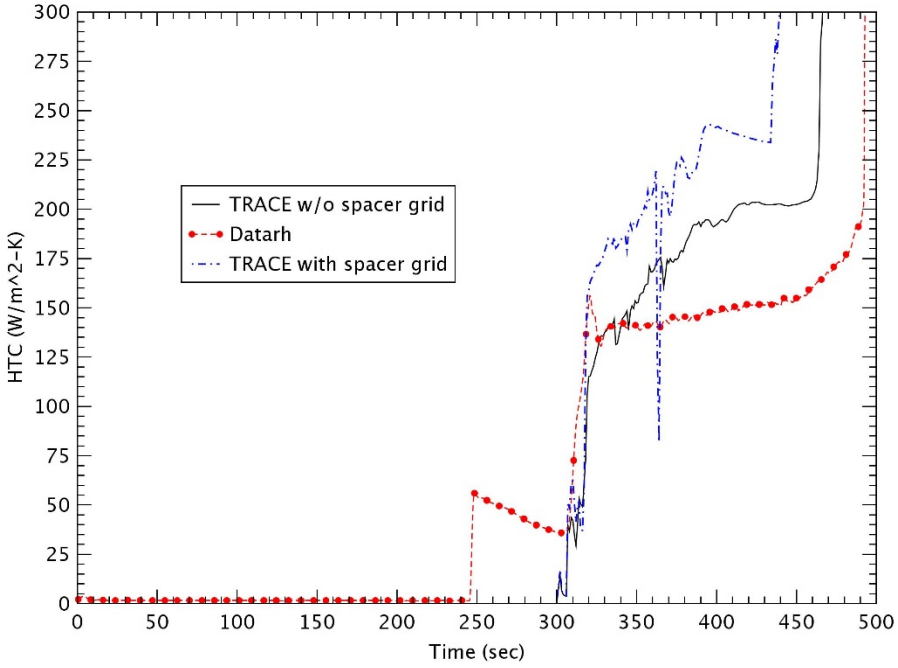

Figure 3-47 Heat Transfer Coefficient at 1.88 m – Test 1170

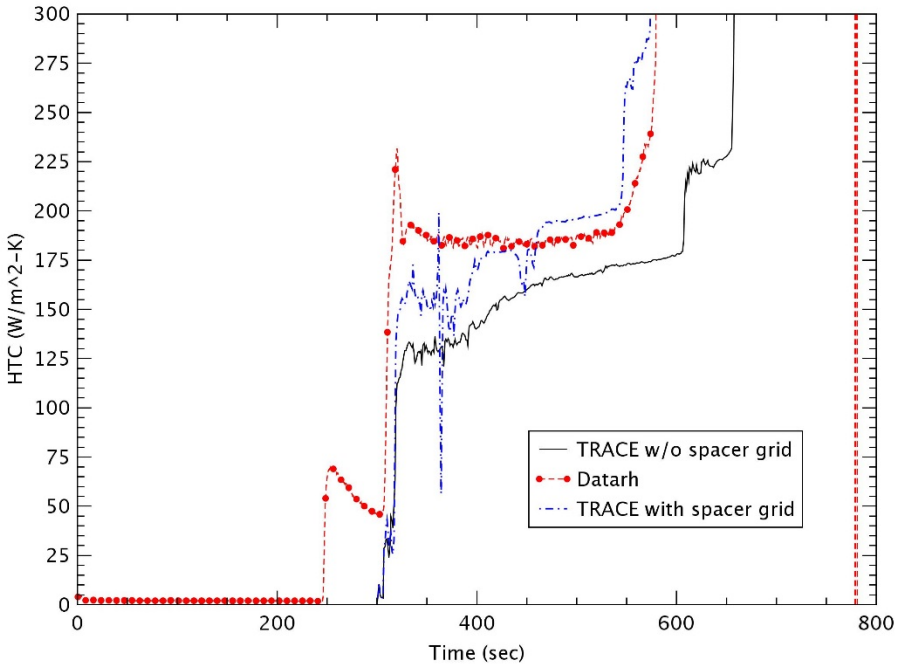

Figure 3-48 Heat Transfer Coefficient at 2.54 m – Test 1170

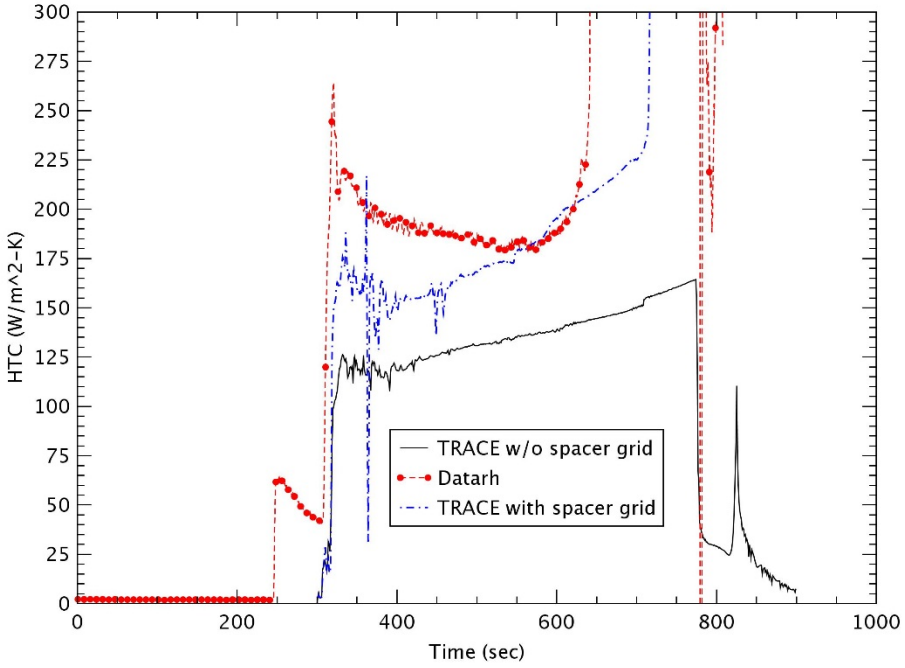

Figure 3-49 Heat Transfer Coefficient at 2.93 m – Test 1170

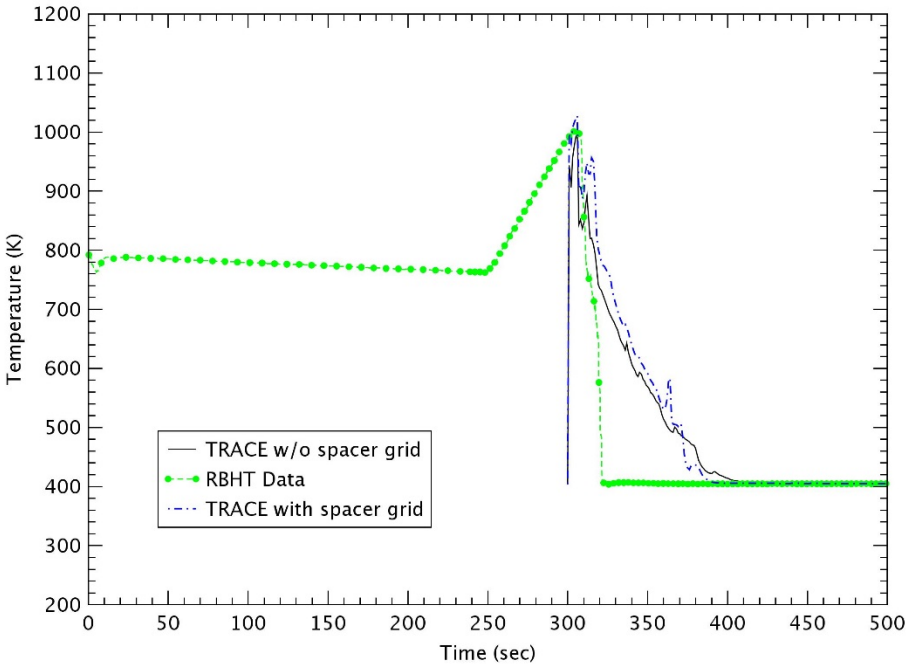

Figure 3-50 Steam Temperature at 1.40 m – Test 1170

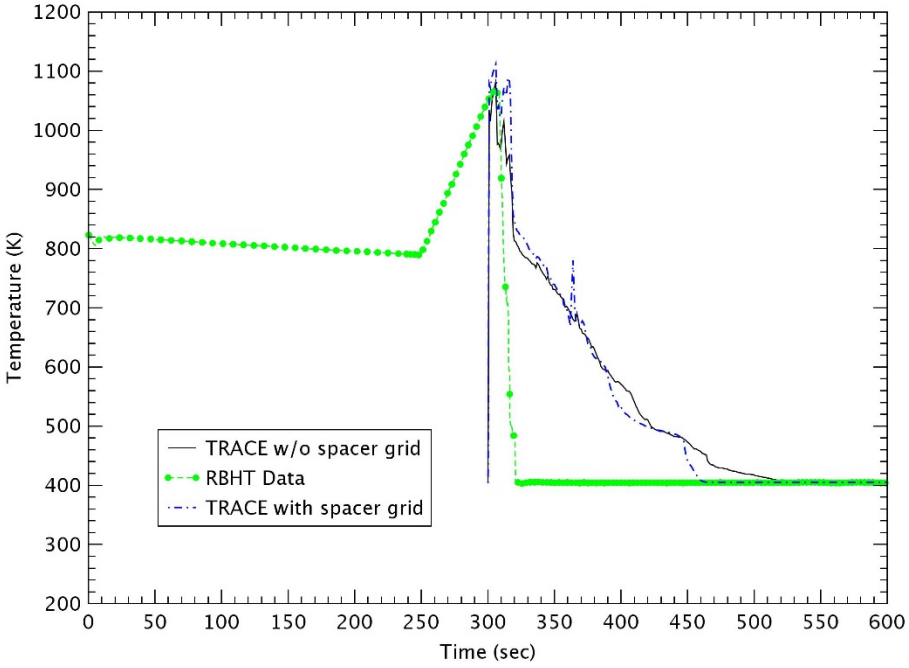

Figure 3-51 Steam Temperature at 1.88 m – Test 1170

5) Test 1196

Test 1196 was a reflood test with 0.74 kg/s (~ 6 in/s) at 0.28 MPa, 59 K subcooling and 1.53 kW/m linear power. This was the same as Test 1170 except for a 43 K increase in the subcooling degree. The test procedures were the same as the other tests. The collapsed liquid level is plotted in Figure 3.52. As in Test 1170, the sudden rise in the liquid level was observed in this test and TRACE under predicted the collapsed liquid level during the beginning of reflood. After that, TRACE had a good prediction result for the collapsed liquid level. When the spacer grid model was applied, the change in the liquid level was not large and the collapsed liquid level increased a little faster than without the spacer grid model.

The rod temperature at various elevations is illustrated in Figures 3.53 through 3.57. The prediction of TRACE for the peak rod temperature and the quenching time agreed well with the RBHT data at lower elevations. However, with a higher elevation, the higher peak rod temperatures and the earlier quenching times were estimated for the experimental data. The rod temperature trend at ~ 3.43 m elevation was not predicted well during the reflood period (300 sec < t < 500 sec). In the case with a spacer grid model, the lower rod temperature and earlier quenching time were calculated, but the peak rod temperature was not significantly modified as in Test 1170. At elevation z~2.77 with the peak power, the reduction of peak rod temperature was ~ 4.4 K and the decrease in amount of quenching time was ~ 24 sec by the spacer grid model.

Figures 3.58 through 3.60 show the HTC behaviors at various elevations. As in Test 1170, the HTC had better prediction results at the initiating time of the reflood. When the rod was cooled, the earlier sharp increase in HTCs was estimated owing to the earlier rod quenching. When the spacer grid model was used, the steep growth of HTC was expedited due to the faster rod quenching.

The steam temperature at two elevations are plotted in Figures 3.61 and 3.62. TRACE over-estimated the steam temperature as in Test 1170, which is consistent with the trends of the rod temperature and HTCs. At the time of initiating reflood, the high liquid level influenced other parameters such as the rod temperature, HTCs and the steam temperature. This resulted in the rapid decrease of rod temperature after the peak rod temperature.

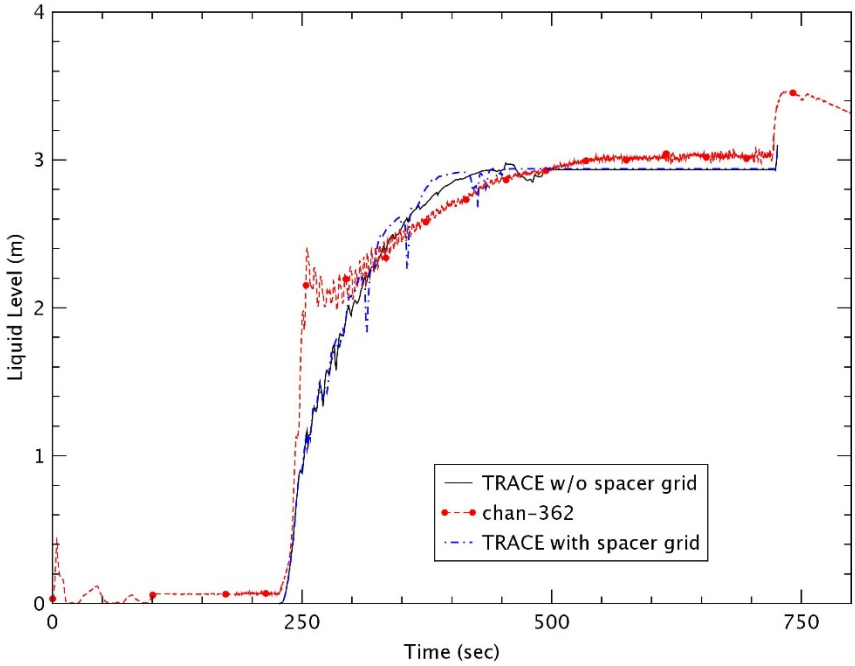

Figure 3-52 Collapsed Liquid Level – Test 1196

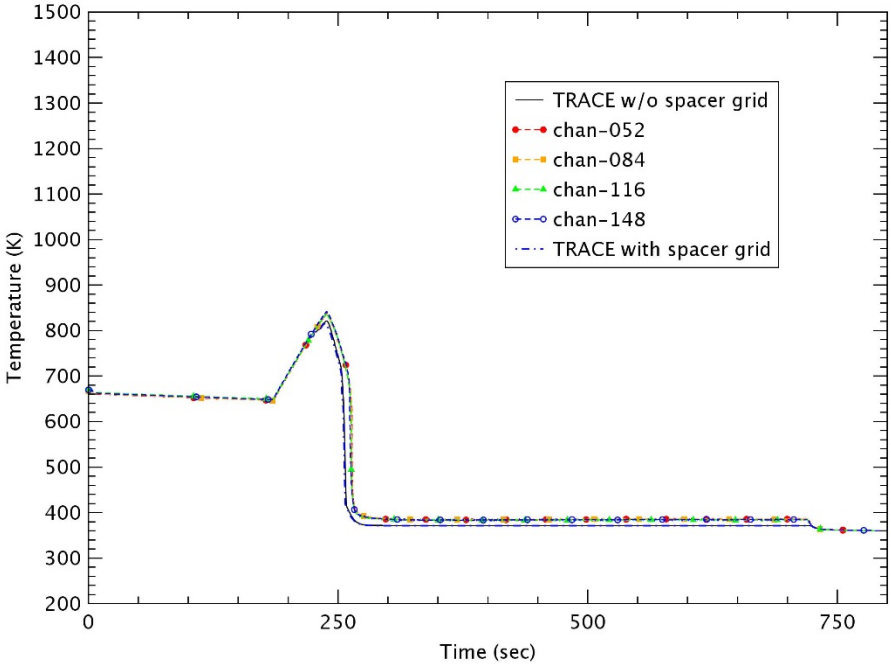

Figure 3-53 Heater Rod Temperature at 0.59 m – Test 1196

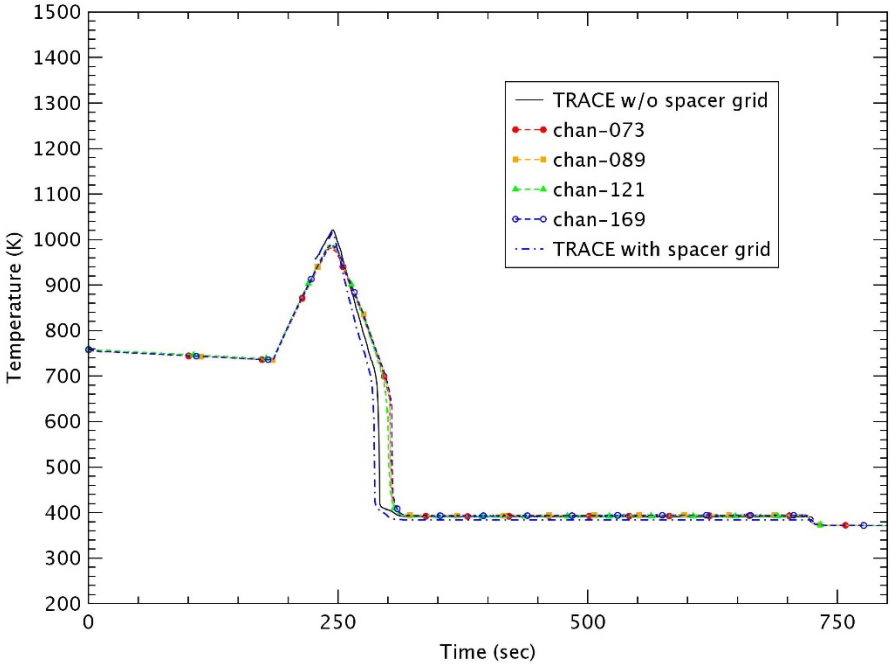

Figure 3-54 Heater Rod Temperature at 1.27 m – Test 1196

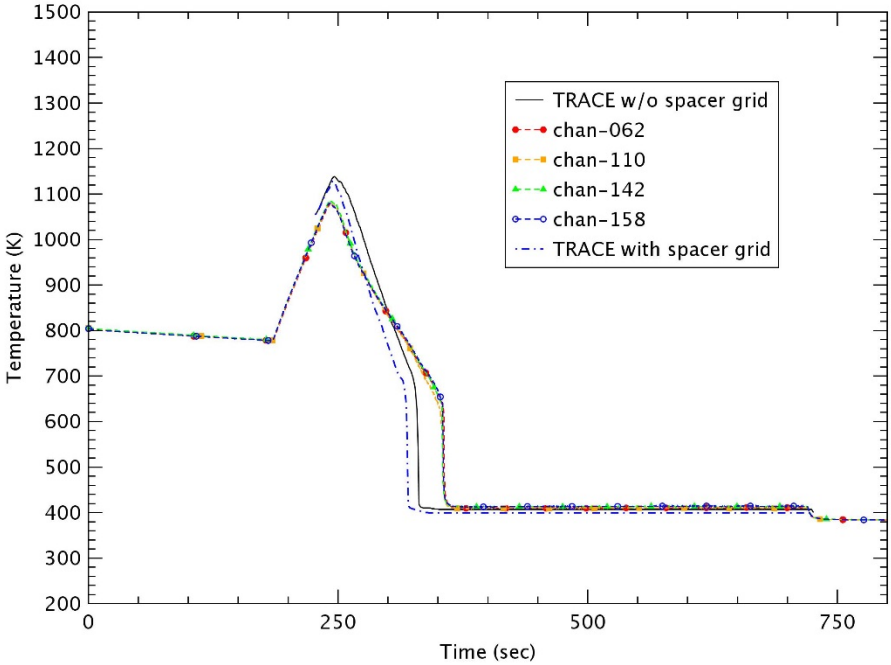

Figure 3-55 Heater Rod Temperature at 1.87 m – Test 1196

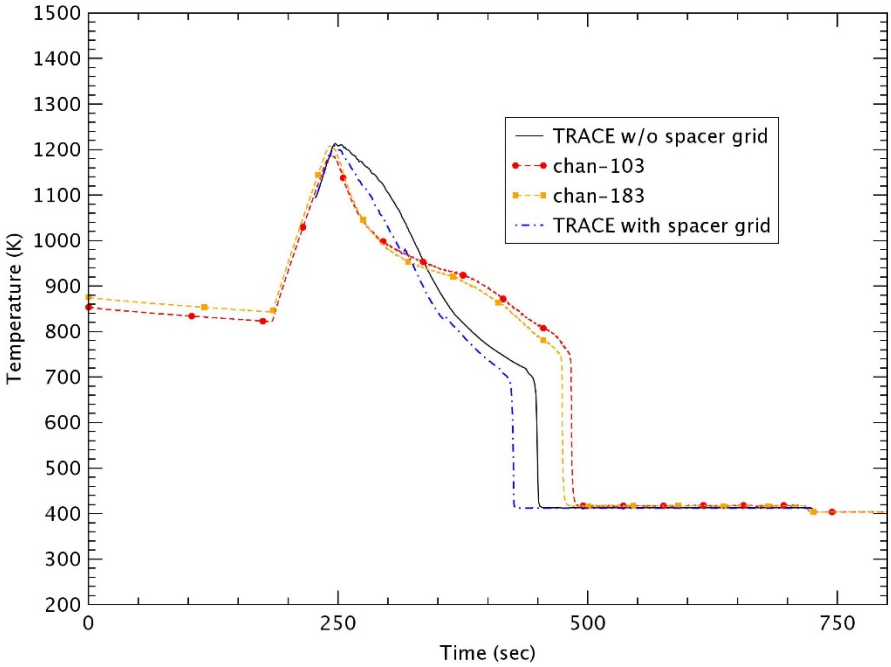

Figure 3-56 Heater Rod Temperature at 2.77 m – Test 1196

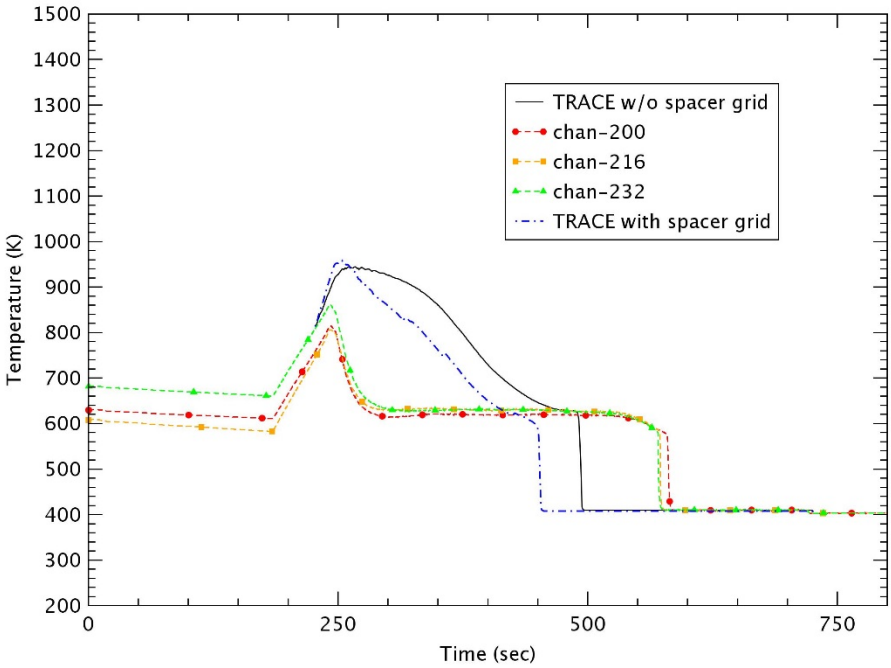

Figure 3-57 Heater Rod Temperature at 3.43 m – Test 1196

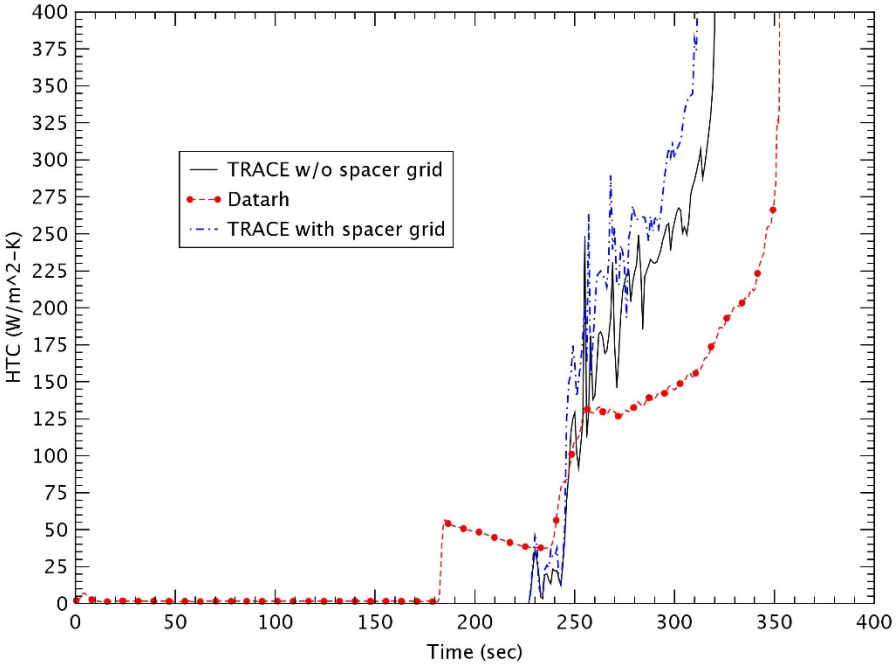

Figure 3-58 Heat Transfer Coefficient at 1.88 m – Test 1196

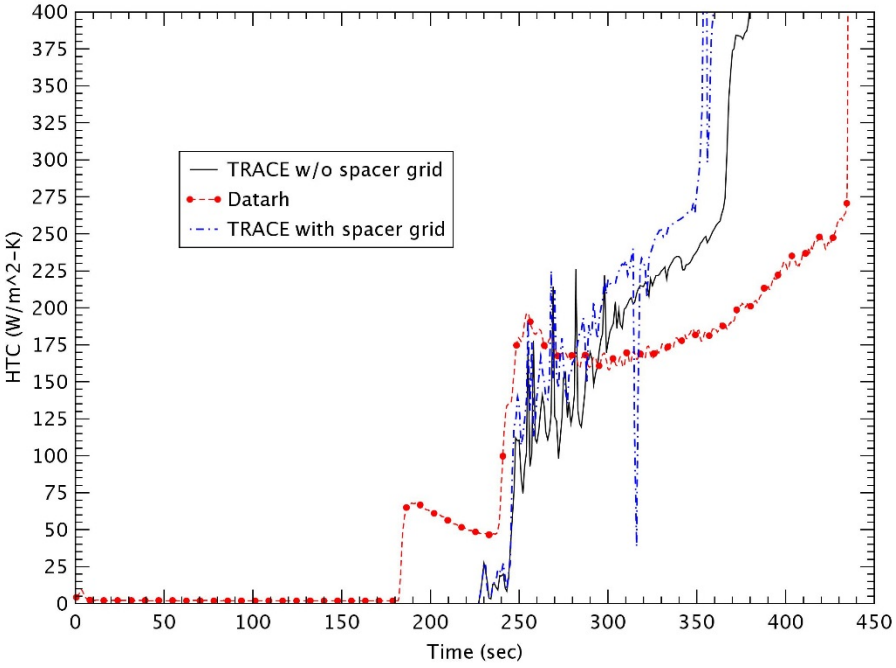

Figure 3-59 Heat Transfer Coefficient at 2.54 m – Test 1196

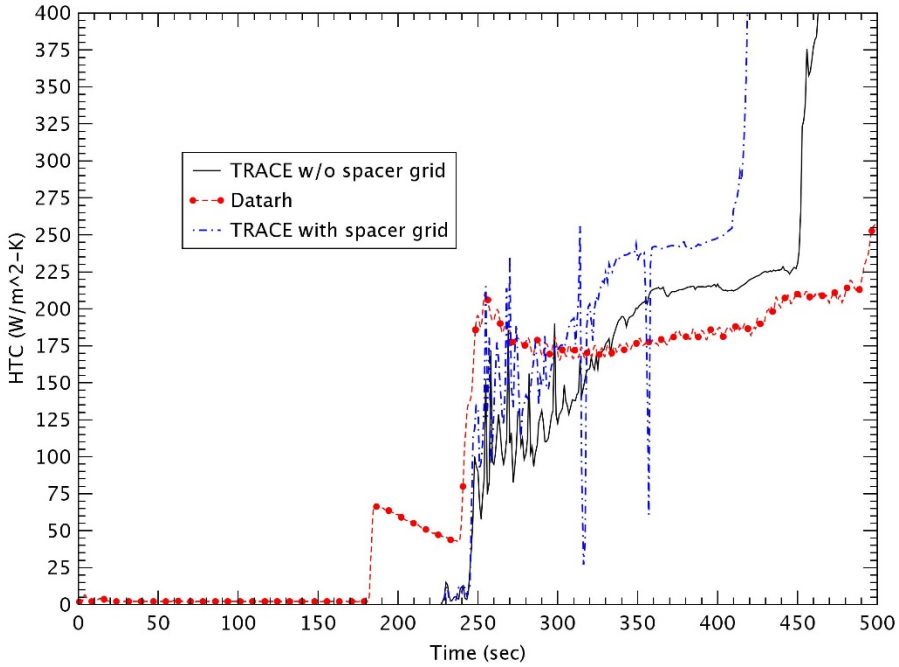

Figure 3-60 Heat Transfer Coefficient at 2.93 m – Test 1196

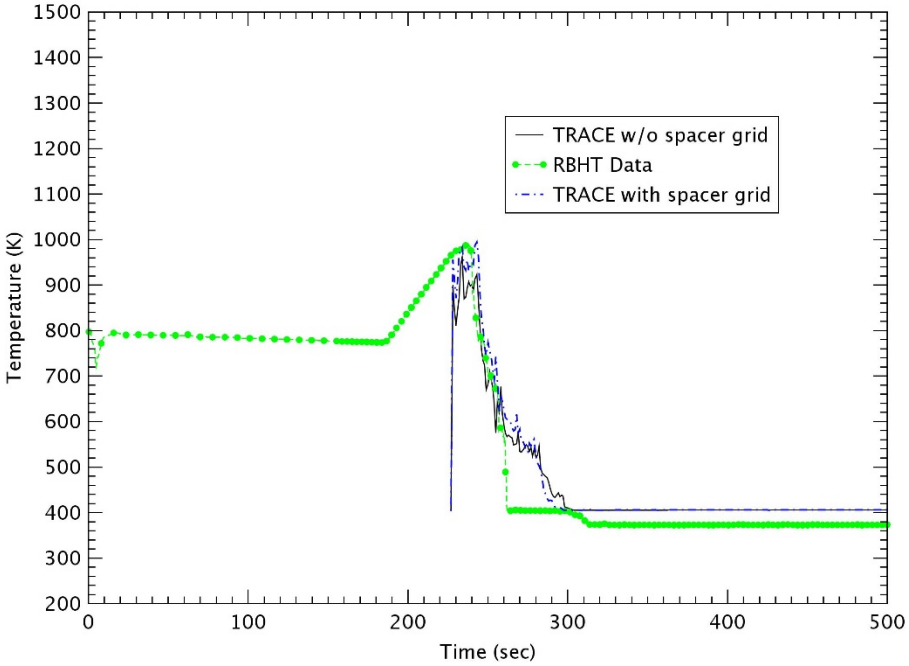

Figure 3-61 Steam Temperature at 1.40 m – Test 1196

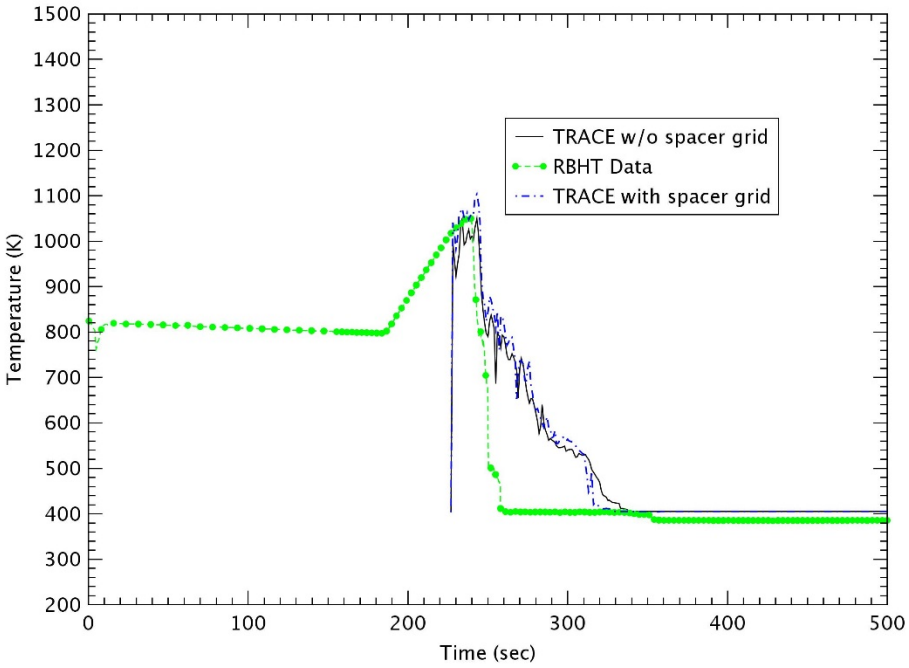

Figure 3-62 Steam Temperature at 1.88 m – Test 1196

6) Test 1285

Test 1285 was conducted with 0.74 kg/s (~ 6 in/s) at 0.28 MPa, 86 K subcooling and 1.53 kW/m linear power. This was the same conditions as for Test 1170 except for a 70 K increase in the subcooling degree. The test bundle was preheated by the steam produced from the boiler and the power was turned on. When the heater rods reached a predetermined temperature, the reflood started by injecting the water. The collapsed liquid level is shown in Figure 3.63. As in Test 1196, a sudden rise in the liquid level occurred at the beginning of the test and TRACE under predicted the collapsed liquid level for this period. After that, TRACE had a good prediction result for the collapsed liquid level up to ~ 260 sec. When the spacer grid model was used, the collapsed liquid level increased slightly faster than without the spacer grid model.

Figures 3.64 through 3.68 gives the rod temperatures at various elevations. Similar to Test 1196, TRACE predicted fairly well the rod temperature (< 1.27 m) and the quenching time (< 1.87 m) at lower elevations. However, at the high elevations, the peak rod temperatures were still over predicted and the rod quenching occurred earlier compared to the RBHT data. The entire trend of the rod peak temperature and the rod quenching for TRACE had the better prediction results compared to Tests 1170 and 1196. By using the spacer grid model, lower rod temperature and earlier rod quenching were estimated than without the spacer grid model, but the peak rod temperature was just a little changed as in Test 1196. At elevation z~2.77 with the peak power, the loss of peak rod temperature was ~ 7.2 K and the decrease in quenching time was ~ 12 sec by the spacer grid model. Since Test 1285 had the large subcooling degree as Test 1108, the high reflood rate and the high heat transfer rate due to the large subcooling resulted in the small change of quenching time by applying the spacer grid model. The HTCs at various elevations are plotted in Figures3.69 through 3.71. TRACE reasonably predicted the initiating time of the reflood, but the steep growth of HTCs at the rod cooling was predicted earlier than the RBHT data. And the spacer grid model resulted in the earlier increase of HTC due to the enhancement of heat transfer when the rod was quenched.

Figures 3.72 and 3.73 give the steam temperature at two elevations. The over prediction of the steam temperatures reasonably described the behaviors of the rod temperature and HTCs. After the rod had a peak temperature, the rapid drop of rod temperature was due to the high liquid level during the reflood as Test 1196.

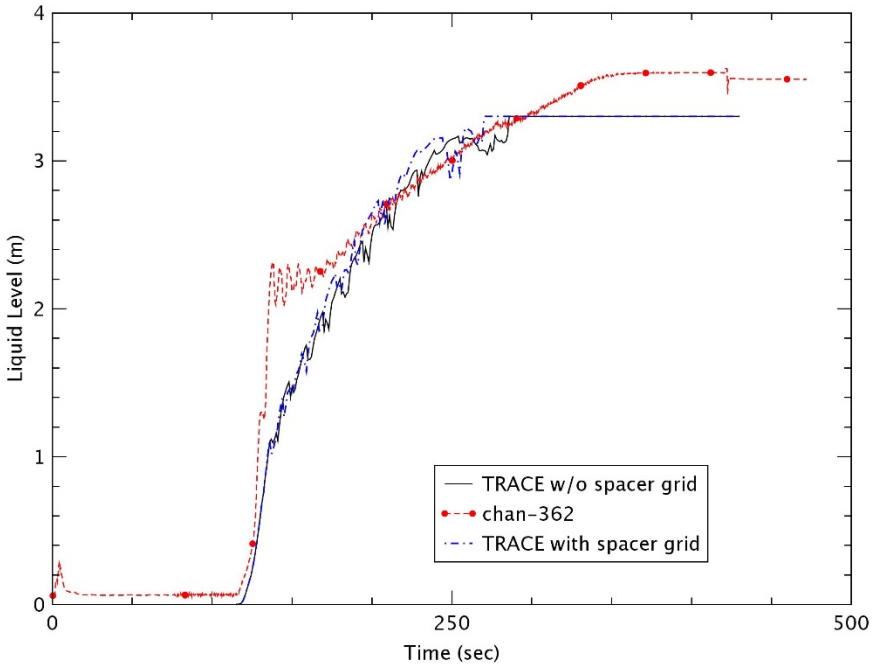

Figure 3-63 Collapsed Liquid Level – Test 1285

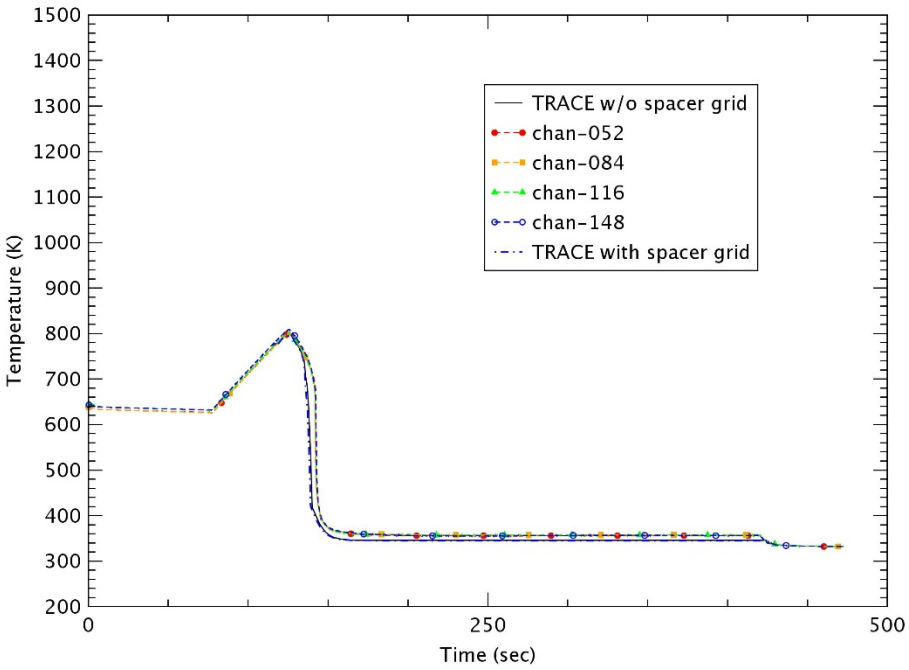

Figure 3-64 Heater Rod Temperature at 0.59 m – Test 1285

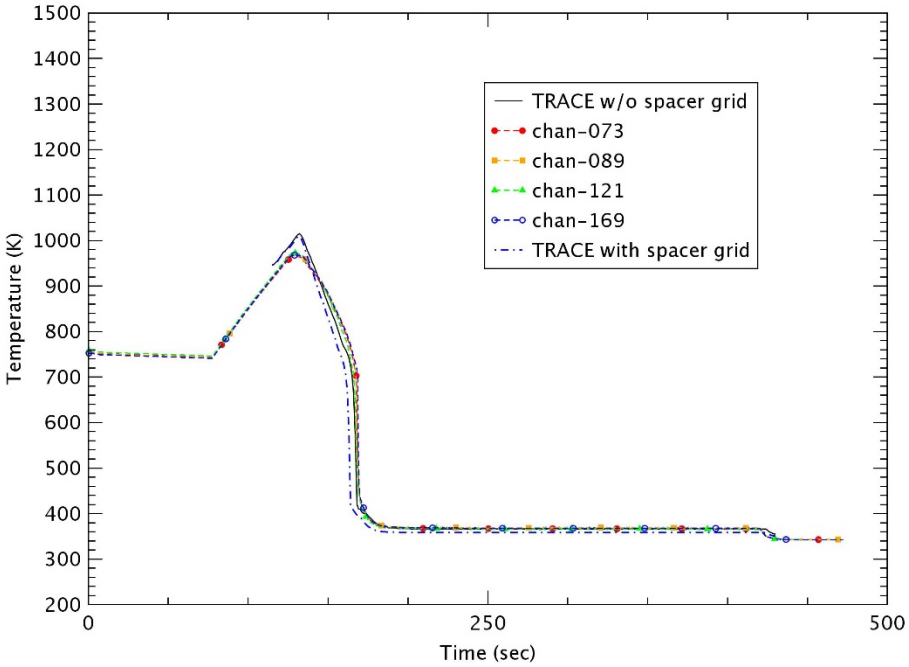

Figure 3-65 Heater Rod Temperature at 1.27 m – Test 1285

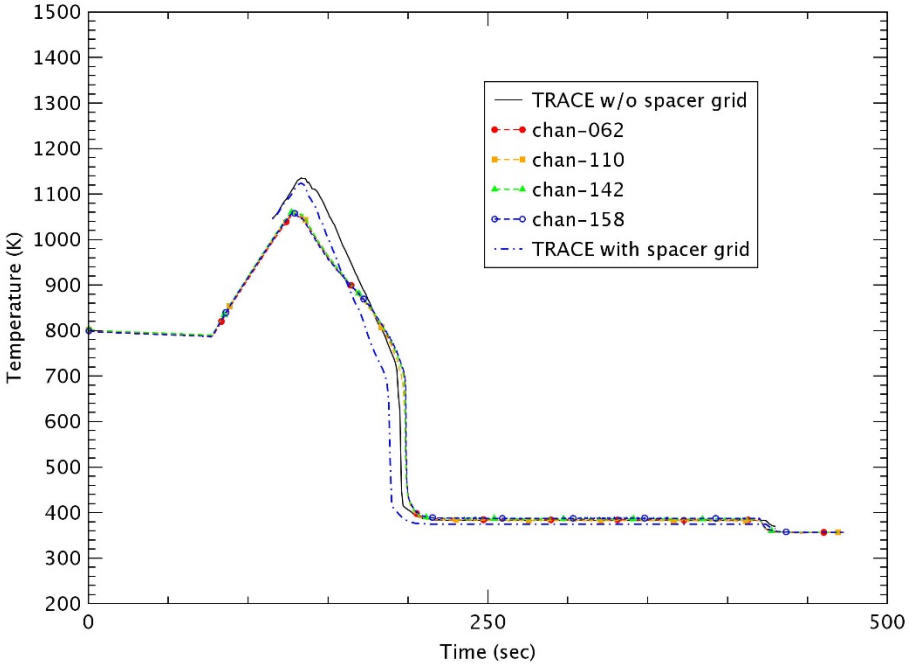

Figure 3-66 Heater Rod Temperature at 1.87 m – Test 1285

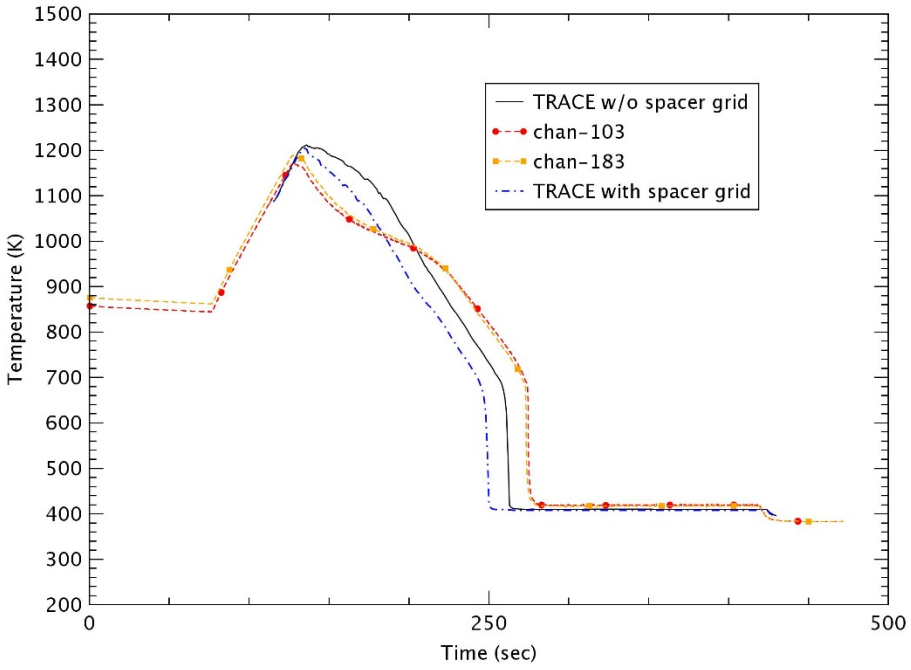

Figure 3-67 Heater Rod Temperature at 2.77 m – Test 1285

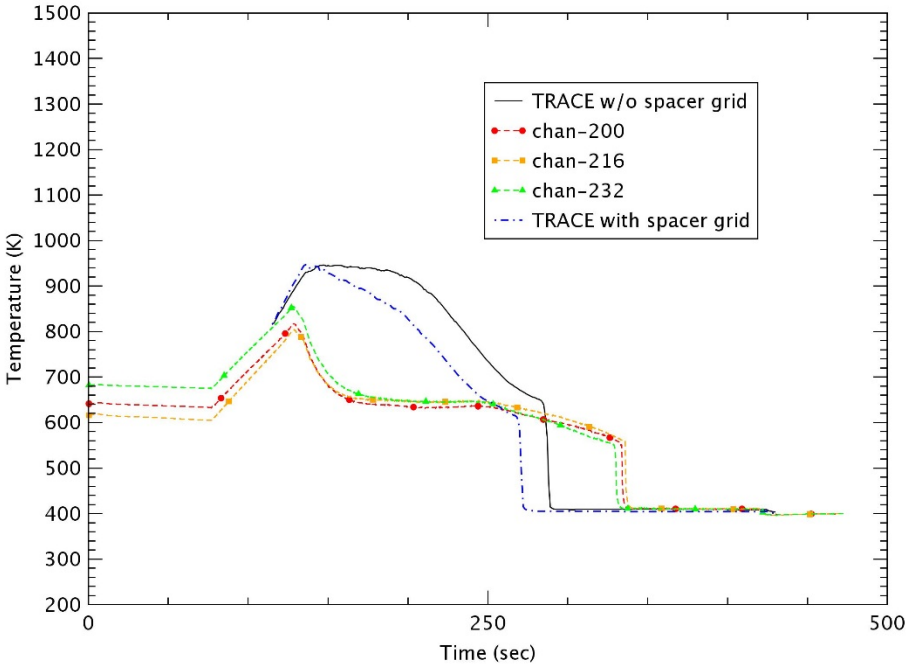

Figure 3-68 Heater Rod Temperature at 3.43 m – Test 1285

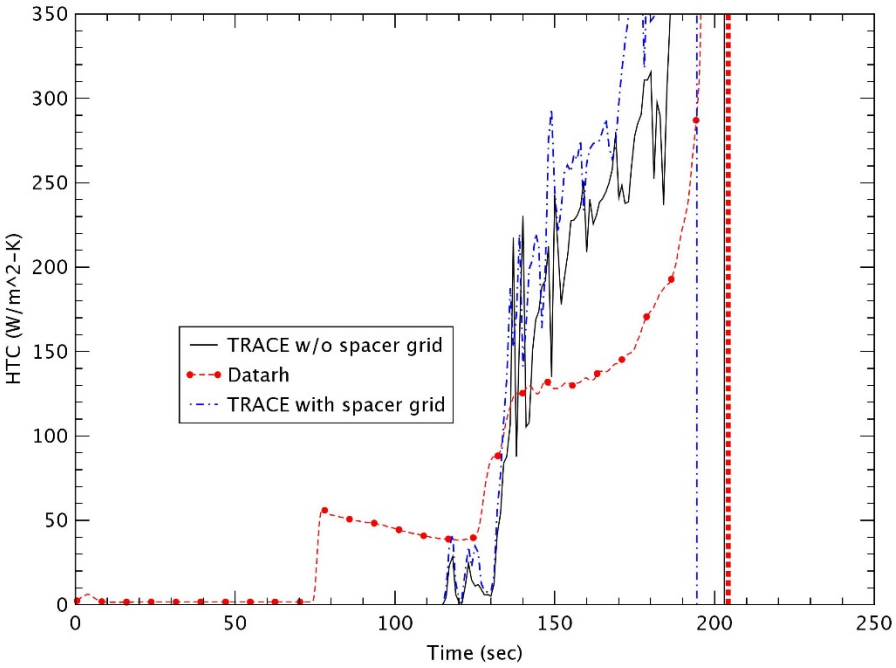

Figure 3-69 Heat Transfer Coefficient at 1.88 m – Test 1285

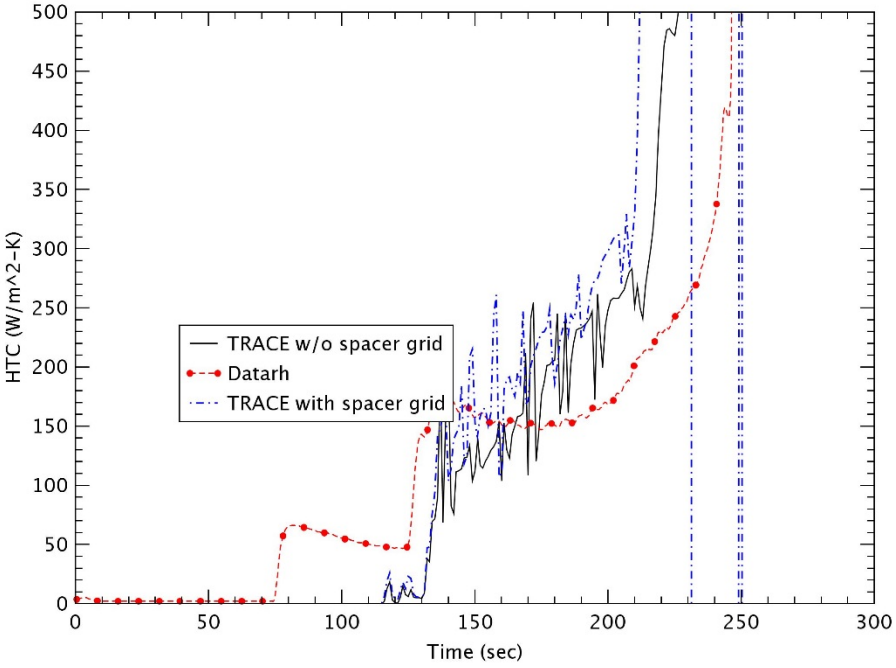

Figure 3-70 Heat Transfer Coefficient at 2.54 m – Test 1285

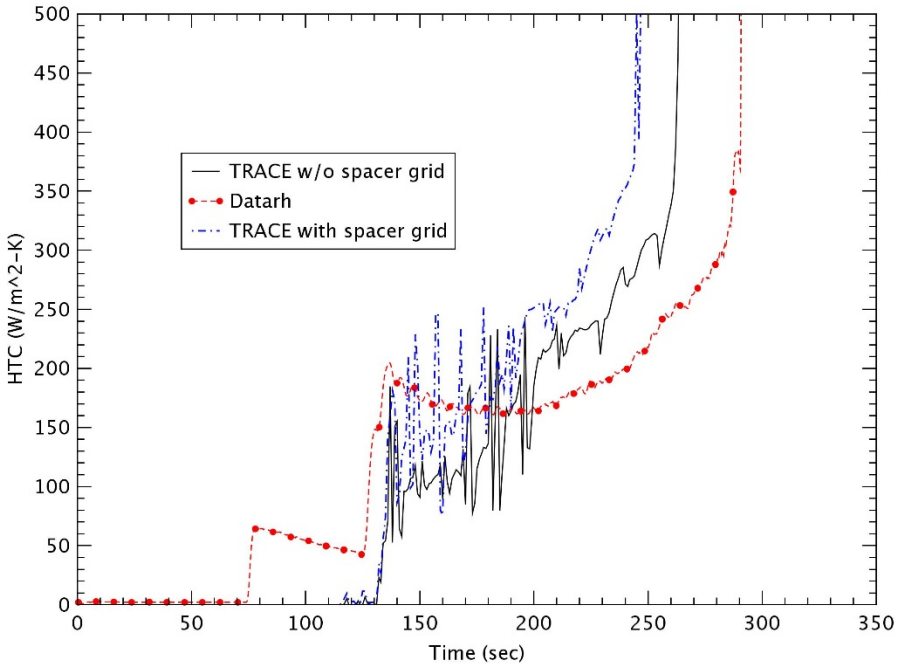

Figure 3-71 Heat Transfer Coefficient at 2.93 m – Test 1285

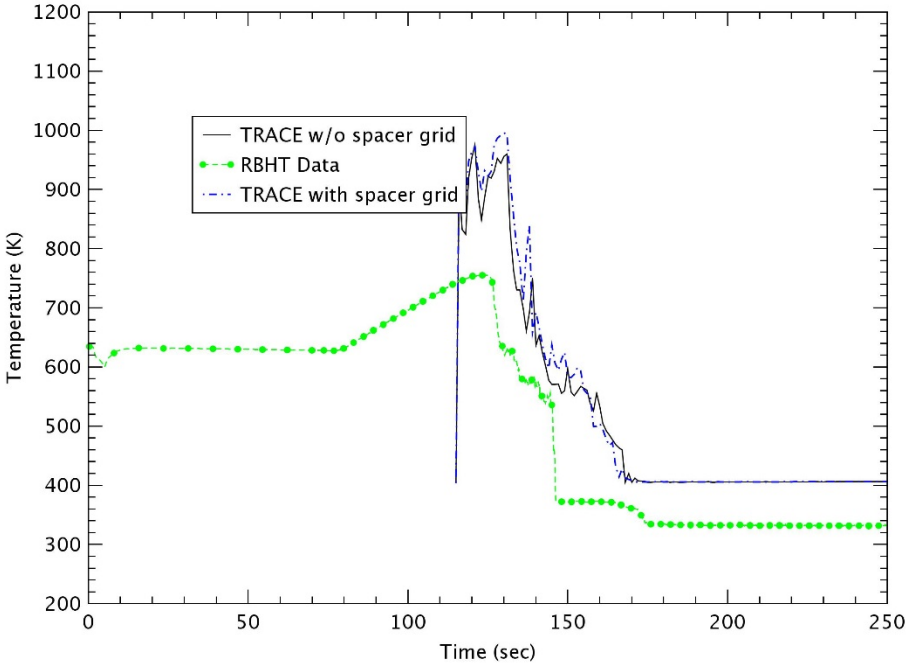

Figure 3-72 Steam Temperature at 1.40 m – Test 1285

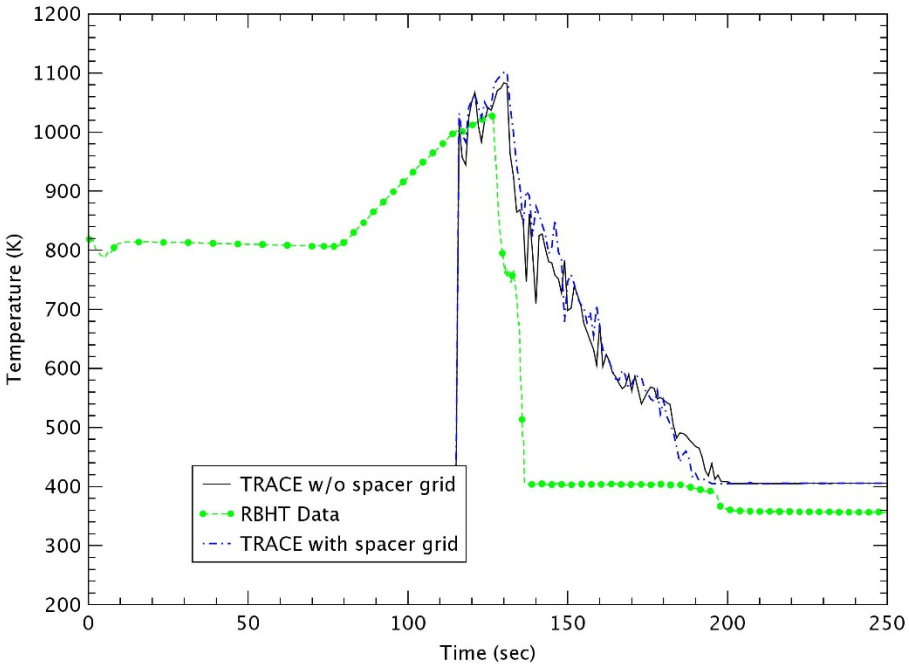

Figure 3-73 Steam Temperature at 1.88 m – Test 1285

7) Summary

Usually, the spacer grid promotes the convective heat transfer due to the flow acceleration and the turbulence increase. Currently, among the four sub-models, the droplet breakup model is not activated and the grid re-wetting model is not fully implemented in TRACE. Therefore, only the enhancement of convective heat transfer and the pressure drop due to the spacer grid were considered in this study. As would be expected, the rod temperatures decreased and the rods were quenched earlier in most of the tests when the spacer grid model was applied. In tests with high power and a high reflood rate, the change in peak temperature due to the spacer grid was not large, which resulted from the short heat up period and the faster increase in the liquid level by the high reflooding rate. Additionally, with a higher subcooling degree, the decreased amount of quenching time due to the spacer grid was reduced since the high subcooling degree enhanced the heat transfer rate. In all the tests, Test 1096 for low power, low reflood rate, low pressure and low subcooling degree was affected most significantly for the peak temperature and the quenching time using the spacer grid model as shown in Figure 3.74 and Table 3.4.

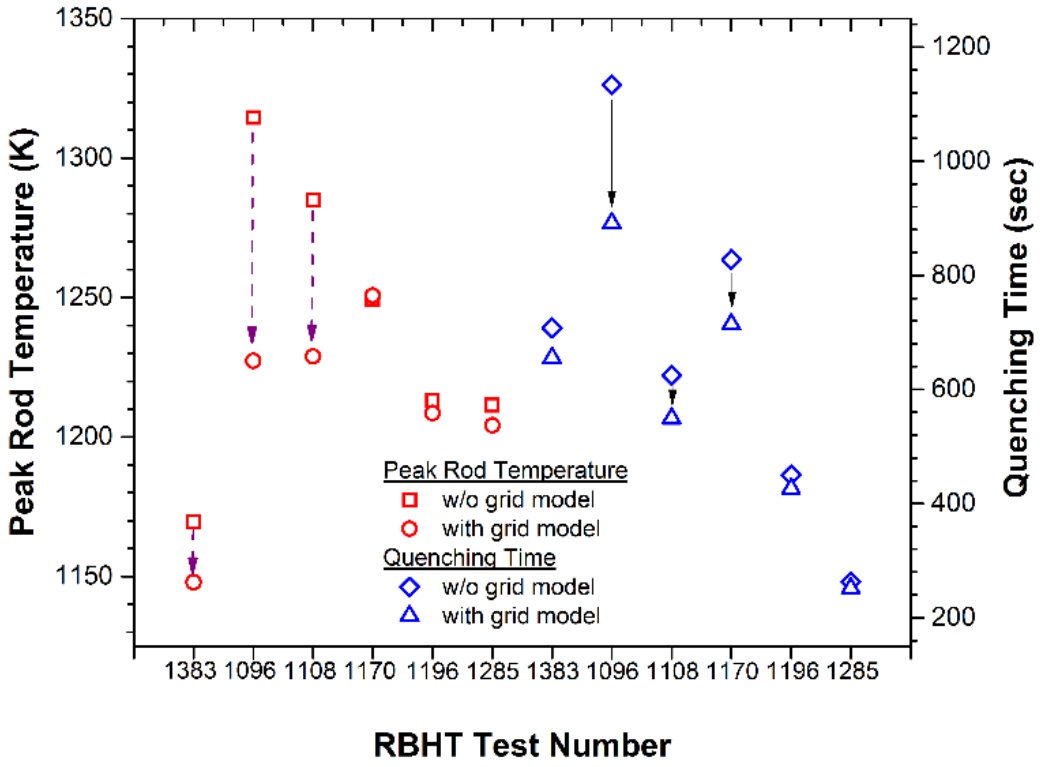

Figure 3-74 Peak Rod Temperature and Quenching Time at elevation z = 2.77 m

Table 3-4 Peak Temperature and Quenching Time at 2.77 elevation

Test	Peak Temperature (K) (at time)			Quenching Time (sec)		
	W/O grid	With grid	Δ Temp	W/O grid	With grid	Δ Time
1383	1169.6 (402 sec)	1147.9 (394 sec)	21.7	708	655	53
1096	1314.5 (441 sec)	1227.3 (329 sec)	87.2	1134	891	243
1108	1284.9 (256 sec)	1228.9 (240 sec)	56	625	549	76
1170	1249.5 (319 sec)	1250.7 (318 sec)	-1.2	828	714	114
1196	1213 (247 sec)	1208.6 (246 sec)	4.4	450	426	24
1285	1211.4 (136 sec)	1204.2 (135 sec)	7.2	263	251	12

4 SENSITIVITY ANALYSIS

4.1 Effect of the Number of Nodes

The selection of the proper number of nodes has been one of the long-term issues for the computational fluid dynamic calculations. In particular, the number of nodes influence the calculation results for the LBLOCA analysis. The use of a coarse node normally results in the loss of accuracy and the savings of calculations resources. However, if the detailed cladding temperature needs to be obtained from the complicated thermal hydraulic problems, more detailed nodes is required. Therefore, the nodes for the core, steam generator, reactor coolant pump and pressurizer must be carefully determined by the sensitivity studies for the number of nodes. By using a relatively coarse node, TRACE and RELAP5 tend to produce a stepwise increase of quench front during the transient.

Currently, the test section of the RBHT assessment manual [12] is modeled as a VESSEL component. The VESSEL is divided into 17 axial levels including 15 heated length levels with 3.66 m. There are two cells between each gird. The bottom of the spacer grid is located in the bottom of the corresponding cell as shown in Figure 4.1 (a). In this study, 8 nodes and 30 nodes for the heated section were selected as the sensitivity study to identify the effect of the number of nodes as shown in Figure 4.1.

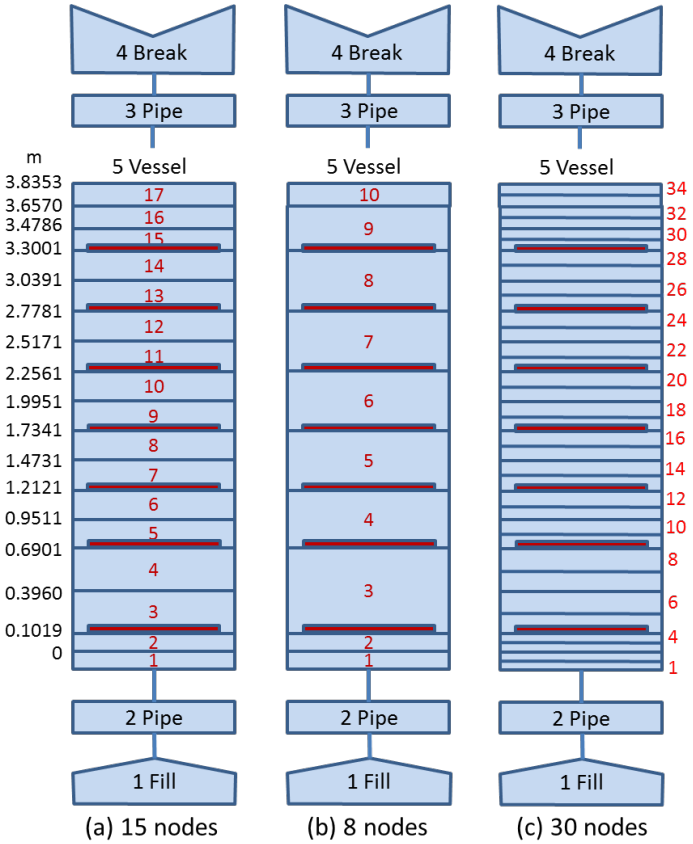

Figure 4-1 Number of Nodes for Sensitivity Calculation

There is a fine mesh reflood option in the HTSTR component of the TRACE code and then the maximum number of axial nodes can be defined in the reflood calculations. In this study, 125, 250 and 500 were used as the maximum number of axial nodes in the fine mesh calculation for 8, 15 and 30 nodes, respectively. Among the six tests in Table 3.3, Tests 1096 and 1108 and Tests 1170 and 1285 were selected for the node sensitivity calculations in low and high reflood tests, respectively.

1) Test 1096

Test 1096 was a reflood test with 0.12 kg/s (~ 1 in/s) at 0.14 MPa, 16 K subcooling and 0.88 kW/m linear power. The collapsed liquid level for the number of nodes is shown in Figure 4.2. The spacer grid model was applied in the calculations. Nodes 15 and 30 followed a similar trend for the collapsed liquid level, and TRACE reasonably predicted the experimental data with the injected water. However, the case with 8 nodes experienced a little delayed growth of the liquid level and under-predicted the collapsed liquid level during all times of the test. The relatively coarse node weakened the computation accuracy for the thermal hydraulic variables and then resulted in the delayed increase and the under-estimation for the collapsed liquid level.

For the number of nodes, the rod temperatures at various elevations are shown in Figures 4.3 through 4.5. There were no significant differences in the predicted rod temperatures for the three cases of Figure 4.1 at low elevations ($z < 1.27$ m). However, at elevation $z \sim 2.77$ m with the peak power, the coarse node case (8 nodes) had a lower peak temperature and earlier quenching time than the other two cases. In general, this result was the opposite of the behavior of the water level. The rod temperature and quenching were influenced by the complicated thermal hydraulic mechanism. The rod temperatures for 8 nodes under-predicted possibly due to the relatively higher heat transfer to the fluid and then the water temperature increased more than other cases as shown Figure 4.6. This delayed the steam quenching upstream and the growth of the water level was expedited according to the conditions for the reflood rate and the subcooling degree. At elevation $z = 3.43$ m near the exit, it was interesting that the rod quenching for 8 nodes occurred at the latest time as shown in Figure 4.5. Usually, the rod is quenched for a short time as the flow regime changes from the dispersed film boiling to the nucleate boiling heat transfer. This may be due to the low final liquid level due to the high water temperature in the coarse node as shown in Figure 4.6.

Figures 4.7 and 4.8 show the change in rod temperatures for cases with 8 and 30 nodes, respectively. The elevation was $z \sim 2.77$ m with the peak power. As would be expected, if the spacer grid model was applied, the lower rod temperatures and earlier rod quenches were predicted in the two cases. When the spacer grid model was applied, the peak rod temperature at elevation $z \sim 2.77$ m was the highest in the case with 30 nodes as shown in Table 4.1. As the number of nodes increased, the effect of the spacer grid model decreased for the peak rod temperature and the quenching time.

Table 4-1 Peak Temperature and Quenching Time at 2.77 m elevation in Test 1096

No. of nodes	Peak Temperature (K) (at time)			Quenching Time (sec)		
	W/O grid	With grid	Δ Temp	W/O grid	With grid	Δ Time
8 nodes	1262.4 (464 sec)	1155.5 (332 sec)	106.9	1224	867	357
15 nodes	1314.5 (441 sec)	1227.3 (329 sec)	87.2	1134	891	243
30 nodes	1311.3 (428 sec)	1234.4 (321 sec)	76.9	1137	942	195

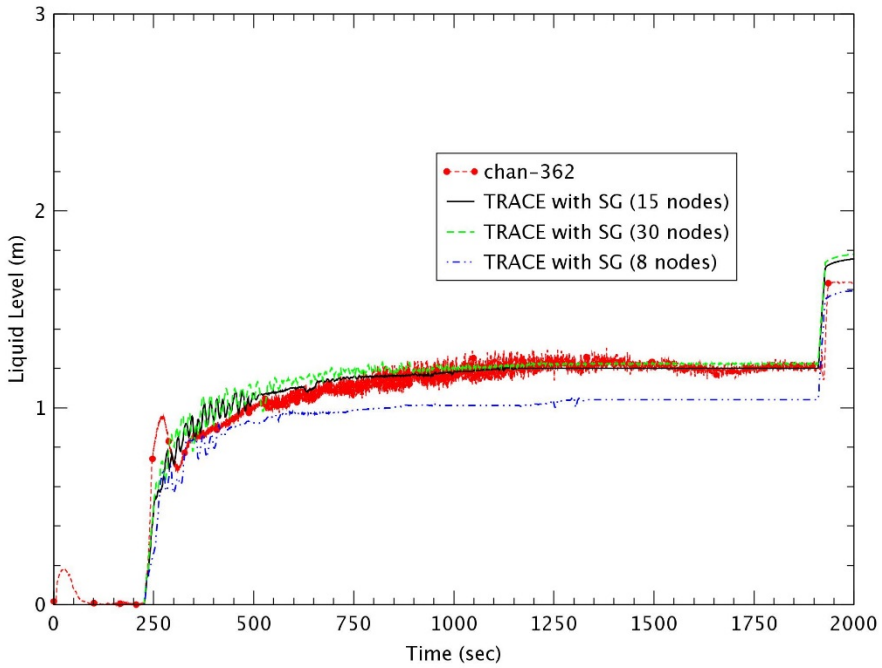

Figure 4-2 Collapsed Liquid Level – Test 1096

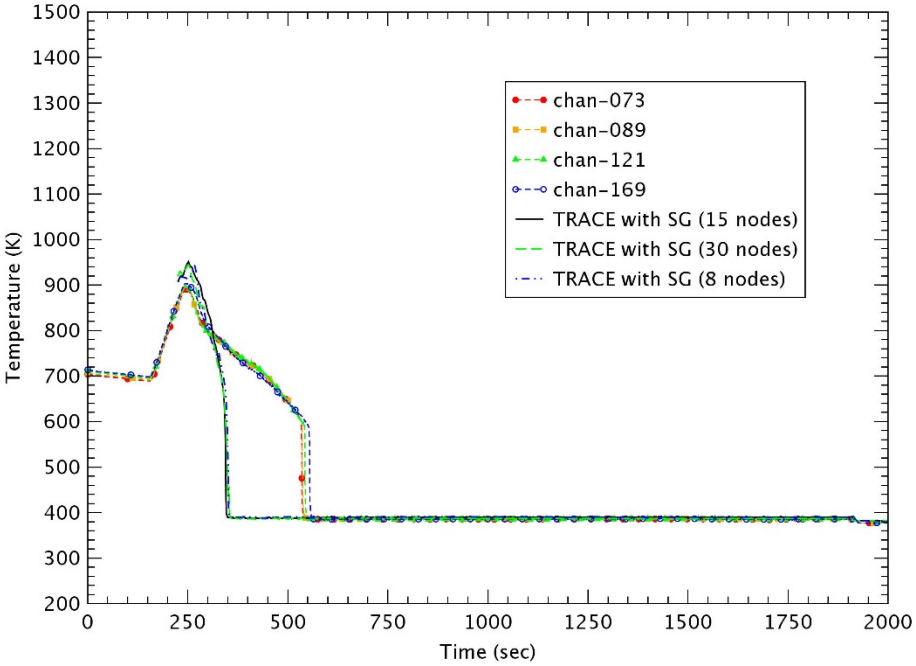

Figure 4-3 Heater Rod Temperature at 1.27 m – Test 1096

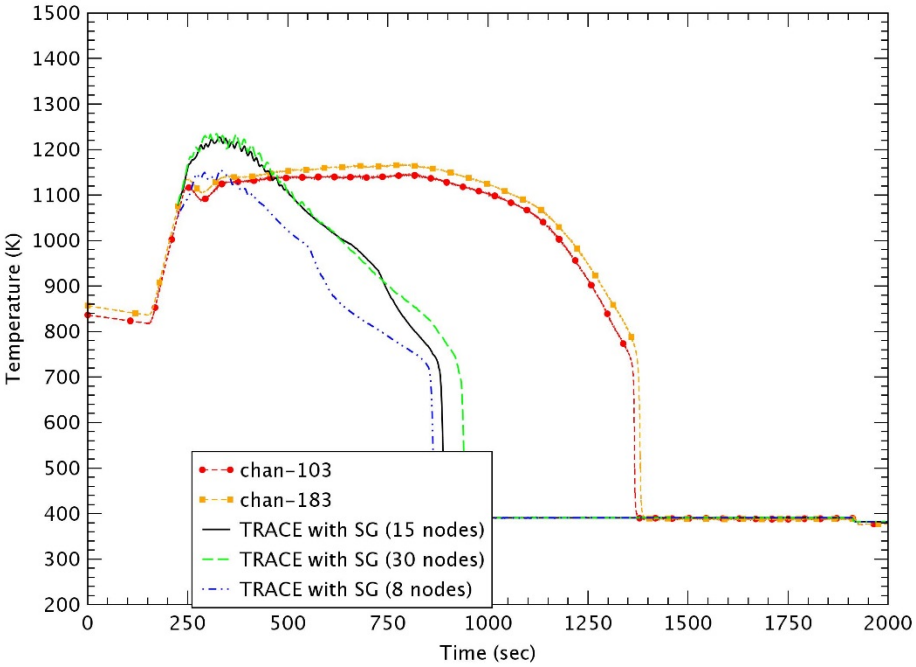

Figure 4-4 Heater Rod Temperature at 2.77 m – Test 1096

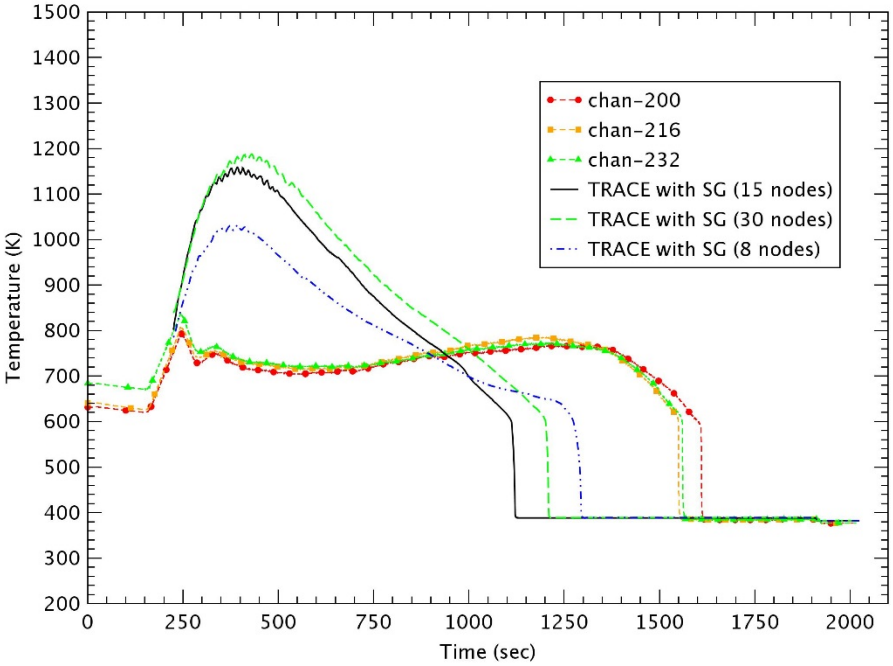

Figure 4-5 Heater Rod Temperature at 3.43 m – Test 1096

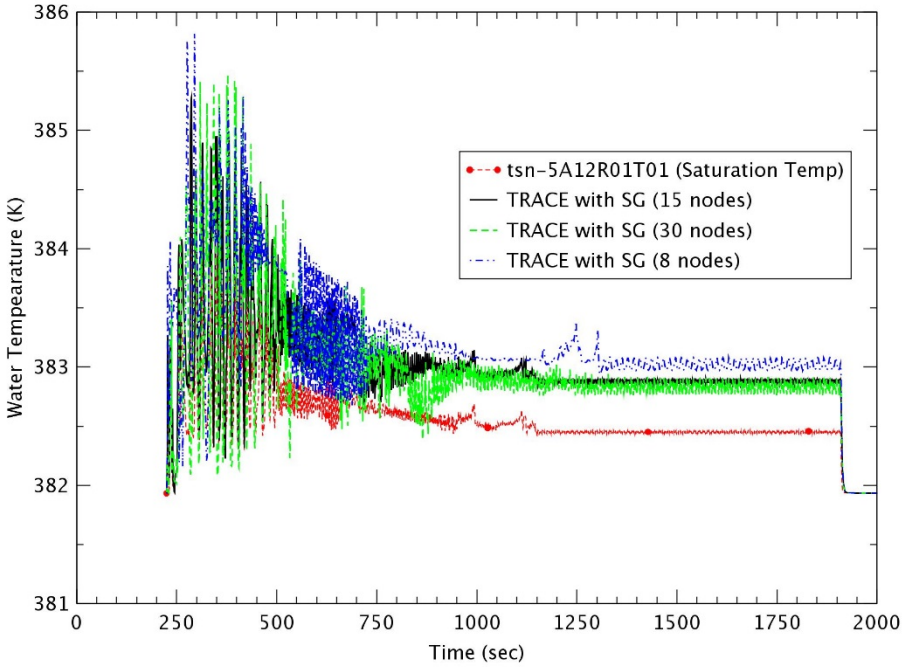

Figure 4-6 Water Temperature at 2.77 m – Test 1096

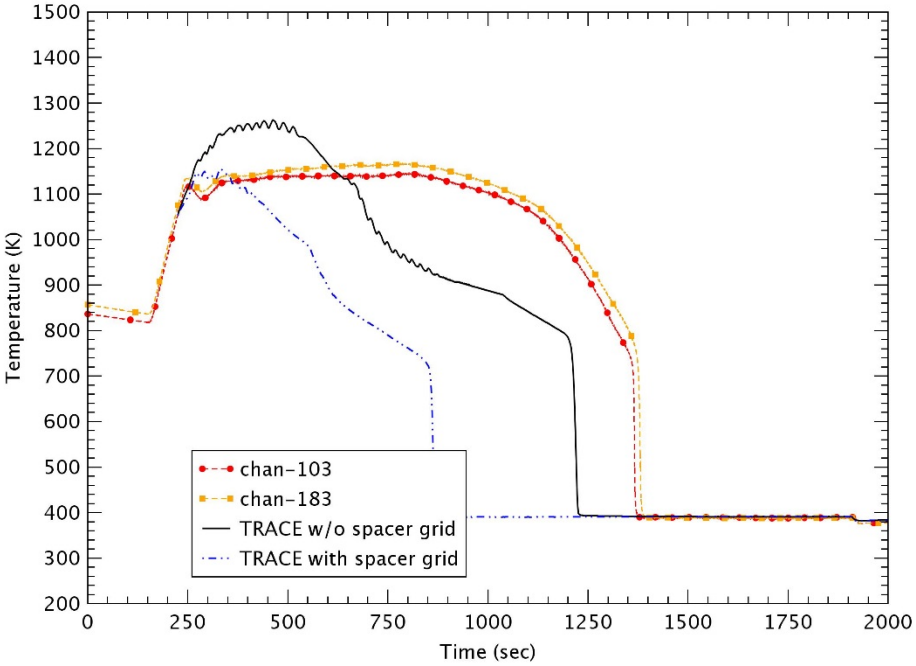

Figure 4-7 Heater Rod Temperature at 2.77 m for 8 nodes – Test 1096

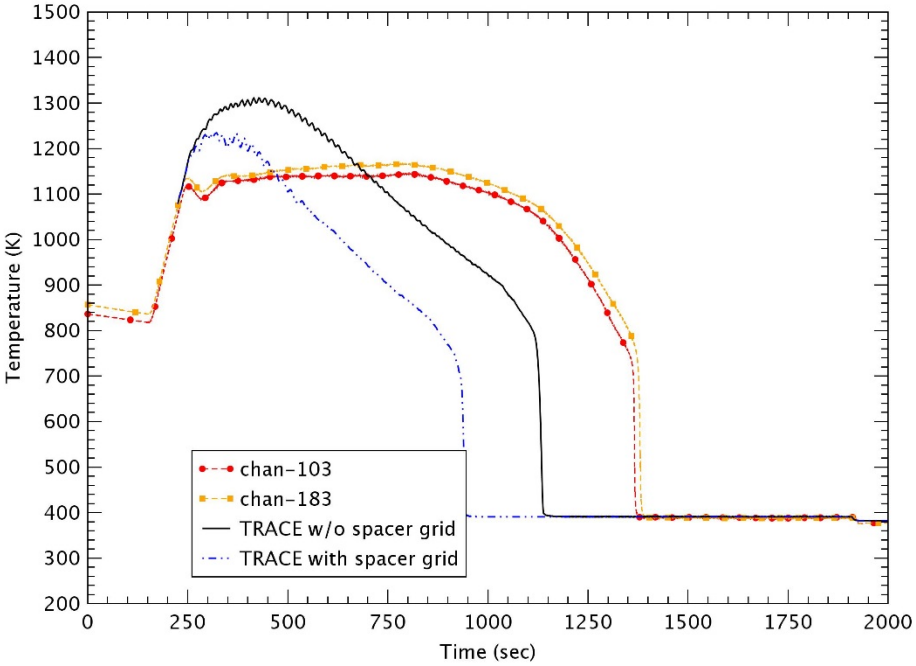

Figure 4-8 Heater Rod Temperature at 2.77 m for 30 nodes – Test 1096

2) Test 1108

Test 1108 was a reflood test with 0.13 kg/s (~ 1 in/s) at 0.14 MPa, 82 K subcooling and 0.88 kW/m linear power. This was the same as Test 1096 except for the subcooling degree. The collapsed liquid level for the number of nodes is shown in Figure 4.9. For three nodes, TRACE could reasonably predict the experimental level trend. However, as shown in Test 1096, the case with 8 nodes under-predicted the collapsed liquid level during all times of the test. The collapsed liquid level for 30 nodes was higher than that for 15 nodes and the difference for the number of nodes was large due to the high subcooling degree as compared to Test 1096.

Figures 4.10 through 4.12 show the rod temperatures for the number of nodes at various elevations. According to the number of nodes, the differences for the rod temperature and the quenching time were not big at lower elevations (< 1.27 m). At elevations z ~2.77 m and 3.43 m, the lower peak rod temperature and the earlier quenching time were predicted for the coarse node case (8 nodes). This result was also the opposite of the behavior of the collapsed liquid level. For 8 nodes, the lower rod temperature due to the high heat transfer might have resulted in the earlier quenching time. The difference between 15 nodes and 30 nodes was not big for the rod temperature.

The change in the rod temperatures for cases with 8 and 30 nodes is illustrated in Figures 4.13 and 4.14. At the elevation z ~2.77 with the peak power, the lower rod temperature and the earlier rod quenching were predicted as the spacer grid model was applied. The case with 30 nodes had the highest peak rod temperature with the spacer grid model as shown in Table 4.2. For this test, the connective heat transfer increased due to the increase of the subcooling degree and then the peak rod temperature without the spacer grid model decreased as compared to Test 1096. Therefore, the effect of the spacer grid model decreased for the rod temperature and the quenching time as shown in Table 4.2. The case with 8 nodes had a lower rod temperature and earlier quenching time, but the results for 15 nodes were similar to those for 30 nodes.

Table 4-2 Peak Temperature and Quenching Time at 2.77 m elevation in Test 1108

No. of nodes	Peak Temperature (K) (at time)			Quenching Time (sec)		
	W/O grid	With grid	Δ Temp	W/O grid	With grid	Δ Time
8 nodes	1222.1 (235 sec)	1148.6 (204 sec)	73.5	569	478	91
15 nodes	1284.9 (256 sec)	1228.9 (240 sec)	56	625	549	76
30 nodes	1288.5 (250 sec)	1253.6 (223 sec)	34.9	628	548	80

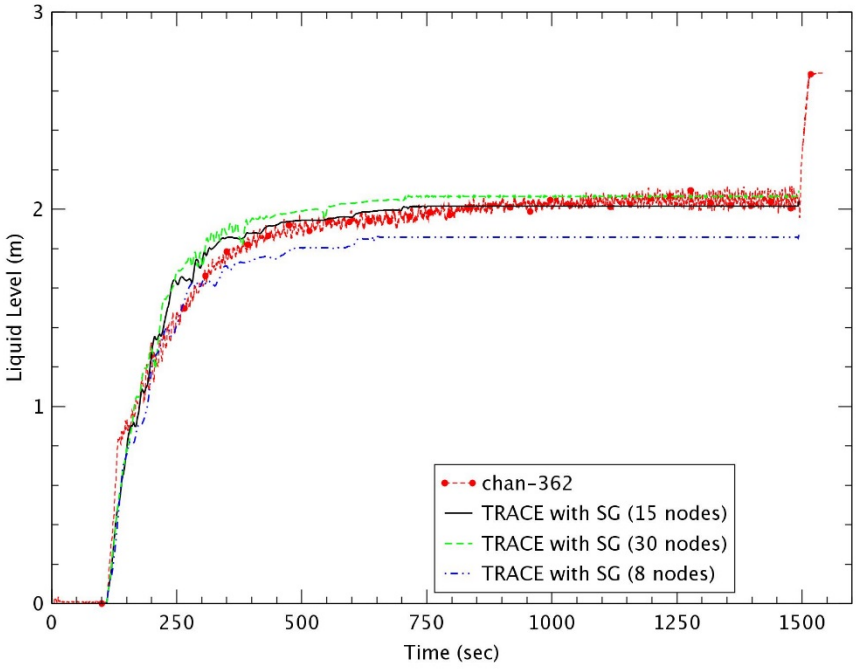

Figure 4-9 Collapsed Liquid Level – Test 1108

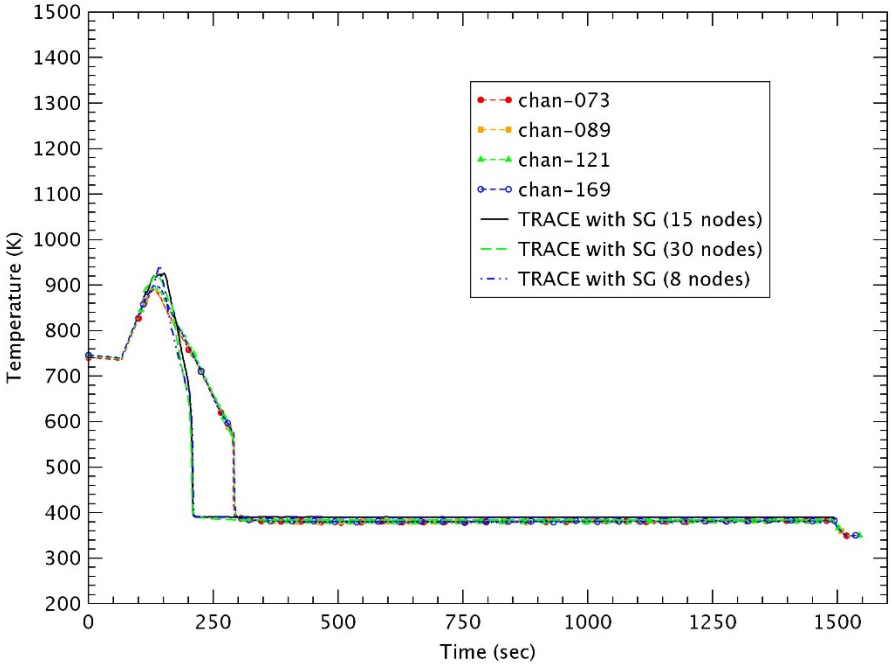

Figure 4-10 Heater Rod Temperature at 1.27 m – Test 1108

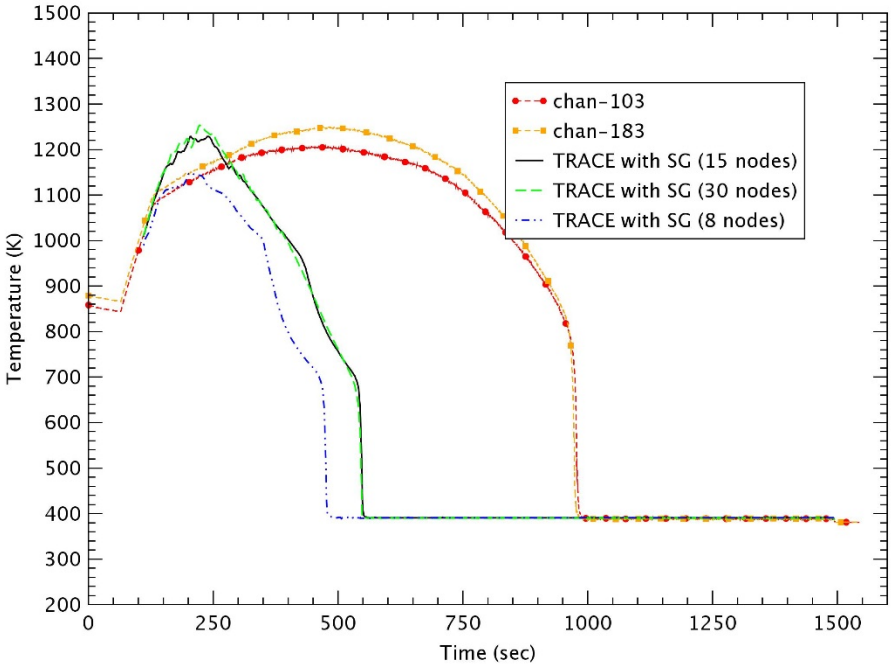

Figure 4-11 Heater Rod Temperature at 2.77 m – Test 1108

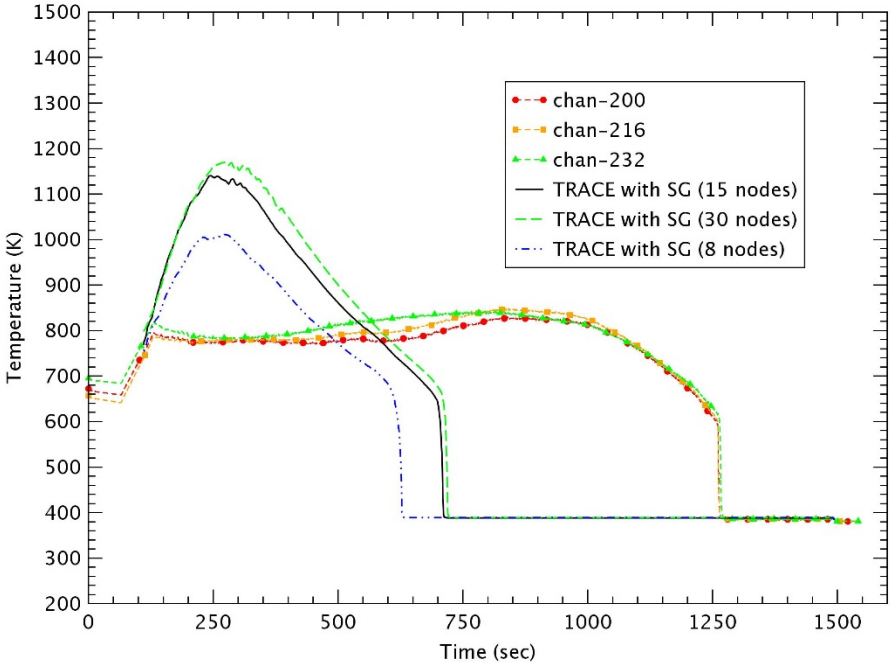

Figure 4-12 Heater Rod Temperature at 3.43 m – Test 1108

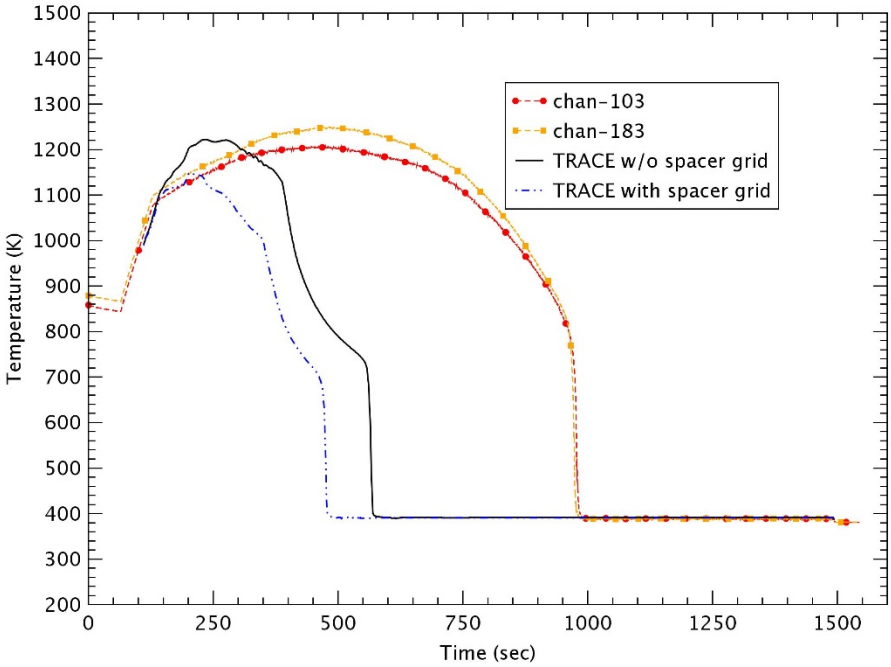

Figure 4-13 Heater Rod Temperature at 2.77 m for 8 nodes – Test 1108

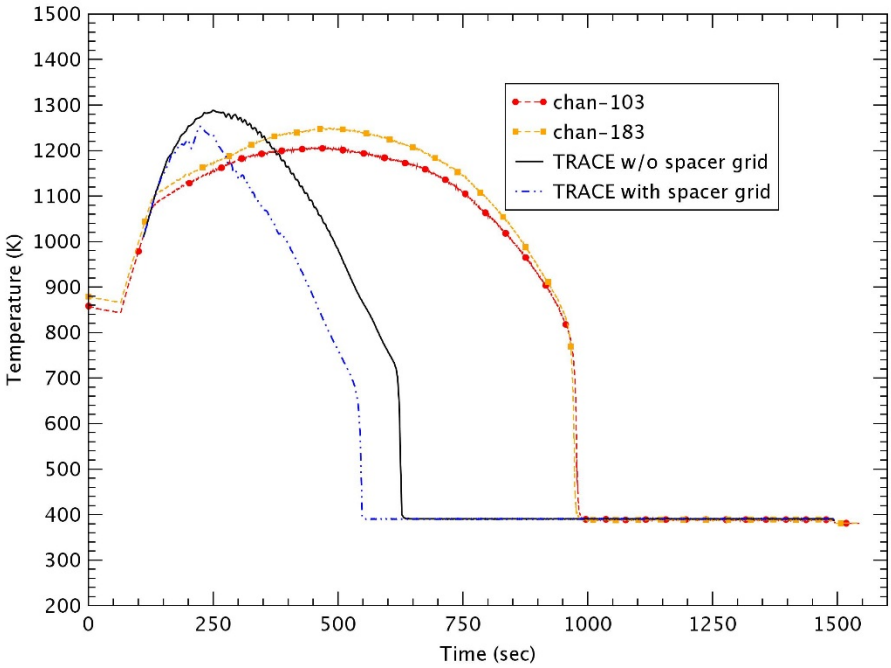

Figure 4-14 Heater Rod Temperature at 2.77 m for 30 nodes – Test 1108

3) Test 1170

Test 1170 was the first of three high power and high reflood rate cases in the test matrix of Table 3.3. Test 1170 was a reflood test with 0.75 kg/s (~ 6 in/s) at 0.28 MPa, which was a relatively high pressure and high reflooding rate, 16 K subcooling and 1.53 kW/m linear power. Figure 4.15 shows the collapsed liquid level for the number of nodes. TRACE for three nodes significantly under-predicted the liquid level. The calculation for 8 nodes showed the lowest level and the slowest growth in the three cases. The water level for 30 nodes increased a little earlier than that for 15 nodes.

The rod temperature for the number of nodes at various elevations is shown in Figures 4.16 through 4.18. In spite of the under-prediction of the liquid level, the rod temperatures were predicted reasonably well and the effect of the node number was not very significant at lower elevations (z < 1.27 m). However, the rod quenching time was significantly delayed at higher elevations (z < 2.77 m) compared with the RBHT data. For 8 nodes, the lower peak rod temperature and the delayed quenching time were predicted at higher elevations. This low peak temperature might be due to the high heat transfer for the coarse nodes and the late quenching could come from the growth of the liquid level. The peak rod temperature for 30 nodes was a value similar to 15 nodes because of the high reflood rate, but the rod temperature for 30 nodes was quenched at the earliest time.

The change in rod temperatures for 8 and 30 nodes is shown in Figures 4.19 and 4.20. As the spacer grid model was used, the lower rod temperature and the earlier rod quenching were predicted due to the enhancement of heat transfer. At elevation z~2.77 with the peak power, the highest peak rod temperature was predicted in the case with 30 nodes, but the difference in the peak temperature between 15 nodes and 30 nodes was not large as shown in Table 4.3. However, in this test with high power and high reflood rate, the change in peak temperature due to the spacer grid was not large, which resulted from the short heat up period and the faster increase in liquid level by the high reflooding rate.

Table 4-3 Peak Temperature and Quenching Time at 2.77 m elevation in Test 1170

No. of nodes	Peak Temperature (K) (at time)			Quenching Time (sec)		
	W/O grid	With grid	∆ Temp	W/O grid	With grid	∆ Time
8 nodes	1210.3 (317 sec)	1195.6 (316 sec)	14.7	821	719	102
15 nodes	1249.5 (319 sec)	1250.7 (318 sec)	-1.2	828	714	114
30 nodes	1255.8 (319 sec)	1251.1 (318 sec)	4.7	808	671	137

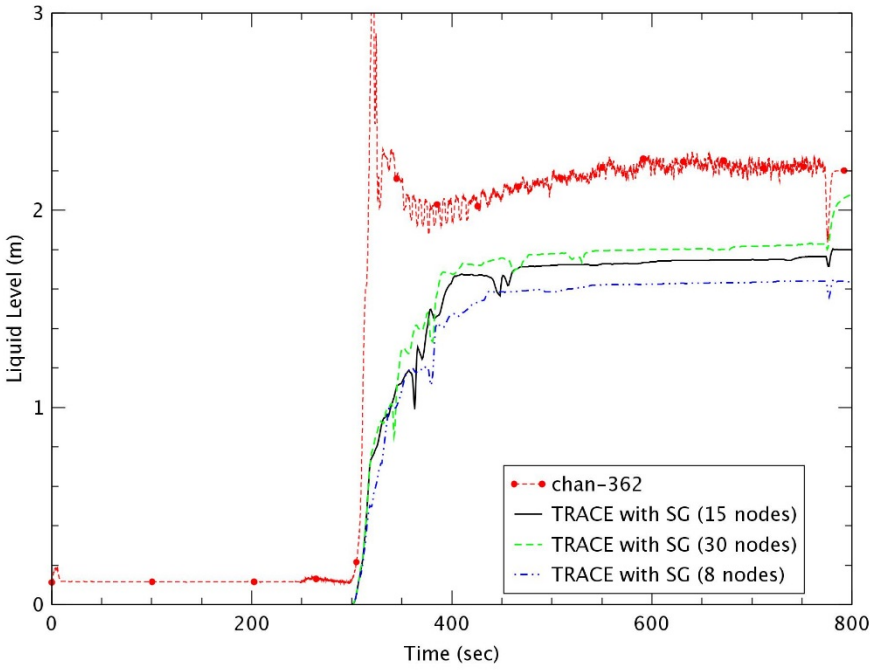

Figure 4-15 Collapsed Liquid Level – Test 1108

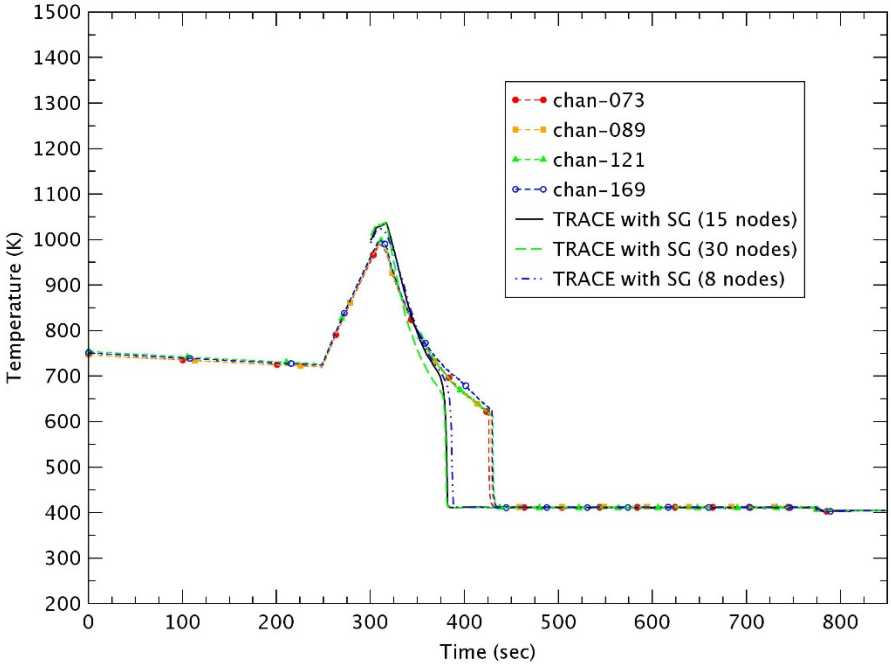

Figure 4-16 Heater Rod Temperature at 1.27 m – Test 1170

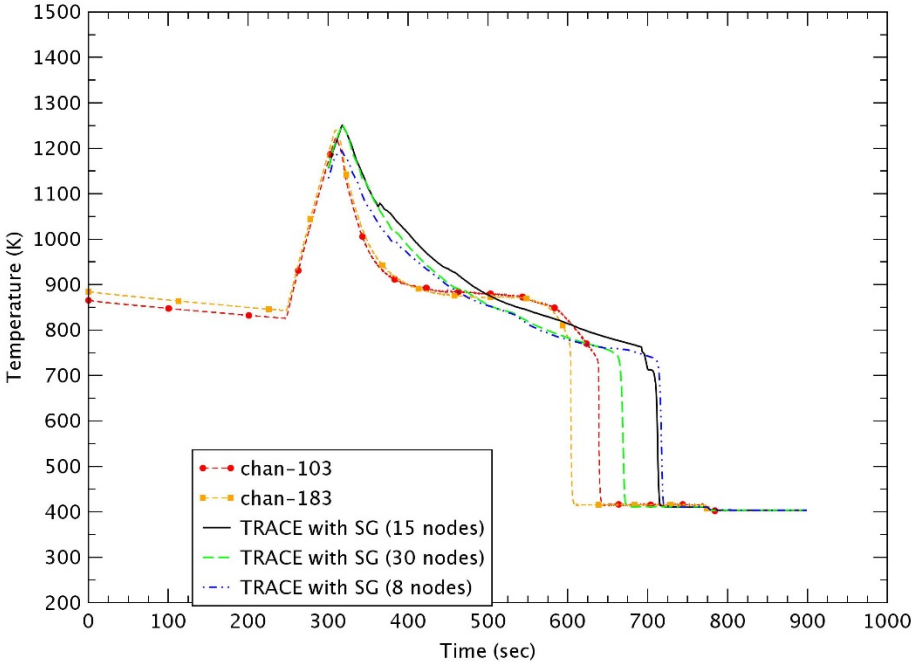

Figure 4-17 Heater Rod Temperature at 2.77 m – Test 1170

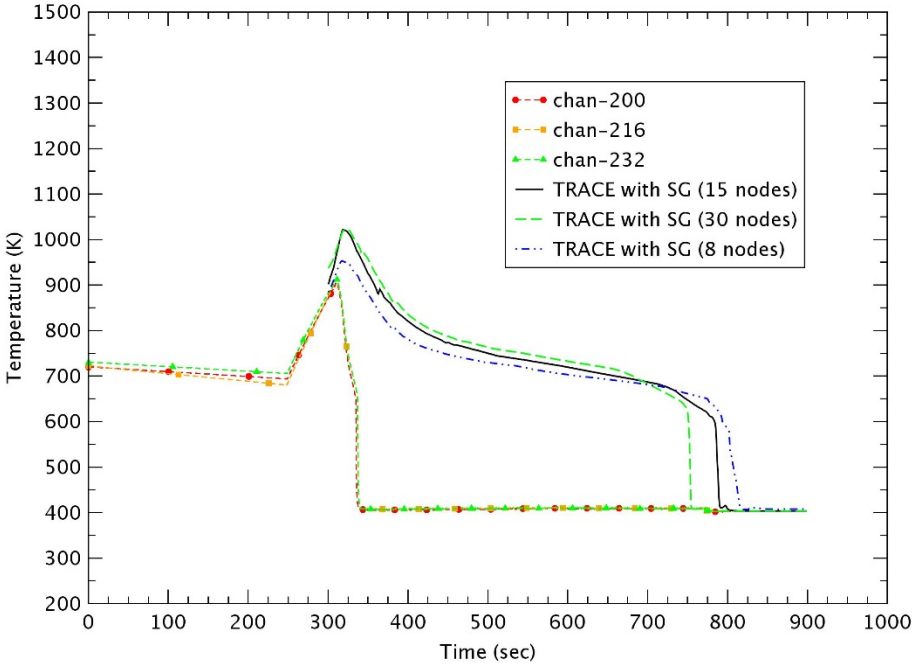

Figure 4-18 Heater Rod Temperature at 3.43 m – Test 1170

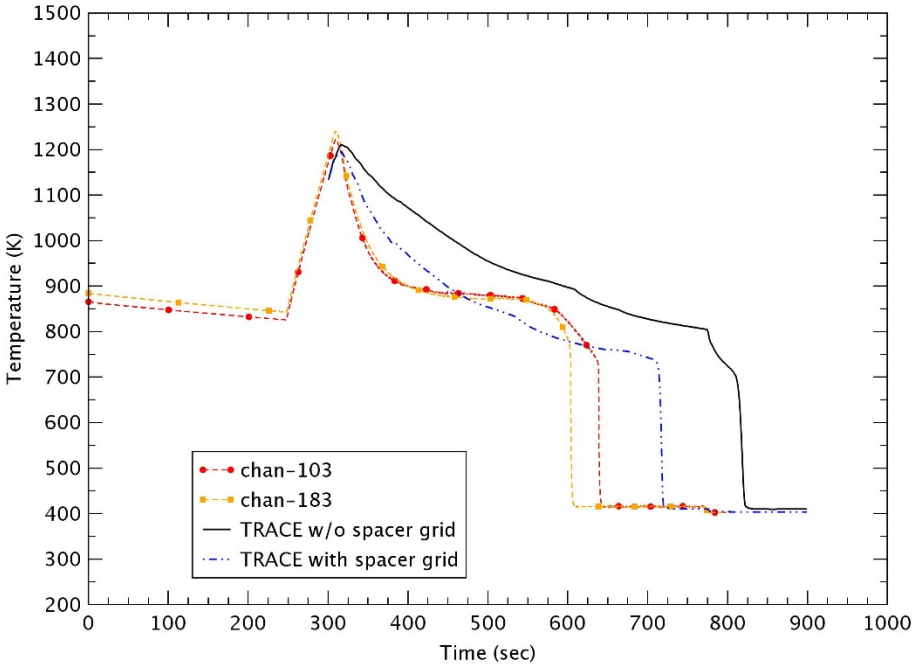

Figure 4-19 Heater Rod Temperature at 2.77 m for 8 nodes – Test 1170

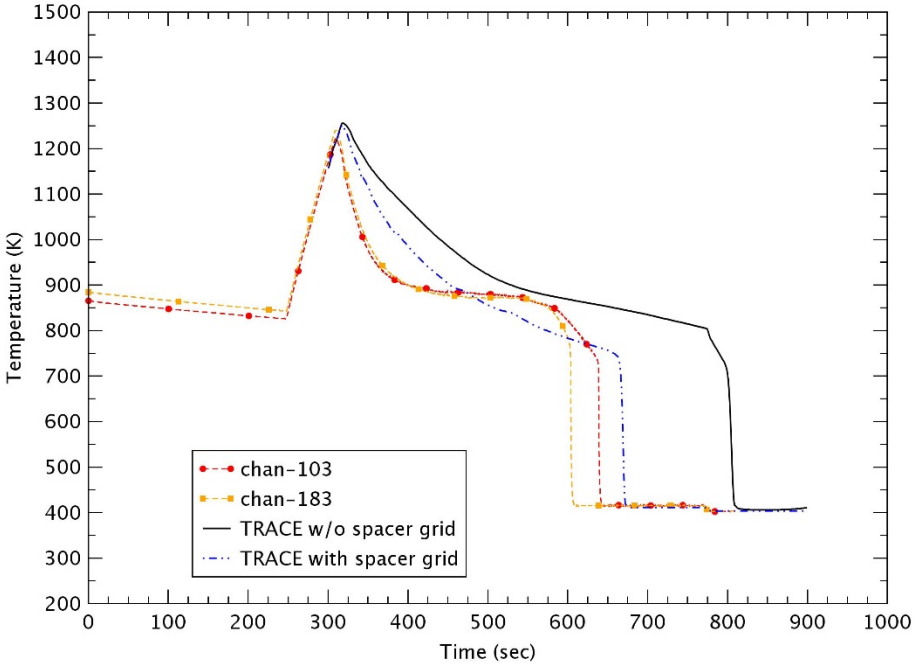

Figure 4-20 Heater Rod Temperature at 2.77 m for 30 nodes – Test 1170

4) Test 1285

Test 1285 was conducted with 0.74 kg/s (~ 6 in/s) at 0.28 MPa, 86 K subcooling and 1.53 kW/m linear power. This test had a relatively high reflood rate and subcooling degree. This were the same conditions as Test 1170 except for a 70 K increase in the subcooling degree. The collapsed liquid level for the number of nodes is shown in Figure 4.21. For three nodes, TRACE could not predict the sudden rise in the liquid level at the beginning of test. After that, TRACE showed a better prediction for the collapsed liquid level up to ~ 260 sec. As in Test 1096, the case with 8 nodes under-predicted the liquid level, and the difference between 15 and 30 nodes decreased due to the high reflood rate. Further, the collapsed liquid level with 30 nodes increased faster than that with 15 nodes.

Figures 4.22 through 4.24 give the rod temperatures for the number of nodes at various elevations. TRACE predicted fairly well the rod temperature and the quenching time at lower elevations (< 1.27 m) and the differences for the number of nodes were not large in the rod temperatures and the quenching times. At elevations z ~2.77 m and 3.43 m, the coarse node case (8 nodes) had a lower peak temperature but the quenching time was delayed in comparison with other nodes. The rod quenching occurred at earlier as the increase of the liquid level was faster for the three cases.

Figures 4.25 and 4.26 plot the change in rod temperatures for cases with 8 and 30 nodes, respectively. The elevation was z ~2.77 m with the peak power. By using the spacer grid model, a lower rod temperature and earlier rod quenching were estimated than that without the spacer grid model. The peak rod temperature for 30 nodes was just a little changed from that for 15 nodes. When the spacer grid model was applied, the peak rod temperature at elevation z ~2.77 m was the highest in the case with 30 node as shown in Table 4.4. As the number of nodes increased, the effect of the spacer grid model decreased for the peak rod temperature and the quenching time. As this test had a high reflood rate and high subcooling degree, the effect of the spacer grid was not big for the rod temperature due to the faster rise in the liquid level and the amount of change for the quenching time was also large since the high subcooling degree promoted the heat transfer rate.

Table 4-4 Peak Temperature and Quenching Time at 2.77 m elevation in Test 1285

No. of nodes	Peak Temperature (K) (at time)			Quenching Time (sec)		
	W/O grid	With grid	Δ Temp	W/O grid	With grid	Δ Time
8 nodes	1191.6 (140 sec)	1166.6 (139 sec)	25	274	258	16
15 nodes	1211.4 (136 sec)	1204.2 (135 sec)	7.2	263	251	12
30 nodes	1211.3 (135 sec)	1209.4 (135 sec)	1.9	254	244	10

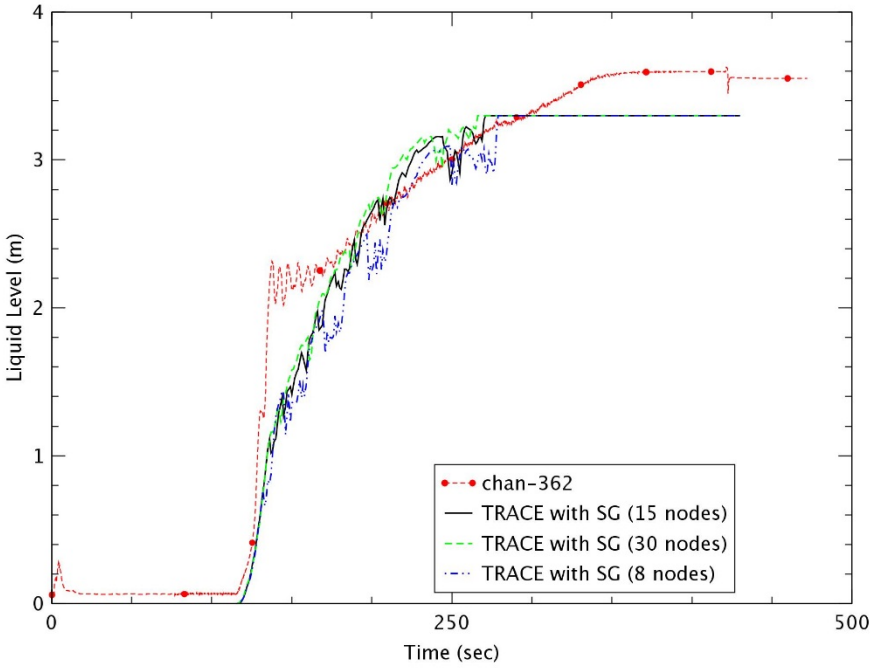

Figure 4-21 Collapsed Liquid Level – Test 1285

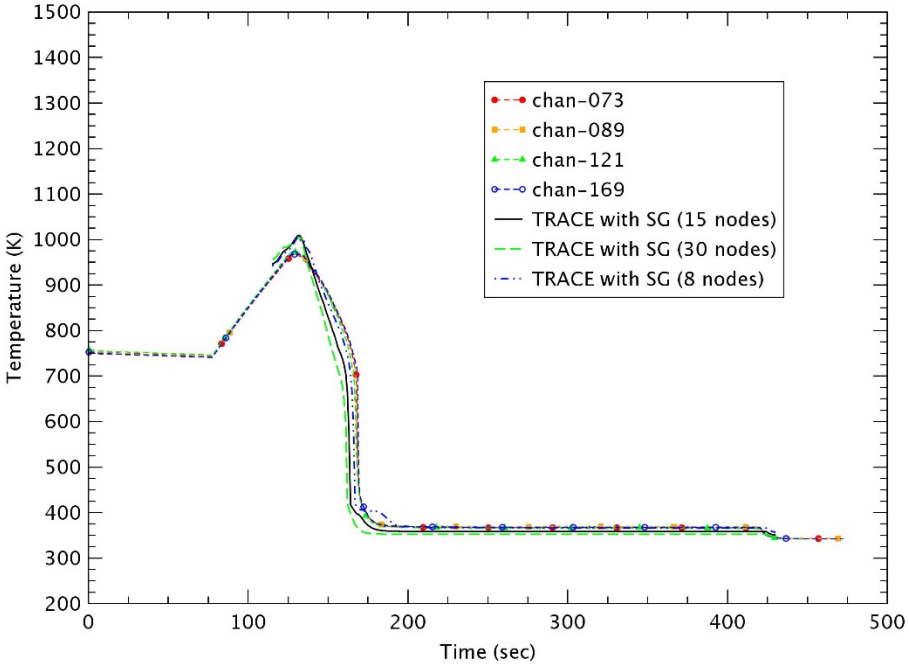

Figure 4-22 Heater Rod Temperature at 1.27 m – Test 1285

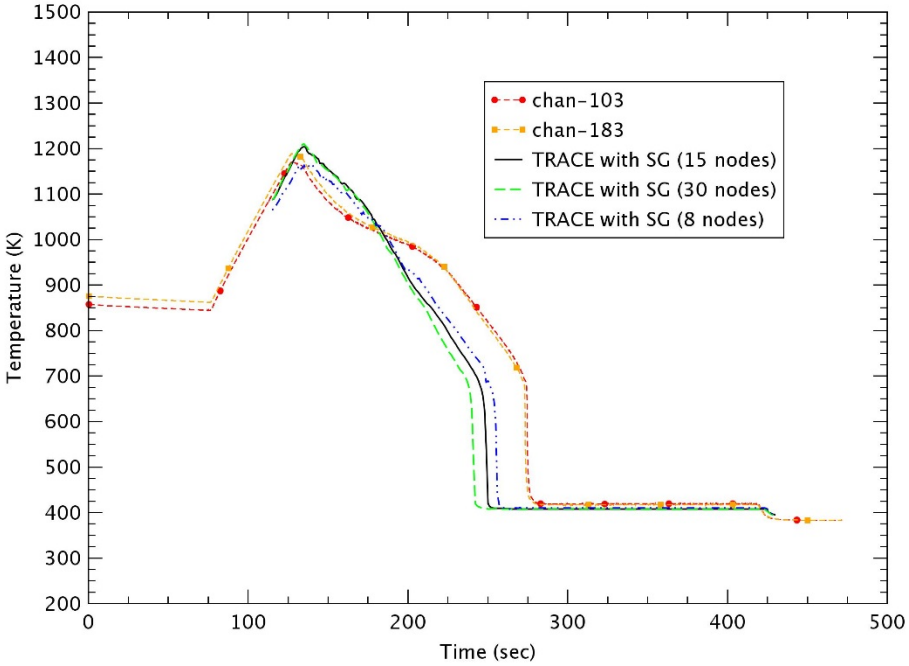

Figure 4-23 Heater Rod Temperature at 2.77 m – Test 1285

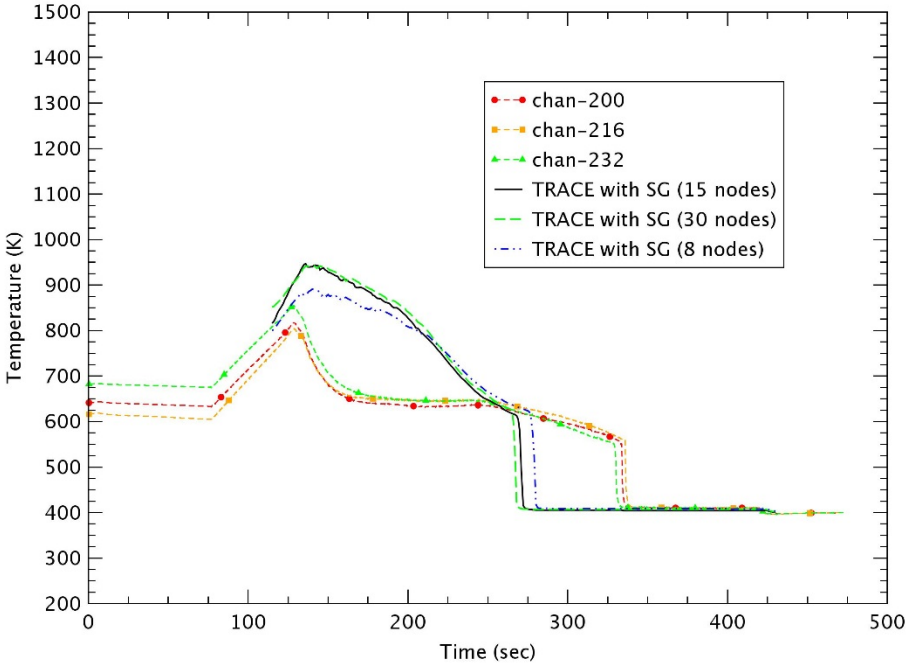

Figure 4-24 Heater Rod Temperature at 3.43 m – Test 1285

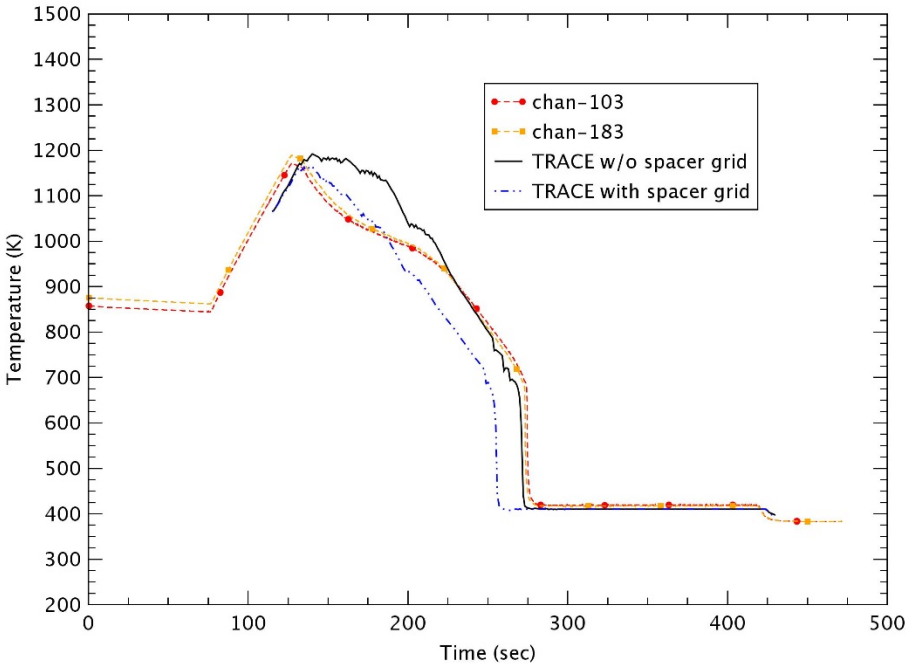

Figure 4-25 Heater Rod Temperature at 2.77 m for 8 nodes – Test 1285

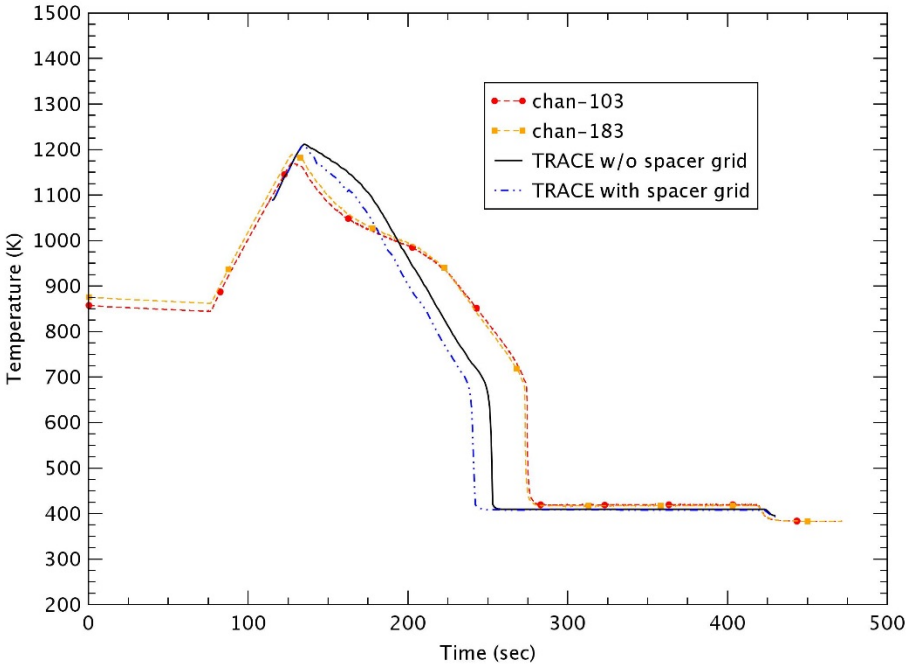

Figure 4-26 Heater Rod Temperature at 2.77 m for 30 nodes – Test 1285

4.2 Effect of Spacer Grid Parameters

There are several input parameters in the current spacer grid model of TRACE. Seven input parameters are defined for a separate grid model as follows:

- spbloc : Spacer grid flow blockage area ratio
- vnbloc : Mixing vane flow blockage area ratio
- phi : Mixing vane angle measured from parallel with the top of the spacer grid to the mixing vane
- wetperim : Spacer grid wetted perimeter
- height : Spacer grid axial height
- strthick : Grid strap thickness of modeled spacer grid
- spmatid : Grid material ID

A review of the spacer grid model revealed that the spacer grid and the mixing vane flow blockage ratio and the mixing vane angle influenced the convective heat transfer, the pressure drop and the droplet breakup model among the four sub-models. The spacer grid axial height, wetted perimeter and the strap thickness were related more significantly to the droplet breakup model and the grid re-wetting model. There, the sensitivity analysis was performed for several parameters in order to identify the effects of the grid parameters. The calculations were performed in the base case with 15 nodes. Test 1096 was selected as the base case because it had the largest effect for the peak rod temperature by using the spacer grid model. Test 1096 was a reflood test for low power, low reflood rate, low pressure and low subcooling degree.

Table 4-5 Conditions and Results for Sensitivity Analysis

	Base Case	spbloc-up	spbloc-down
spbloc	0.362	0.4344 (+20%)	0.2896 (-20%)
PCT (K) (at time)	1227.3 (329 sec)	1229.2 (328 sec)	1224.1 (336 sec)
Quenching time (sec) (at z ~ 2.77m)	891	869	924
- ± 20 % for vnbloc (0.188), wetperm (1.912), Height (0.045) - For phi (20° & 40°, nominal 30°) - For strthick (0.5E-4 & 2.0E-3, nominal 1.0E-3) - Material property (Inconel600, ZrO_2, SS316) ➔ Results were little changed from base case			

The conditions and results for the sensitivity analysis are shown in Table 4.5. Among seven parameters, the only thing that showed a meaningful change for the rod temperature was the spacer grid flow blockage area ratio (spbloc). Figures 4.27 through 4.29 give the rod temperature results at z ~2.77 m according to the spacer grid flow blockage area, the mixing vane flow blockage area and the mixing vane angle. As the spacer grid flow blockage area increased, the peak rod temperature increased a little and the quenching time fairly decreased in this test.

To model the convective heat promotion due to the spacer grid, the enhanced Nusselt number was added to the nominal Nusselt number. The model can be divided into two parts: the enhancement due to the acceleration of the flow and the increased turbulence due to the mixing vane. Therefore, if the spacer grid flow blockage area increased, the convective heat transfer rate was enhanced and then decreased with the axial distance from the downstream of the spacer grid as shown in Figure 4.30. For a large spacer grid flow blockage area, the small growth of the peak rod temperature might have resulted from the reduction of the local nominal heat transfer due to the high vapor temperature for the enhanced heat transfer upstream. However, the difference of the peak rod temperature was not significant at z ~2.77 m with the peak power. The earlier quenching was predicted at the large spacer grid flow blockage area since a faster growth of the liquid level occurred because of the enhancement of heat transfer and the increase of the pressure drop.

As shown in Figures 4.28 and 4.29, the effect of the mixing vane flow blockage area and the mixing vane angle were not significant for the rod temperature. Figure 4.30 presents the heat transfer enhancement due to the spacer grid, where the laminar enhancement factor was assumed to be one. The variation of the heat transfer (Nusselt number) for the mixing vane flow blockage area and the mixing vane angle seemed very small compared to the variation for the spacer grid flow blockage area. The sum of the spacer grid and mixing vane blockage area was used to calculate the pressure drop for the spacer grid. The behavior of the rod temperature changed little for the variation of the mixing vane flow blockage. Therefore, the effect of the spacer grid flow blockage area was dominant for the enhancement of heat transfer due to the spacer grid.

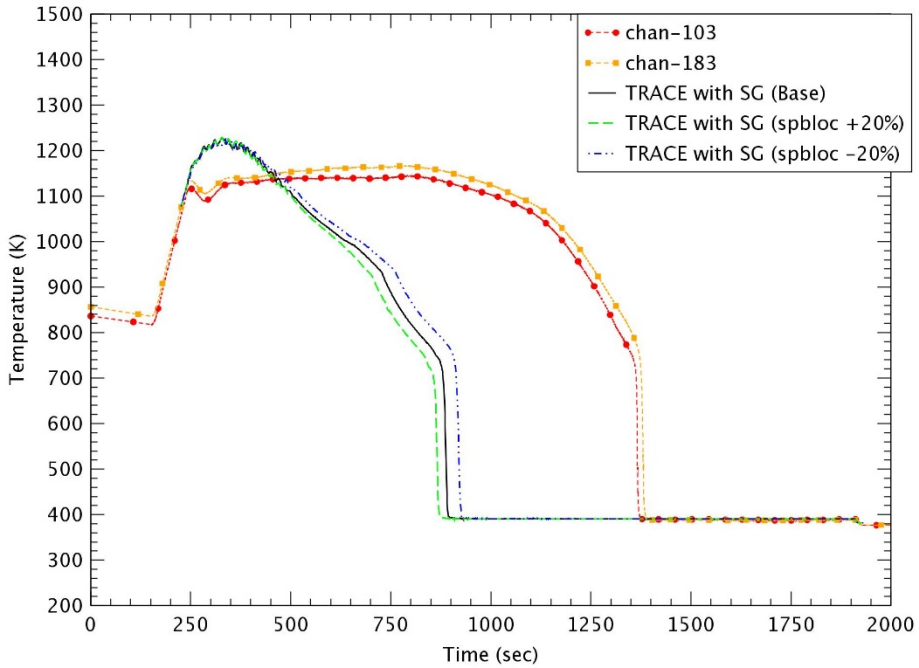

Figure 4-27 Heater Rod Temperature at 2.77 m for spbloc– Test 1096

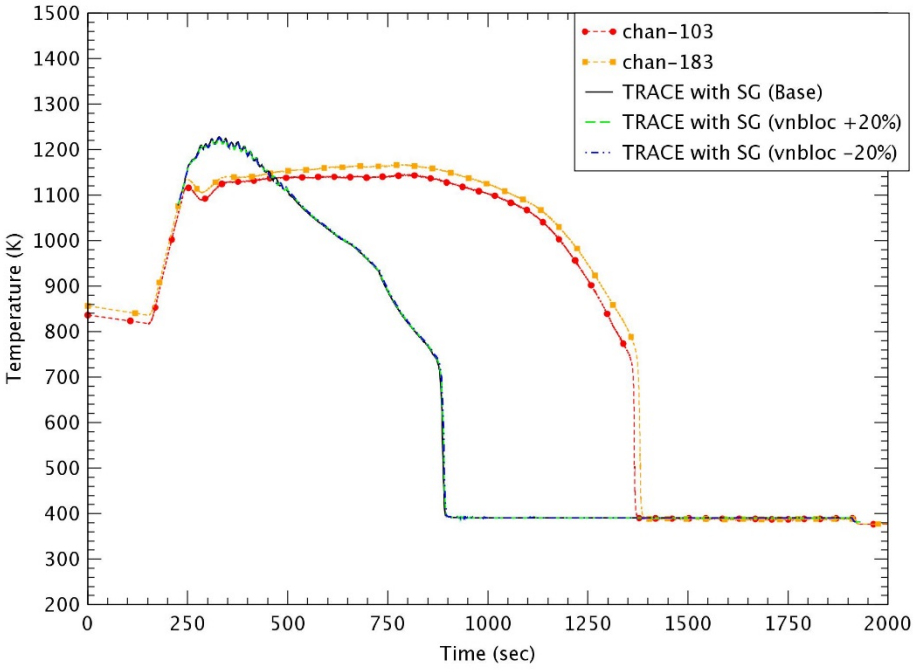

Figure 4-28 Heater Rod Temperature at 2.77 m for vnbloc– Test 1096

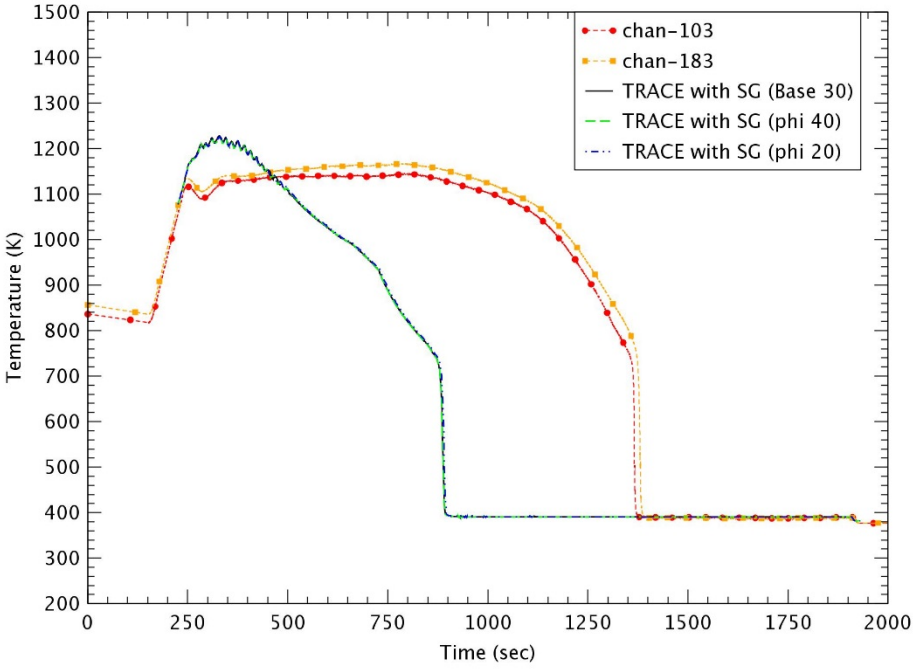

Figure 4-29 Heater Rod Temperature at 2.77 m for phi – Test 1096

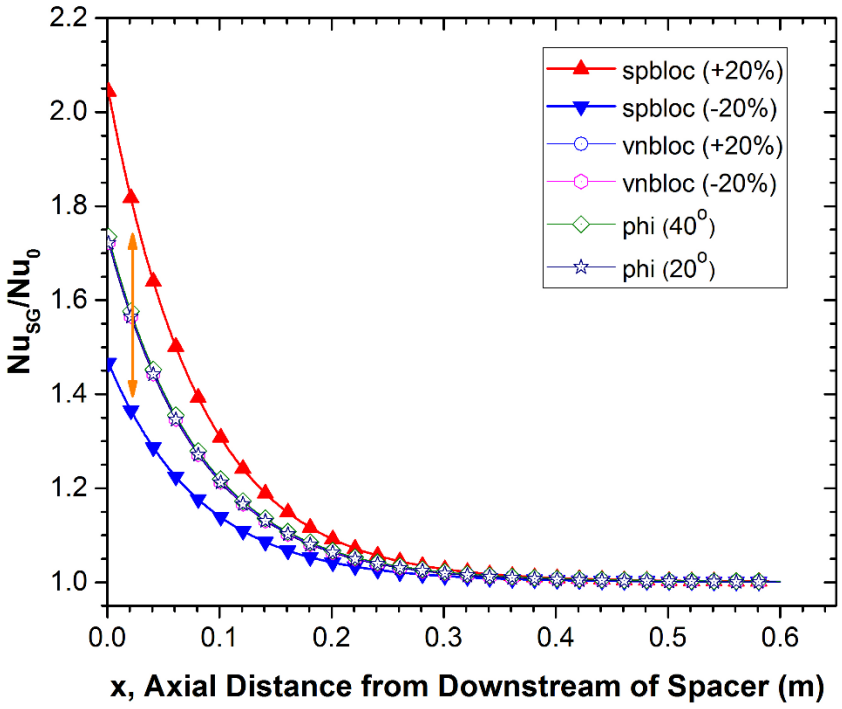

Figure 4-30 Heat Transfer Enhancement for Spacer Grid Parameters

Figures 4.31 through 4.34 give the rod temperature results at z ~2.77 m according to the spacer grid wetted perimeter, the axial height, the strap thickness and the material property. As the figures show, the behavior of the rod temperature was not changed by the variation of these parameters. In TRACE, among the four sub-models, the droplet breakup model and the grid re-wetting model were not fully implemented, as described above. Full implementation for the droplet breakup model will be done after the completion of the droplet field modeling [3]. Additionally, the grid re-wetting model is only implemented to calculate the spacer grid temperatures and then the calculation for the critical film thickness would be needed to fully implement the model. The parameters in Figures 4.31 through 4.34 could be mainly used to calculate the grid surface temperature and area in the grid re-wetting model. Figures 4.35 and 4.36 show the grid temperature variations for the spacer grid wetted perimeter and the strap thickness. The grid temperature would be a little affected by the change in these parameters, but it was not large enough to influence the rod temperature. Furthermore, the grid temperature was not varied by the axial height and the material property as shown in Figures 4.37 and 4.38. Therefore, it is clear that varying of these parameters would have little effect on the rod temperature because some models were not fully implemented.

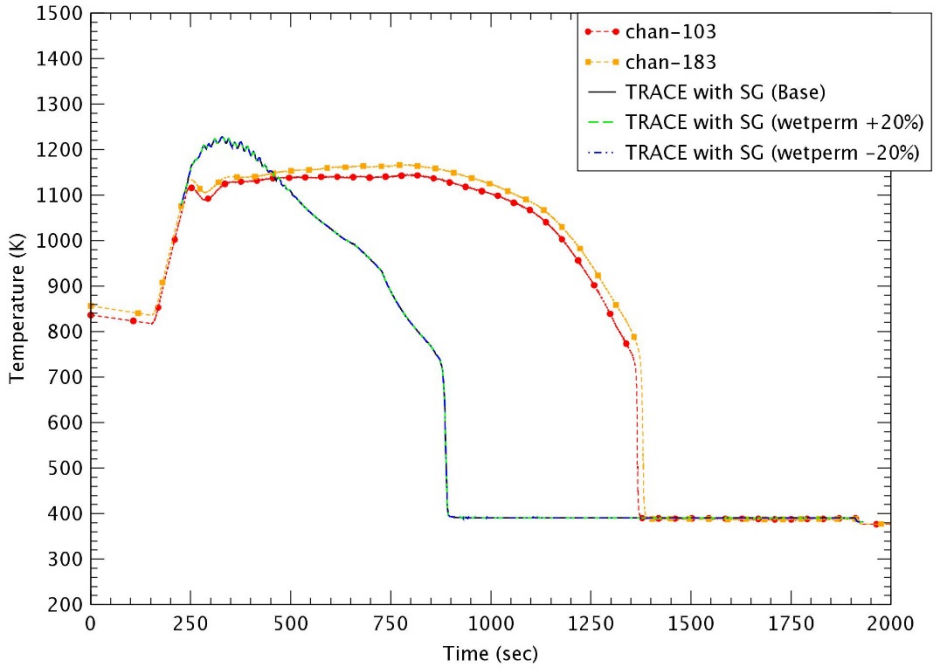

Figure 4-31 Heater Rod Temperature at 2.77 m for wetperm – Test 1096

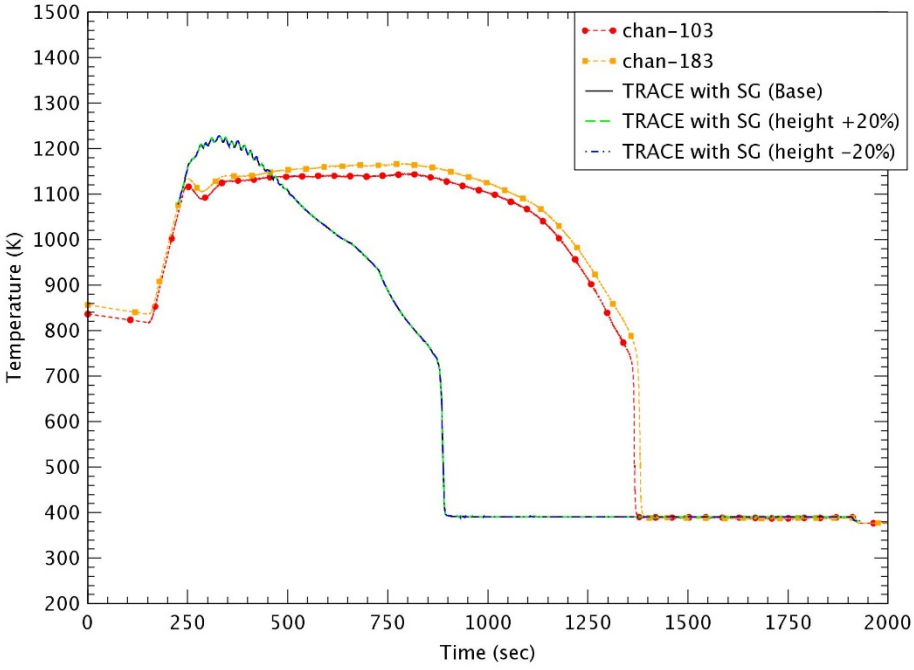

Figure 4-32 Heater Rod Temperature at 2.77 m for height – Test 1096

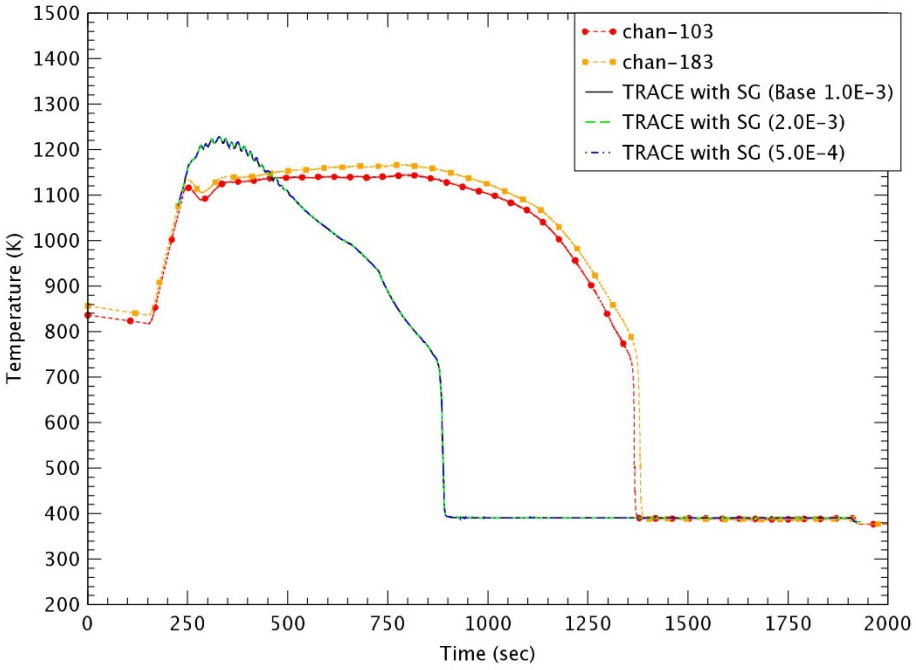

Figure 4-33 Heater Rod Temperature at 2.77 m for strthick – Test 1096

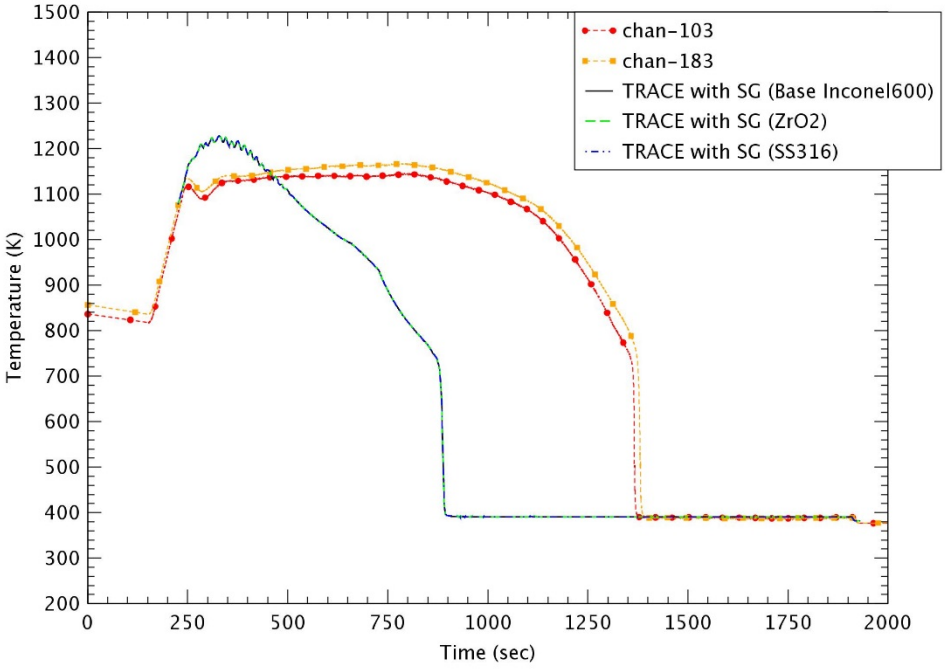

Figure 4-34 Heater Rod Temperature at 2.77 m for material property – Test 1096

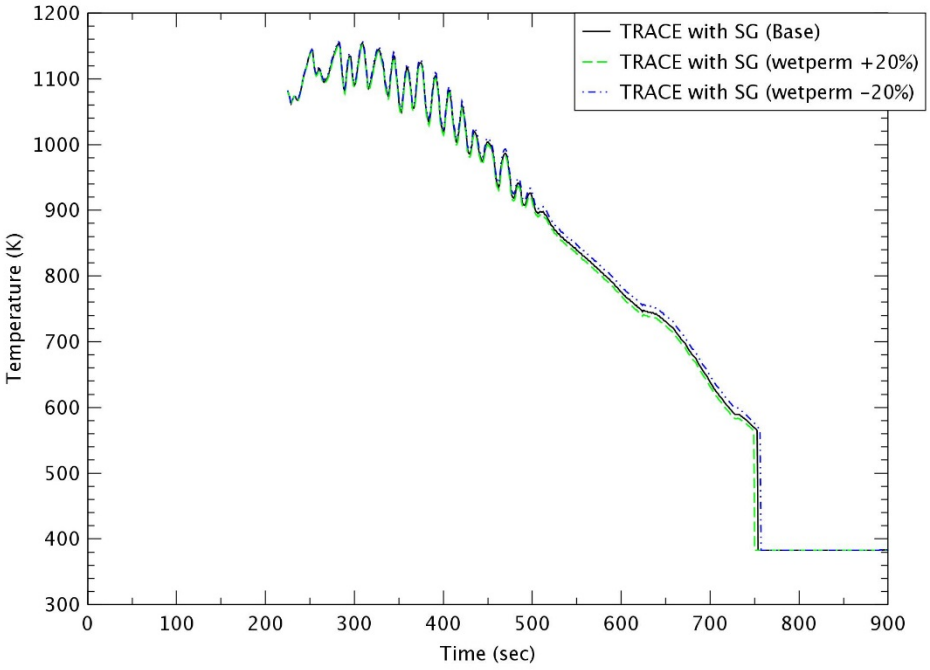

Figure 4-35 Grid Temperature at 2.77 m for wetperm – Test 1096

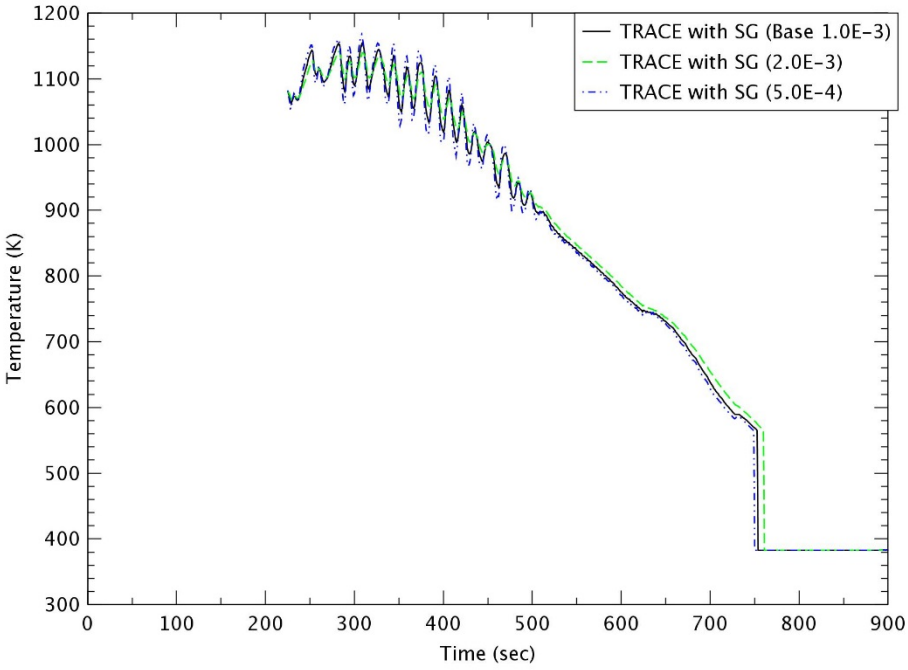

Figure 4-36 Grid Temperature at 2.77 m for strthick – Test 1096

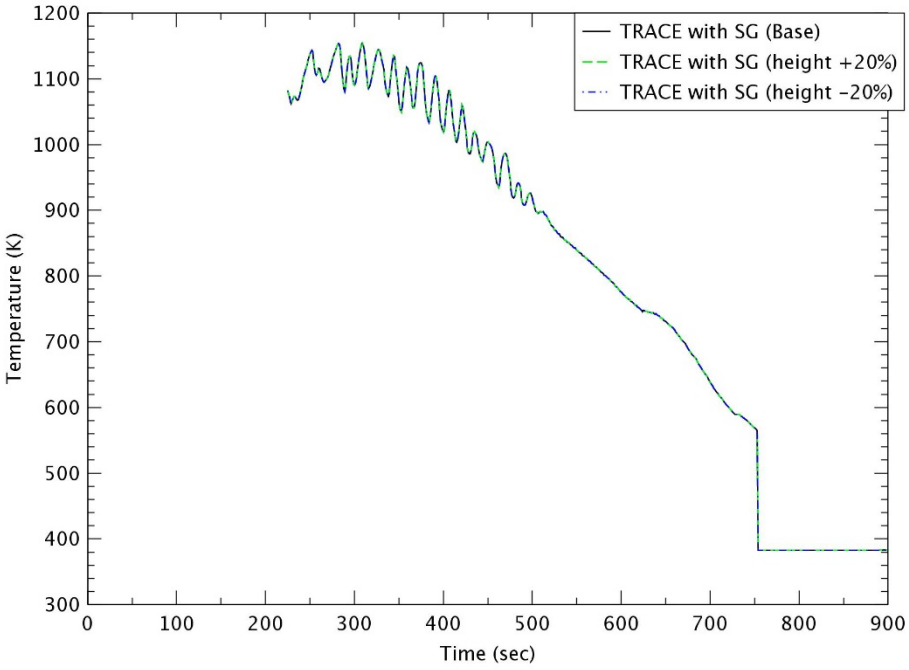

Figure 4-37 Grid Temperature at 2.77 m for height – Test 1096

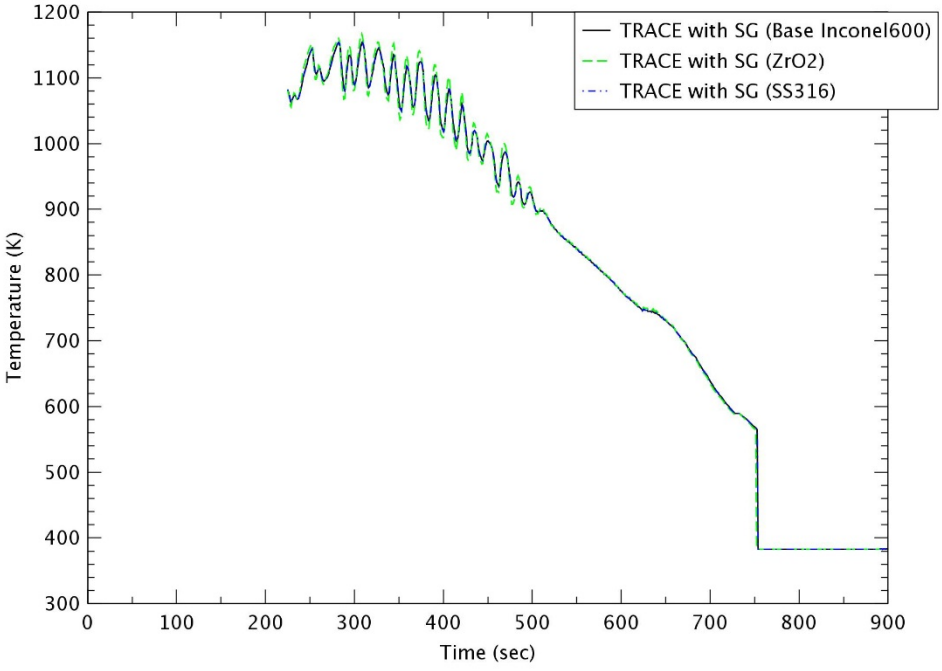

Figure 4-38 Grid Temperature at 2.77 m for material property – Test 1096

4.3 Effect of the Mixing Vane

As described in Chapter 2, the convective heat transfer enhancement due to the spacer grid was composed of two parts: 1) the heat transfer enhancement due to the acceleration of the flow and the increased turbulence due to the spacer grid, and 2) the effects of mixing vanes. In this study, the effects of mixing vanes was also evaluated for RBHT Test 1096. When it was assumed that the egg-crate grids without the mixing vanes were installed in RBHT, Part 2 of Eq. (1) could be 1.0 and the effect of mixing vanes disappeared. Figures 4.39 through 4.42 give the rod temperatures at various elevations for the effect of the mixing vanes. The effect of the mixing vane was considered with parameters such as the mixing vane flow blockage area ratio and the angle of the vane and decayed exponentially downstream of a spacer grid as shown in Figure 4.43. For RBHT tests, the heat transfer enhancement for mixing vanes was far lower than that due to the flow acceleration, but it increased by ~ 20% of the enhancement due to the flow acceleration up to ~ 0.4 m downstream of the spacer grid.

As shown in Figures 4.39 through 4.42, the rod temperature without the mixing vanes had patterns that were similar to those with the mixing vanes. When the mixing vanes were not considered, the rod temperatures slightly increased and the rod quenches were delayed due to the decrease of the heat transfer enhancement due to the mixing vanes. Table 4.6 shows the variations of the rod temperature and the quenching time for the mixing vane at elevation z ~ 2.77 m with the peak power. The decreasing peak rod temperature without the mixing vane was ~ 69.6 K and the reduction of quenching time without the mixing vane was ~ 201 sec due to the spacer grid model. This variation for the rod temperature was 20% smaller than that with the mixing vane. It was hard to determine the effect of the mixing vanes quantitatively since the rod temperature could be influenced by the power shape, the reflood rate, the initial temperature, the initial pressure, etc. However, it is clear that the mixing vanes could meaningfully change the behaviors of the rod temperature.

Table 4-6 Peak Temperature and Quenching Time for Mixing Vane in Test 1096

Test No. 1096 (~ 2.77 m)	Peak Temperature (K) (at time)			Quenching Time (sec)		
	W/O grid	With grid	∆ Temp	W/O grid	With grid	∆ Time
With mixing vane	1314.5 (441 sec)	1227.3 (329 sec)	87.2	1134	891	243
Without mixing vane		1244.9 (349 sec)	69.6		933	201

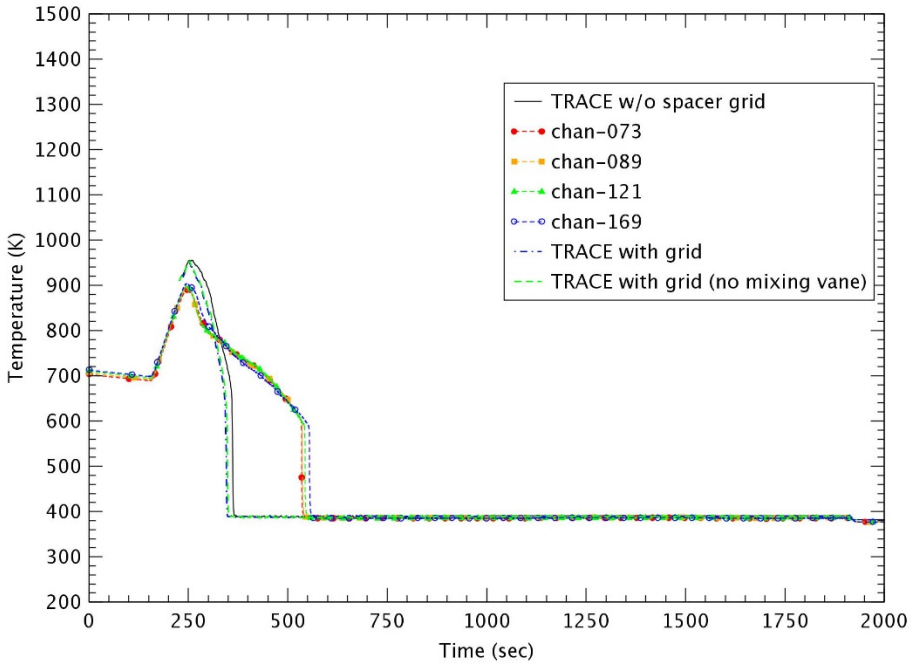

Figure 4-39 Heater Rod Temperature at 1.27 m – Test 1096

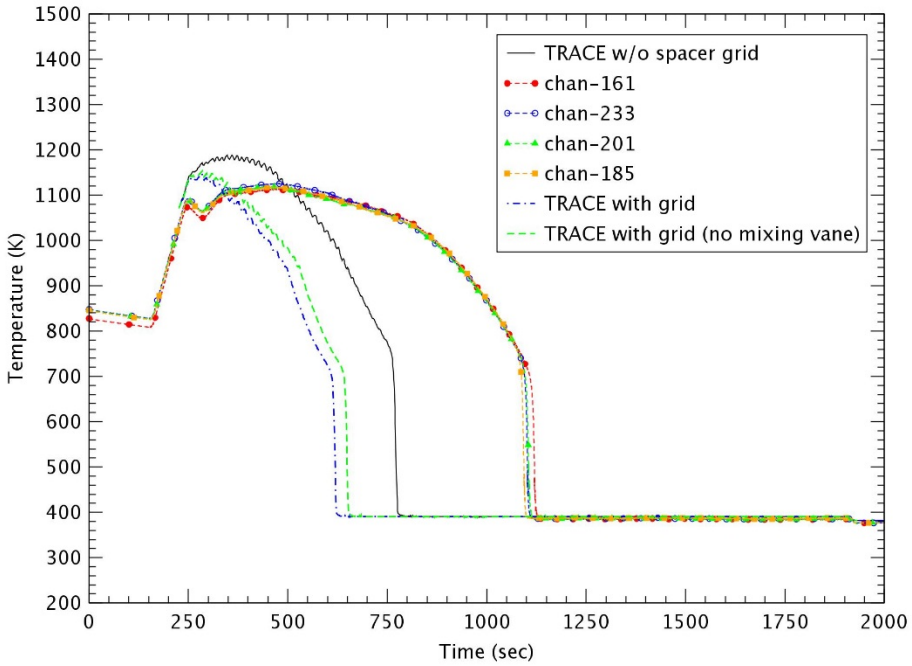

Figure 4-40 Heater Rod Temperature at 2.25 m – Test 1096

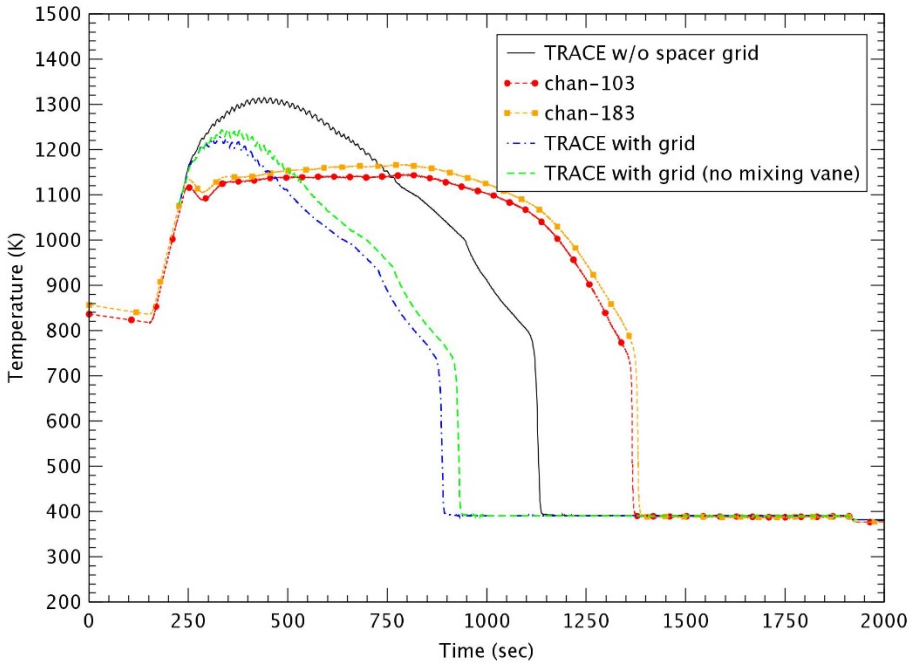

Figure 4-41 Heater Rod Temperature at 2.77 m – Test 1096

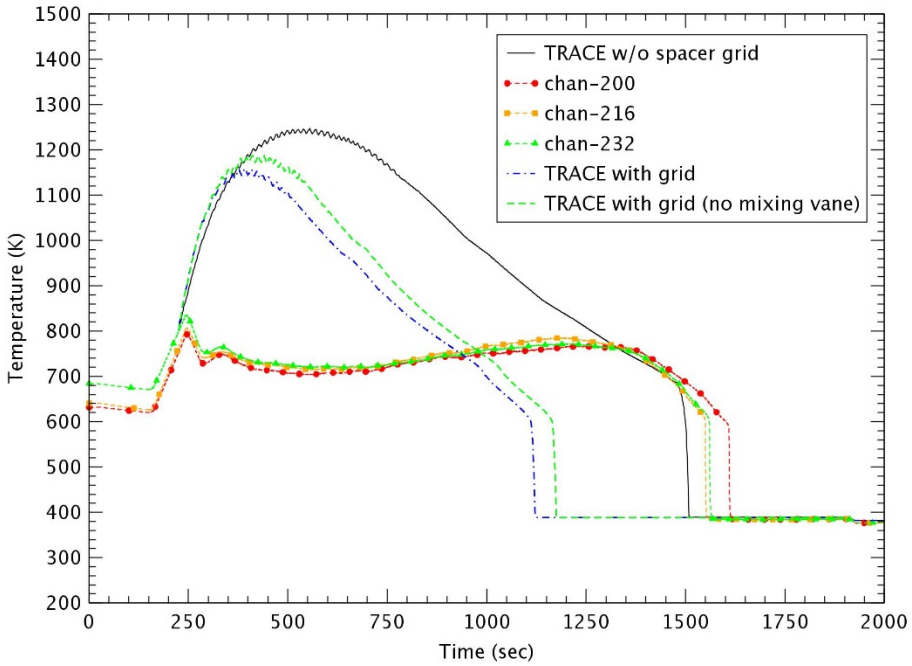

Figure 4-42 Heater Rod Temperature at 3.43 m – Test 1096

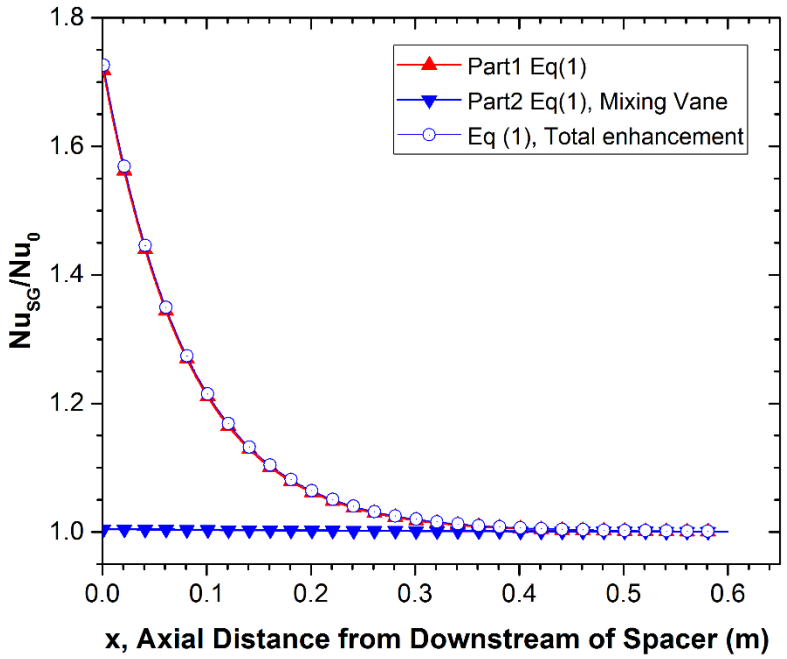

Figure 4-43 Heat Transfer Enhancement for RBHT Tests

5 CONCLUSIONS

The effect of the spacer grid of TRACE V5.0 patch4 were evaluated for Rod Bundle Heat Transfer (RBHT) reflood heat transfer experiments. These RBHT experiments were conducted to obtain data for developing reflood heat transfer models of the USNRC's thermal-hydraulic codes such as TRACE, RELAP5. The RBHT test section was modeled in the VESSEL and HTSTR components of TRACE, which was based on a previous study [12]. Two PIPE components were modeled as the lower plenum and upper plenum respectively. The injected flow was provided by the FILL component, which was connected to the bottom of the lower plenum. The BREAK component was used to set the pressure boundary at the top of the test section. The times for the injected flow and power were modified to precisely consider the experimental data, especially for tests 1108, 1170 and 1196. The main parameters of the spacer grid were defined by the experimental data and seven mixing vane grids were modeled in the test section of TRACE.

Six tests of RBHT were calculated by TRACE, and the tests covered a range of power from 0.88 kW/m to 1.53 kW/m, subcooling from 16 K to 86 K, liquid injection flow rate from 0.12 kg/sec to 0.75 kg/sec and pressure from 0.13 MPa to 0.28 MPa. When the spacer grid model was applied, the calculation results revealed that the rod temperatures decreased and the rods were quenched earlier in most of the tests. That was because the spacer grid enhanced the convective heat transfer due to the flow acceleration and the turbulence increase. In tests with high power and a high reflood rate, the effect of the spacer grid for the peak temperature was not big, which came from the short heat up period and the faster rise of the liquid level. As the subcooling degree was higher, the reduced degree of quenching time due to the spacer grid also decreased more. Consequently, in Test 1096 for low power, a low reflood rate, low pressure and low subcooling degree, the peak rod temperature and the quenching time was changed most significantly by the spacer grid.

Sensitivity studies were performed to identify 1) the effect of the number of nodes, 2) the effect of the spacer grid parameters and 3) the effect of the mixing vane. For modeling the number of nodes of test section as 8, 15 and 30, the coarse node case (8 nodes) had the lower peak temperature at elevation z ~ 2.77 m with the peak power. The peak rod temperature for 30 nodes was predicted slightly higher compared to that for 15 nodes, but their difference was not large. For sensitivity calculations of seven grid parameters, such as the spacer grid flow blockage area ratio, the mixing vane flow blockage ratio, the mixing vane angle, etc., the effect of the spacer grid flow blockage area was dominant, but the effect of other parameters was not significant for the enhancement of heat transfer due to the spacer grid. That could also be because there was no full implementation of the droplet breakup model and the grid re-wetting model in TRACE. Without the mixing vane, the rod temperatures were slightly increased and the rod quenches were delayed due to the reduction of the heat transfer enhancement due to the mixing vane.

In conclusion, the effect of the spacer grid model in TRACE was shown well to simulate the RBHT reflood heat transfer experiments. However, there are some limitations to quantitatively predicting the effect of the droplet breakup and the grid rewetting models. Therefore, comparative studies with other codes with a spacer grid model should be performed, and the TRACE code needs to be improved to implement the droplet breakup and the grid rewetting models in future studies.

6 REFERENCES

1. USNRC, “Improvement of RELAP5/MOD3.3 Reflood Model Based on the Assessments against FLECHT-SEASET Tests”, NUREG/IA-0251, 2011.

2. USNRC, “TRACE V5.840 User’s manual, Volume 1: Input Specification”, 2014.

3. USNRC, “TRACE V5.840 Theory Manual, Field Equations, Solution Methods, and Physical Models”, 2013.

4. USNRC, “RBHT Reflood Heat Transfer Experiments Data and Analysis”, NUREG/CR-6980, 2012.

5. USNRC, “Rod Bundle Heat Transfer Test Facility Test Plan and Design”, NUREG/CR-6975, 2010.

6. T.S. Choi, “Development of an Improved Reflood Model for RELAP5 and SPACE”, PhD Thesis of KAIST, 2013.

7. Yao, S. C., L. E. Hochreiter, and W. J. Leech., "Heat-Transfer Augmentation in Rod Bundles Near Grid Spacers", Journal of Heat Transfer, 104, 76-81, 1982.

8. Yao, Shi-Chune, M. Loftus, and L. Hochreiter., "Hydraulics of Blocked Rod Bundles", Nuclear Technology, 65, 444-453, 1984.

9. Rehme, Klaus, J. Marek, and K. Maubach. "Heat Transfer and Pressure Drop Performance of Rod Bundles Arranged in Square Arrays", International Journal of Heat and Mass Transfer, 16, 2215-2228, 1973.

10. Yao, S. C., L. E. Hochreiter, and K. Y. Cai. "Dynamics of Droplets Impacting on Thin Heated Strips," 23rd National Heat Transfer Conference, American Society of Mechanical Engineers, Heat Transfer Division. New York, 1985.

11. USNRC, “Analysis of FLECHT-SEASET 163-Rod Blocked Bundle Data Using COBRA-TF”, NUREG/CR-4166, 1985.

12. USNRC, “TRACE V5.0 Assessment Manual, Appendix B: Separate Effects Tests”, 2007.

NRC FORM 335
(12-2010)
NRCMD 3.7

U.S. NUCLEAR REGULATORY COMMISSION

BIBLIOGRAPHIC DATA SHEET

(See instructions on the reverse)

1. REPORT NUMBER
(Assigned by NRC, Add Vol., Supp., Rev., and Addendum Numbers, if any.)
NUREG/IA-0480

2. TITLE AND SUBTITLE
TRACE Assessment for Effect of Spacer Grid in RBHT Reflood Heat Transfer Experiments

3. DATE REPORT PUBLISHED

MONTH	YEAR
February	2018

4. FIN OR GRANT NUMBER

5. AUTHOR(S)
Byung-Gil HUH, Ae-Ju CHEONG, Kyung-Won LEE

6. TYPE OF REPORT
Technical

7. PERIOD COVERED (Inclusive Dates)

8. PERFORMING ORGANIZATION - NAME AND ADDRESS (If NRC, provide Division, Office or Region, U. S. Nuclear Regulatory Commission, and mailing address; if contractor, provide name and mailing address.)
Korea Institute of Nuclear Safety
62 Gwahak-ro, Yuseong-gu
Daejeon, 34142, Korea

9. SPONSORING ORGANIZATION - NAME AND ADDRESS (If NRC, type "Same as above", if contractor, provide NRC Division, Office or Region, U. S. Nuclear Regulatory Commission, and mailing address.)
Division of Systems Analysis
Office of Nuclear Regulatory Research
U.S. Nuclear Regulatory Commission
Washington, DC 20555-0001

10. SUPPLEMENTARY NOTES
K.Tien, NRC Project Manager

11. ABSTRACT (200 words or less)
The spacer grid model in the TRACE V5.0 patch4 were evaluated for Rod Bundle Heat Transfer (RBHT) reflood experiments. The RBHT test section was modeled with VESSEL and HTSTR components. Two PIPE components were modeled as the lower and upper plenum and injected flow was provided by the FILL component. The BREAK component set the pressure boundary. The calculations for six tests of RBHT confirmed that when the spacer grid model was used, the rod temperatures decreased and the rods were quenched at an earlier time. This was due to enhanced convective heat transfer and turbulence increase. In Test 1096 the peak rod temperature and the quenching time were most significantly affected by the spacer grid. Sensitivity studies were also performed to identify 1) the effect of the nodes, 2) the effect of the spacer grid parameters and 3) the effect of the mixing vane. The effect of the spacer grid model in TRACE is largely shown to simulate the RBHT reflood heat transfer. The droplet breakup and the grid rewetting models were not yet fully implemented, therefore these features in TRACE code will needs to be improved in the future.

12. KEY WORDS/DESCRIPTORS (List words or phrases that will assist researchers in locating the report.)
Rod Bundle Heat Transfer Test Facility (RBHT)
Mixing Vane Spacer Grid
TRACE Version 5.0 Patch Release 4
Reflood Heat Transfer
Droplet Breakup
Spacer Grid Rewetting

13. AVAILABILITY STATEMENT
unlimited

14. SECURITY CLASSIFICATION
(This Page)
unclassified
(This Report)
unclassified

15. NUMBER OF PAGES

16. PRICE

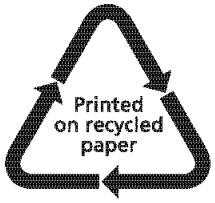

Federal Recycling Program

UNITED STATES
NUCLEAR REGULATORY COMMSSION
WASHINGTON, DC 20555-0001

OFFICIAL BUSINESS